Calibrating the Long-Range Backbone Dynamics of Polymers in Solution Using Two Different Models

by

Hunter Little

A thesis
presented to the University of Waterloo
in fulfilment of the
thesis requirement for the degree of
Master of Science
in
Chemistry

Waterloo, Ontario, Canada, 2022

AUTHOR'S DECLARATION

I hereby declare that I am the sole author of this thesis. This is a true copy of the thesis, including any required final revisions, as accepted by my examiners.

I understand that my thesis may be made electronically available to the public.

ABSTRACT

The fluorescence decays of a series of 41 pyrene-labeled poly(oligo(ethylene glycol)methyl ether methacrylate)s (Py-PEG$_n$MA where n = 0, 1, 2, 3, 4, 5, 9, 16, 19) were prepared by free-radical polymerization of 1-pyrenebutyl methacrylate and oligo(ethylene glycol)methyl ether methacrylate. The more polar oligo(ethylene glycol) side chains increased the range of solvent polarities in which these polymers were soluble. The Py-PEG$_n$MAs were dissolved in four solvents, namely tetrahydrofuran, toluene, dimethyl formamide, and dimethylsulfoxide which represented a broad range of solvent polarities and viscosities. The pyrene monomer and excimer decays were acquired for the different Py-PEG$_n$MA solutions and then analyzed globally using the fluorescence blob model (FBM) and the model free analysis (MFA).

The FBM analysis yielded the parameters k_{blob} and N_{blob} along with the product $k_{blob}\times N_{blob}$. The parameter N_{blob}, which reports on the number of structural units within an imaginary volume known as a *blob*, describes the ability of a polymer to bend, while $k_{blob}\times N_{blob}$ reports on the encounter frequency between structural units. Together, N_{blob} and $k_{blob}\times N_{blob}$ provide information on the long-range backbone dynamics (LRBD) of the polymer. Interestingly, since a single structural parameter, the length of the side-chain, was changed in this study, it was easy to parametrize both of N_{blob} and $k_{blob}\times N_{blob}$ in terms of the molecular weight of the structural unit and the solvent viscosity. The resulting equations were used to construct a calibration curve against which the dynamics of other polymers could be compared. This represents a great step forward as previous calibration curves were limited to a single solvent in which the benchmark polymers were soluble. Additionally, N_{blob} was used to extract the persistence length of the polymers from a modified version of the Kratky-Porod equation.

Analysing the same decays with the MFA provided a unique opportunity to compare the two very different models. The FBM assumes the polymer has been randomly labeled with pyrene which are distributed into imaginary volumes called *blobs* according to a Poisson distribution and fits the monomer and excimer decays globally with an infinite sum of exponentials. Conversely, the MFA makes no assumption about the fluorophore distribution and fits the decays with a sum of 2–3 exponentials. This makes the MFA particularly apt to study any type of fluorophore-labeled macromolecules, many of which would be incompatible with the FBM. Regardless of the very different approaches, both models retrieved values representing the average rate constant of excimer formation, $\langle k \rangle$ for the MFA and $k_{blob} \times \langle n \rangle$ for the FBM, which were identical within experimental error. This result shows that the MFA is capable of reporting on the local pyrene concentration, which in turn provides important structural information. Therefore normalizing $\langle k \rangle$ for pyrenyl labels incapable of forming excimer yielded the parameter $\langle k^{MF} \rangle^{blob}$ which was also parameterized in terms of the molecular weight of the structural unit and solvent viscosity, resulting in a universal calibration curve for long-range backbone dynamics. More importantly though, the equivalency between the key parameters retrieved between the two models implied that there existed a similar parameter to N_{blob} within the results of the MFA which described the number of structural units probed by an excited state pyrene. This parameter highlighted a crucial difference between the two models: in the analysis of the FBM the dynamic component, represented as k_{blob}, and the structural component, represented as $\langle n \rangle$, are separated in the analysis whereas in the MFA they are merged into the single parameter $\langle k \rangle$. Additional knowledge about the dynamics of the polymer chain is needed in order to accurately extract the structural information contained within the parameters reported by the MFA.

ACKNOWLEDGEMENTS

I would like to start by thanking my supervisor, Prof. Jean Duhamel, who has guided me in my career as a scientist since I first joined his lab as an excited undergraduate in the spring of 2014. I would also like to thank the numerous members of the Duhamel and Gauthier groups who have overlapped with me, including Janine Toma, Remi Casier, Mike Fowler, Shiva Farhangi, Lu Li, Damin Kim, Justin Rambault, Kiarash Gholami, Sanjay Patel, Abdullah Basalem, Jasmine Zheng, Zehou You, Jingqi Wang, Franklin Frasca, Alex Liu, Kristijan Lulic, Joanne Fernandez, Tori Hisko, Natun Dasgupta, Sebastian Soo, Maria Tzoganakis, Raymond Yeung, and Ryan Lloyd.

I would also like to thank my committee members Prof. Derek Schipper and Prof. Xiaosong Wang. The chemistry department administrative team, especially Cathy Van Esch, Kim Rawson, and Pat Gruber who were always willing to help answer any questions I had about the administrative side of my time here.

I would like to thank my parents, Dawn and Mark Little, my sister Emma, and brother Holden, for supporting me during the course of my studies here at the University of Waterloo.

Finally, I feel I must thank and acknowledge the person who, so many years ago, first inspired my love of chemistry. Had Amy Massiccotte not inspired me as she did, in all likelihood, I would never have set myself on this path, and this thesis would almost certainly never have been written.

TABLE OF CONTENTS

LIST OF FIGURES

LIST OF TABLES

LIST OF ABBREVIATIONS

a.u.	arbitrary units
AIBN	2,2'-azobisbutyrontrile
DCC	dicyclohexylcarbodiimide
DCM	dicholoromethane
DMAP	4-(dimethylamino)pyridine
DMF	*N*,*N*-dimethyl formamide
DMSO	Dimethylsulfoxide
DP	degree of polymerization
DRI	differential refractive index
EG_nMA	oligo(ethylene glycol)methyl either methacrylate
FBM	Fluorescence blob model
FDQ	fluorescence dynamics quenching
GPC	Gel permeation chromatography
LRBD	Long-range backbone dynamics
MALLS	multiangle laser light scattering
meq	molar equivalent
MFA	model free analysis
MMO	molecular mechanics optimizations
MWD	molecular weight distribution
PDMS	poly(dimethyl siloxane)
PEF	pyrene excimer formation
PIMA	poly(isobutylene-*alt*-maleic anhydride)

PLM	pyrene-labeled macromolecules
PMA	poly(methyl acrylate)
PMMA	poly(methyl methacrylate)
PS	polystyrene
PyBMA	1-pyrenebutyl methacrylate
Py-PAMA	Pyrene-labeled poly(alkyl methacrylate)s
Py-PEG$_n$MAs	Pyrene-labeled poly(oligo(ethylene glycol)methyl ether methacrylates) with a degree of polymerization equal to *n*.
SSF	steady-state fluorescence
SU	Structural units
THF	tetrahydrofuran
TRF	time-resolved fluorescence

LIST OF SYMBOLS

D^*	poorly-stacked pyrene excimer
$E0^*$	well-stacked pyrene excimer
f_{agg}	fraction of pyrene that form excimer by pre-aggregation equal to $f_{E0} + f_{EL}$
f_D	fraction of pyrene that form poorly stacked excimer
f_{diff}	fraction of pyrene that form excimer by diffusion
f_{E0}	fraction of pyrene that form well-stacked excimer
f_{free}	fraction of pyrene that remain isolated in solution
f_{k2}	fraction of pyrene that form excimer by rapid re-arrangement
η	solvent viscosity
$[\eta]$	intrinsic viscosity
I_E	fluorescence intensity of the pyrene excimer
I_M	fluorescence intensity of the pyrene monomer
$<k>$	average rate-constant of excimer formation
k_{blob}	rate constant for excimer formation within a *blob*
k_{diff}	bimolecular rate constant describing the diffusive encounters between a dye and a quencher
$<k^{MF}>^{blob}$	normalized average rate-constant of excimer formation
l_p	Persistence length
λ_{Py}	pyrene content given as mmol pyrene per gram of polymer
M	molecular weight
M_n	molar mass of the non-pyrene structural unit
M_{Py}	molar mass of the pyrene labeled structural unit

MW_{SU}	Molecular weight of the structural unit
$\langle n \rangle$	average number of pyrenyl labels within a blob
N_{bb}	number of backbone atoms
N_{blob}	Number of structural units within a *blob*
n_C	number of overlapping carbons between two pyrenyl moieties during MMO
N_S	number of non-hydrogen atoms in the side-chain
Py_{diff}*	pyrenes that form excimer through diffusion
Py_{free}*	pyrene that are isolated and do not form excimer
Py_{k2}*	pyrenes that form excimer through fast re-arrangement
$[Py]_{loc}$	local concentration of pyrene
$\langle r_{EE}^2 \rangle_{blob}$	average squared end-to-end distance of the polymer segment within a blob
R_g	radius of gyration
τ_C	correlation time
τ_D	lifetime lifetime of the pyrene monomer
τ_{E0}	lifetime of the well-stacked pyrene excimer
T_g	Glass transition temperature
τ_M	natural lifetime of a fluorphore
V_{blob}	volume of a blob
Ω_{SU}	frequency of encounter between structural units
x_{Py}	molar fraction of pyrene-labeled structural units

CHAPTER 1

INTRODUCTION AND LITERATURE REVIEW

1.0 FOREWORD

The focus of this thesis is to prepare calibration curves against which the long-range backbone dynamics (LRBD) of polymer chains can be compared in solvents of varying viscosity and polarity. LRBD describe the ability of a polymer to bend and the rate at which bending occurs. Consequently, this chapter begins with a discussion on polymer flexibility and how it is quantified, followed by an introduction to fluorescence which was used to probe the LRBD of polymers in solution. An explanation of the two models, namely the fluorescence blob model (FBM) and model free analysis (MFA), used to handle the fluorescence response of fluorescently labeled polymers is presented, followed by a review of a calibration curve that was established earlier by applying these two models to a series of poly(alkyl methacrylate)s. This chapter concludes with a summary of the research conducted in the subsequent chapters.

1.1 LONG-RANGE BACKBONE DYNAMICS OF POLYMERS

The flexibility of a macromolecule, be it that experienced by a synthetic polymer subject to a deformation or a biological polypeptide folding into its native conformation, is an important parameter that defines the properties of the macromolecule. The flexibility of a macromolecule depends on the time and length scale over which it is being deformed. It can be characterized by conducting a tensile test experiment on a polymer dogbone where the physical properties experienced by the dogbone at the macroscopic level are expected to be reflected at the molecular level by the polymer chains in terms of the extent of their deformation and the frequency at which they bend.

1.1.1 Persistence Length:

The ability of a polymer chain to bend is often quantified by its persistence length (l_p). l_p represents the distance over which the orientation of a linear chain persists starting from an arbitrary structural unit (SU).[1,2] This is depicted in Figure 1.1, where the short and long l_p of a flexible and rigid polymer are compared, respectively.

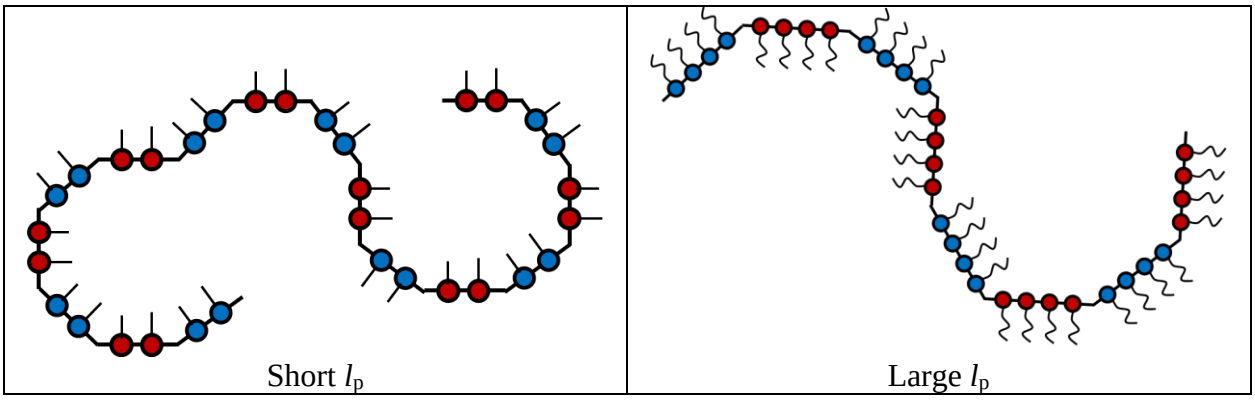

Figure 1.1. Comparison between a flexible polymer with a short l_p and a rigid polymer with a large l_p.

Experimentally, l_p was first retrieved by plotting $(M/\langle R_g^2\rangle)^{1/2}$ as a function of M^{-1} to generate a conformation plot, whereby M and $\langle R_g^2\rangle$ were, respectively, the molecular weight and radius of gyration measured by static light scattering for a series of polymers prepared with a narrow molecular weight distribution (MWD).[1,3–6] While this procedure might appear straightforward at first glance, it turned out to be very demanding in practice. First, the preparation of polymer samples with a narrow MWD requires the use of controlled polymerization methods, which might not always be available depending on the nature of the monomer to be polymerized.[7] Second, the scattering signal recorded in these experiments reports on the entire polymer, which combines the scattering from the polymer backbone, which would yield the l_p, along with the scattering from the side chains.[8] The determination of l_p requires that the unknown scattering from the side chains be subtracted from the scattering for the whole polymer. Since the scattering

component of the side-chains is unknown, assumptions must be made to subtract the contribution of the side chains from the total scattering, leading to erroneous results unless the side chains are exceedingly short. Further complications arise from *x*-axis of this conformation plot scaling as the reciprocal of *M*; the low molar-mass data points which are most effected by noise, become the most influential in the linear regression to retrieve the intercept and slope of the conformation plot which in turn are used to determine l_p.[1] Due to these complications, the application of other techniques to measure the l_p of linear chains have been examined.

The l_p of polymers synthesized with a broad MWD can be determined by gel permeation chromatography (GPC) as long as the instrument is equipped with a differential refractive index (DRI) detector to measure the polymer mass concentration, a multiangle laser light scattering (MALLS) detector to determine the absolute molecular weight and R_g, or a pressure detector to measure the absolute molecular weight and the intrinsic viscosity ($[\eta]$).[1,9,10] Since the GPC column separates the polymers into populations of monodisperse chains, the signal of all the detectors provides the M, R_g, and $[\eta]$ at each elution volume along the entire MWD of the polymer, which allows the construction of conformation plots based either on R_g or $[\eta]$ across the MWD of the polymer sample.[1,6,11–13] While GPC appears to solve the problem of dealing with polymer samples having a broad MWD, the use of a GPC instrument requires that all detectors be perfectly calibrated, a task that is sometimes challenging. Second, most GPC systems are designed to operate with a single solvent as the eluent. Consequently, polymers that are insoluble in the selected solvent cannot be injected into the GPC and their l_p cannot be determined. Finally, and like the original scattering experiments, the entirety of the polymer chain is probed, not just the backbone, requiring similar assumptions to be made to separate the signal of the side chains from the signal emanating from the entire polymer.

In summary, while l_p can be measured by scattering and GPC experiments, both techniques have significant drawbacks whose combination makes l_p a much sought-after but seldom measured parameter in polymer science. An ideal technique would, therefore, need to meet the three following requirements. It would have to 1) be capable of handling polydisperse polymer samples, 2) be applicable to a broad range of solvents so that a solvent, in which the polymer is soluble, can always be found, and 3) retrieve the signal generated exclusively by the backbone from which the l_p can be retrieved.

1.1.2 Bending Frequency:

The bending frequency represents the encounter frequency (Ω_{SU}) between the SUs of a chain segment constituting the polymer. This is often quantified by the glass transition temperature (T_g) or correlation time (τ_c) for a polymer in the bulk or in solution, respectively. T_g quantifies the temperature at which there is enough thermal energy for segments of the polymer chain to undergo interconversion between the *trans* and *gauche* conformations.[14,15] Though useful for understanding the bulk properties of a polymer, T_g is strongly influenced by the free-volume generated by the side chains.[15] This is neatly demonstrated in the work of Rogers and Mandelkern for a series of poly(*n*-alkyl methacrylate)s.[15] Since a longer side chain should slow down the motion of the main polymethacrylate chain, poly(*n*-dodecyl methacrylate) ($PC_{12}MA$) would be expected to have a higher T_g than poly(methyl methacrylate) (PC_1MA). As it turns out, the opposite is found with PC_1MA and $PC_{12}MA$ having a T_g of 105 °C and −65 °C, respectively.[15] In this case, the dodecyl side chains generate a lot of free volume, which enables the polymethacrylate backbone of $PC_{12}MA$ to undergo local motions at a much lower temperature than the polymethacrylate backbone of PC_1MA, hence the much lower T_g.

τ_c, retrieved from ^{1}H, ^{13}C, or ^{15}N NMR, reports on the rotational diffusion of the nuclei being probed.[16–20] Though this provides a quantification of Ω_{SU}, its accuracy is highly dependent on the dynamic-homogeneity between the nuclei being probed and the rest of the polymer. Erroneous results will inevitably be retrieved if the nuclei is part of a flexible segment of an otherwise rigid polymer chain, and vice versa.[21] This same pitfall is present in other techniques probing the rotational diffusion of part of a macromolecule such as scattering techniques[22,23] or fluorescence anisotropy.[24,25] What would be of greater use and interest would be a technique where the translational dynamics of the polymer chain were probed, such that these translational motions would directly describe the rate of encounter between structural units.

1.2 FLUORESCENCE QUENCHING

A complementary technique to those outlined above for probing Ω_{SU} is that of fluorescence quenching. Fluorescence is a photophysical phenomenon whereby a dye molecule emits a photon of light following the absorption of a photon having a specific energy.[26] This process is best described through the Jablonski diagram shown in Figure 1.2.

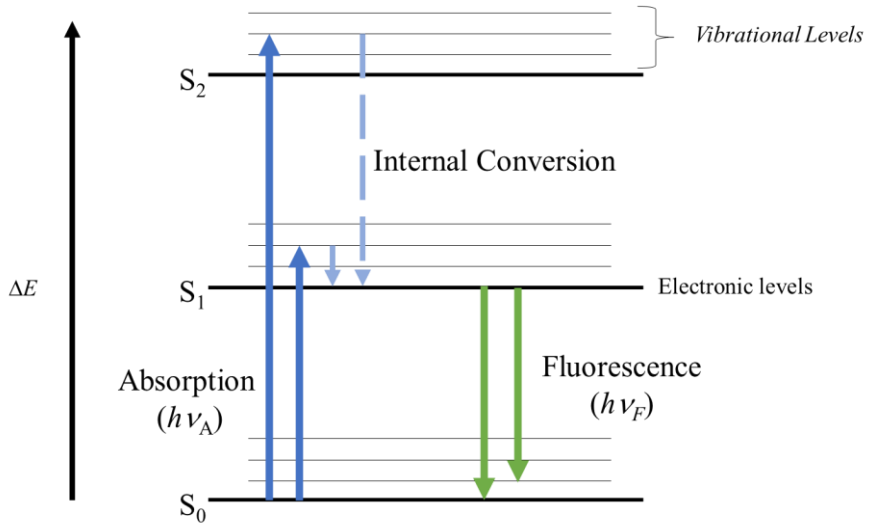

Figure 1.2. Jablonski diagram illustrating the process of (dark blue) absorption, (light blue) internal conversion, and (green) fluorescence. Rotational energy levels are not depicted for clarity.

Upon the absorption of a photon ($h\nu_A$) by a fluorophore, an electron is excited from the ground state ($S_{0,0}$) to a vibrational level of one of the higher excited electronic states (S_1, S_2, or higher). The time taken for this to occur is on the order of 10^{-15} s.[26] The fluorophore then undergoes a process known as internal conversion, that takes place on the order of a few picoseconds, whereby the electron relaxes to the lowest vibrational level of the first electronic state ($S_{1,0}$).[26] Finally, a photon of light is emitted ($h\nu_F$) which returns the fluorophore to one of the vibrational levels of the S_0 electronic state. The time spent in the excited state, usually a few tens of nanoseconds,[26] is known as the natural lifetime (τ_M) of the fluorophore. The emission of a photon described by the Jablonski diagram is referred to as fluorescence.

Any process which reduces the intensity of fluorescence emission is known as fluorescence quenching.[26] Instead of returning to the ground state through the fluorescence pathway, interactions, that can occur on contact or over a distance, between the excited dye and a quencher induces the excited dye to return to the ground state without the emission of a photon.[26–28]

Quenching can occur in a static or dynamic manner depending on whether the fluorescent dye and quencher are either in contact prior to excitation or must undergo diffusive motion to come into contact, respectively.[26] Fluorescence dynamics quenching, depicted in Figure 1.3, is an ideal method to probe the dynamics of macromolecules in solution. A fluorophore and a quencher covalently attached to the macromolecule of interest can only come into contact if the macromolecule is flexible enough to permit dynamic motions that bring the two into contact with a defined pseudo-unimolecular rate constant k_Q, where $k_Q = k_{diff} \times [Q]_{loc}$.[26,28] k_{diff} is the bimolecular rate constant for diffusive encounters, which reflects the flexibility of the macromolecule, while $[Q]_{loc}$ represents the concentration of quenchers experienced locally by an excited dye, where both dye and quencher are covalently attached to the macromolecule. Consequently, $[Q]_{loc}$ and k_Q, which is the parameter that is obtained experimentally, describe the distribution of quenchers attached to the macromolecule.

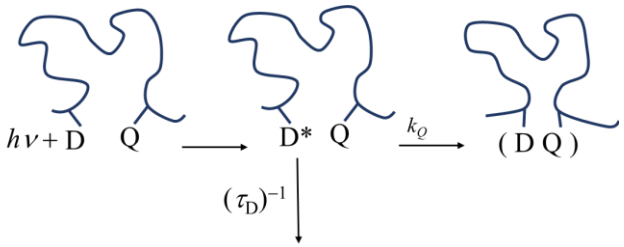

Figure 1.3. Kinetic scheme of fluorescence quenching of an excited dye (D^*) by a quencher (Q) covalently attached to a macromolecule with a rate constant k_Q.

The simplest expression of k_Q corresponds to a polymeric construct where one dye and one quencher are covalently attached to the ends of a monodisperse polymer chain.[27] $[Q]_{loc}$ is then equal to $1/V_{coil}$, as there is one quencher per polymer coil, and k_Q is easily retrieved from the analysis of the fluorescence decays acquired with the fluorescently labeled polymer, since the

decay is monoexponential in this instance.[29.30] In these experiments, k_Q is also known as k_{cy}, the rate constant of end-to-end cyclization, and has been found to scale as $n^{-3\nu}$, where n is the degree of polymerization (DP) and ν is the Flory exponent.[21,27,28] The primary disadvantage of these cyclization experiments is that k_{cy} becomes negligible at very moderate DP's, and is thus better suited for probing the dynamics of oligomers as opposed to true polymers.[27–32] Furthermore, since labeling only occurs at the chain ends, no dynamic information is provided for the interior, unlabeled, portion of the polymer chain, an often overlooked complication as SUs located close to the polymer chain-ends are more mobile than those in the chain interior.[33–35] These disadvantages in the scope of the information retrievable, coupled with the rigorous synthetic protocols needed to label specific sites of the polymer, has seriously limited the utility of these end-to-end cyclization experiments.

Fortunately, there are several ways to overcome these difficulties allowing for dynamic information to be retrieved from fluorescence quenching experiments. To simplify the synthetic protocol, a dye capable of forming an excimer can be used, whereby an excimer is formed between the excited and ground-state version of a same dye.[27,28] This removes the synthetic complexity of preparing two separate labeling protocols, one for the dye and another for the quencher, as an excimer-forming fluorophore requires only one protocol to fluorescently label a macromolecule.[28] For this purpose, pyrene is often chosen for its many excellent photophysical properties, which are described in the following section. In this case, $[Q]_{loc}$ needs to be replaced with $[Py]_{loc}$ in all mathematical derivations.

Pyrene possesses a long fluorescence lifetime capable of probing slow dynamic events[27,28,36] and a strongly reduced $S_{0,0} \rightarrow S_{1,0}$ transition[37,38] which removes the possibility of energy transfer between an excited and ground state pyrene as they diffuse toward each other to

form an excimer. This reduced $S_{0,0} \rightarrow S_{1,0}$ transition is best seen in Figure 1.4 showing the absorption and emission spectrum of a pyrene-labeled poly(mono(ethylene glycol) methyl ether methacrylate) with a pyrene content of 7.5 mol%. The first emission peak of pyrene at 378 nm corresponds to the $S_{1,0} \rightarrow S_{0,0}$ transition, and thus should have a corresponding peak in the absorption spectrum for the $S_{0,0} \rightarrow S_{1,0}$ transition. This peak is so strongly diminished that it is almost unnoticeable in Figure 1.4. The first truly visible peak in the absorbance spectrum at 344 nm represents the $S_{0,0} \rightarrow S_{2,0}$ transition. Also visible in Figure 1.4 is the broad, structureless emission of the pyrene excimer,[28,29,31] centered around 480 nm, well removed from the peaks of the pyrene monomer.

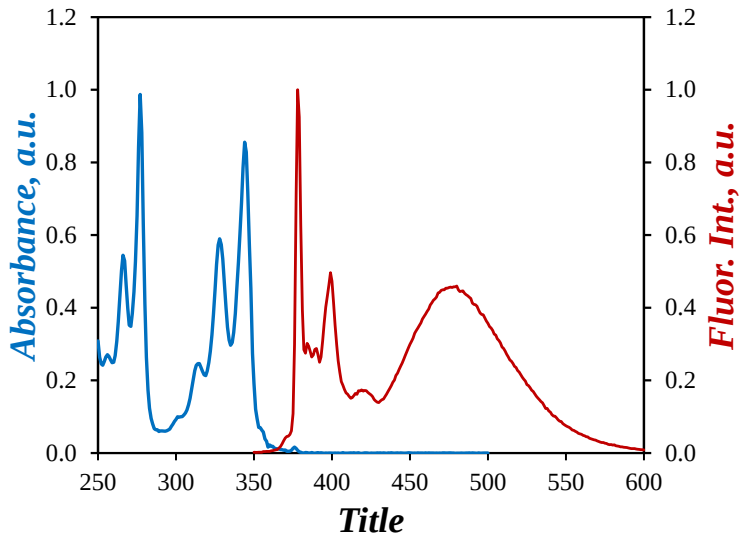

Figure 1.4. Excitation ( ) and emission ( ) spectrum of pyrene-labeled poly(mono(ethylene glycol) methyl ether methacrylate) with a pyrene content of 7.5 mol% dissolved in THF. Absorbance spectrum: [Py] = 20 μM corresponding to a [Poly] = 43 mg/L. Emission spectrum: λ_{ex} = 344 nm, [Py] = 2.3 μM corresponding to a [Poly] = 4.9 mg/L.

The scheme describing the formation of excimer between pyrene labels covalently attached to a polymer is shown in Figure 1.5. Excimer formation occurs when a pyrene moiety is excited by a photon of light ($h\nu_A$) to generate (Py_{diff}*). Slow diffusive motion of the polymer chain is described by the rate constant k_{diff}, which brings Py_{diff}* close to a ground-state pyrene, whereby Py_{diff}* becomes the excited pyrene species Py_{k2}*. Py_{k2}* and the ground-state pyrene can then undergo a rapid rearrangement with a rate constant k_2 to form an excimer (*E0**). This rapid rearrangement occurs on a faster timescale than for the diffusive motions of the backbone.[28] Depicted on the right side of Figure 1.5 is the formation of excimer by the direct excitation of pyrene aggregates. While the use of pyrene as both the dye and quencher reduces the number of reactions for labeling a macromolecule from two to one, a substantial advantage, it addresses neither the lack of encounters between the ends of a long chain nor the lack of information retrieved about the chain interior when only the chain ends are labeled.

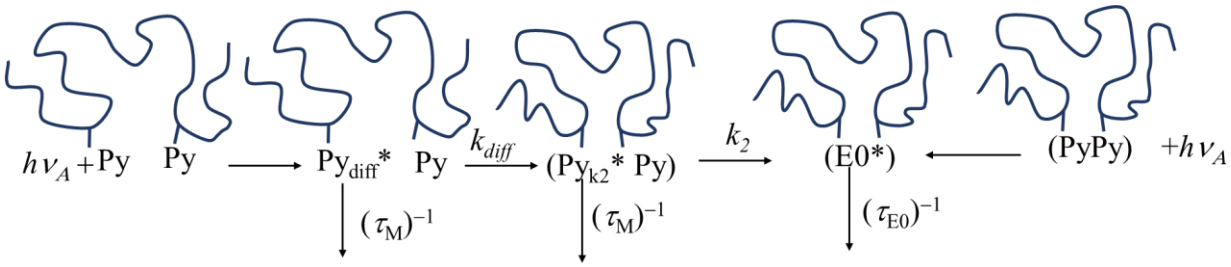

Figure 1.5. Kinetic scheme for pyrene excimer formation. The species Py_{diff}* and Py_{k2}* both emit as pyrene monomer with a lifetime of τ_M, while the excimer emits with a lifetime τ_{E0}.

The obvious solution to counter this problem is to increase the number of pyrene labels across the polymer. Pyrene can be introduced randomly by labeling reactive sites along the polymer backbone ("labeling onto") or through the incorporation of small amounts of pyrene-labeled monomer during the polymerization ("labeling through").[28,39,40] Labeling multiple sites throughout the macromolecule with pyrene increases the amount of excimer formed though it also

introduces an infinite distribution of k_Q values associated with each contour length separating every pair of excited and ground state pyrene.[28] A mathematical means for circumventing this complication was to take advantage of the fact that pyrene excimer formation (PEF) can only take place within the subvolume of the polymer coil being probed by an excited pyrene. This feature has been taken advantage of to derive two global analysis models, namely the fluorescence blob model (FBM)[41] and the model free analysis (MFA).[42]

1.3 GLOBAL ANALYSIS MODELS

1.3.1 Fluorescence Blob Model:

The fluorescence blob model (FBM) was developed in 1999 to analyze the fluorescence decays of macromolecules randomly labeled with pyrene.[41] Using a mathematical derivation that is conceptually similar to that handling the kinetics of excimer formation between pyrenes inside surfactant micelles,[43] the macromolecule is divided into imaginary volumes called *blob*s as depicted in Figure 1.6. Since an excited pyrene remains excited for a finite time, during which its mobility is strongly hindered since it is bound to the macromolecule, it can only probe a finite volume (V_{blob}).[41] The compartmentalization of the polymer coil into a cluster of *blobs* has two main effects. First, the introduction of multiple pyrene labels increases the statistical likelihood of encounters between an excited and ground state pyrene allowing polymers with much larger DP to be studied than what could be done previously with only end-labeled chains.[32] The second advantage is that the compartmentalization of the polymer chain into *blobs* enables the FBM to handle a broad MWD since the focus of the study shifts from the entire chain to a single *blob* whether dealing with a long chain with many *blobs* or a shorter chain with fewer *blobs*.[41]

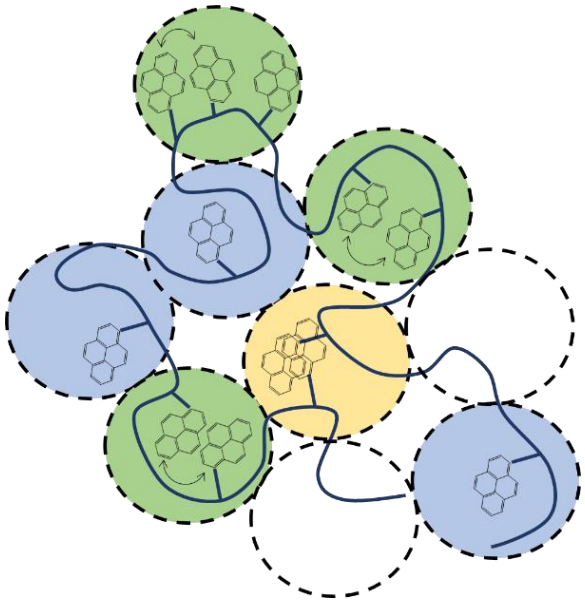

Figure 1.6. Depiction of the FBM with pyrenyl labels that are (blue) isolated and emit as a monomer or can form excimer by (green) diffusive encounters between an excited and a ground-state pyrene or (yellow) direct excitation of aggregated pyrenes. *Blob*s without pyrene (white) are also shown. The pyrene moieties are distributed among the *blobs* according to a Poisson distribution.[28,41,43]

The FBM analysis yields the parameters k_{blob} and $\langle n \rangle$ which represent the rate constant for diffusive encounters between two SUs bearing one excited and one ground state pyrenes located inside a *blob* and the average number of pyrenes inside a *blob*, respectively.[28,41] k_{blob}, is a pseudo-bimolecular rate constant equal to the product $k_{diff} \times (1/V_{blob})$ where $1/V_{blob}$ is the concentration equivalent to one ground-state pyrene in a *blob*.[44] $\langle n \rangle$ is used to determine the number N_{blob} of SUs encompassed inside a *blob* using Equation 1.1. Its purpose is to normalize $\langle n \rangle$ with respect to the pyrene content of the polymer, given by the molar fraction x_{Py} of SUs bearing a pyrenyl label, and the molar fraction f_{Mfree} for those pyrenyl labels located in *blobs* containing only one excited pyrene, which cannot form excimer and are solely detected in the pyrene monomer decay.

N_{blob}, has been found to increase with increasing flexibility of the polymer backbone,[28,45] making N_{blob} a useful structural parameter to quantify the ability of a polymer chain to bend.

$$N_{blob} = \frac{1 - f_{Mfree}}{x_{Py}} < n > \quad (1.1)$$

The product $k_{blob} \times N_{blob}$ reflects the frequency of encounters between SUs, Ω_{SU}.[32,44,45] As with N_{blob}, $k_{blob} \times N_{blob}$ has been found to decrease with decreasing flexibility of the polymer chain.[40] While effective for polymers randomly labeled with pyrene, the FBM fails for polymers where the pyrene labeling is conducted at more than 2 specific positions on the macromolecule, such as with dendrimers where pyrene has been attached to the chain ends.[46] The model free analysis (MFA) was introduced for these types of macromolecules.

1.3.2: Model Free Analysis:

The MFA was developed in 2005[42] and makes no assumptions about the polymer structure or labeling scheme. The MFA merely acknowledges that the fluorescence decay of the pyrene monomer and excimer can be described as a sum of exponentials with linked decay times (τ_i) and pre-exponential factors (a_i).[46] The MFA of the fluorescence decays yields the average rate constant of excimer formation ($<k>$) as described by Equation 1.2,[28,42,46] where $<\tau>$ is the number average lifetime ($<\tau> = \Sigma a_i \tau_i / \Sigma a_i$, where a_i and τ_i are retrieved from the fluorescence decay analysis of the pyrene monomer) and τ_M is the natural lifetime of the pyrene monomer.

$$< k >= \frac{1}{< \tau >} - \frac{1}{\tau_M} \tag{1.2}$$

All experimental evidence gathered to date suggests that <*k*>, retrieved from the MFA of any pyrene-labeled macromolecule, equals the product $k_{diff} \times [Py]_{loc}$. Indeed, it has been shown that <*k*> retrieved by the MFA yields trends that are comparable to those obtained with the rate constants retrieved from the Birks Scheme or the FBM.[47] In particular, normalizing <*k*> according to Equation 1.3 yields $<k^{MF}>^{blob}$, which has been shown to be analogous to $k_{blob} \times N_{blob}$.[47] The MFA could thus be applied to characterize the dynamics of any pyrene-labeled macromolecule, making it a powerful tool in the characterization of macromolecules in solution.[47]

$$< k^{MF} >^{blob} = \frac{1 - f_{free}}{x} < k > \tag{1.5}$$

1.4 CALIBRATION CURVES FOR LRBD

Both the FBM and MFA have been used extensively by the Duhamel group to probe the LRBD of many types of macromolecules in multiple solvents.[32,39,40,48–50] However, due to solubility difference between various macromolecules, and a lack of a polymer soluble in many common solvents, that would act as a true benchmark, the parameters describing the internal dynamics of macromolecules retrieved from one study cannot be directly compared to those of another study. To this end, calibration curves should be generated with a same family of macromolecules, where

a single molecular parameter is modified, such as the length of the alkyl side chains in the series of poly(*n*-alky methacrylate)s, that were randomly labeled with pyrene (Py-PAMAs) as shown in Figure 1.7.[40] Lengthening the alkyl side chain of the PAMA samples generates steric repulsion around the polymethacrylate backbone, which leads to its extension and rigidification to a degree that depends specifically on the alkyl side chain length.

In the case of the Py-PAMA samples, lengthening the alkyl side chains from 1 to 18 carbons led to a decrease in the LRBD of the polymethacrylate backbone of the polymers as illustrated in Figure 1.8 with the parameters $k_{blob}\times N_{blob}$ and $<k^{MF}>^{blob}$ which were obtained from fitting the fluorescence decays according to the FBM and MFA, respectively.[40] $k_{blob}\times N_{blob}$ and $<k^{MF}>^{blob}$ decreased continuously with increasing side chain length reflecting the stiffening of the main chain as the side chain length was increased from 1 to 12 carbons, plateauing for side chains larger than 12 carbons, corresponding to a molecular weight for a repeating unit (MW_{RU}) like dodecyl methacrylate equal to 254 g/mol.[40] The plateau region implies that the side-chains have induced the complete extension of the main chain, when they are longer than 12 carbons. Another interesting point was the similarity of the $k_{blob}\times N_{blob}$ and $<k^{MF}>^{blob}$ values obtained from the analysis of the fluorescence decays acquired with the Py-PAMA samples in THF according to two different models. This equivalence suggested that despite their conceptual and mathematical differences, the MFA and FBM probe a same phenomenon, namely PEF between pyrenyl labels attached onto a same macromolecule, which reflects the LRBD of these Py-PAMA samples in THF.

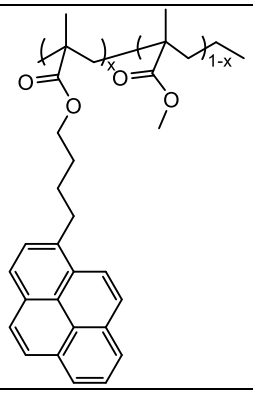	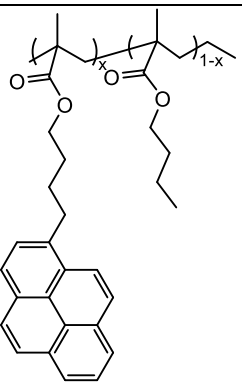	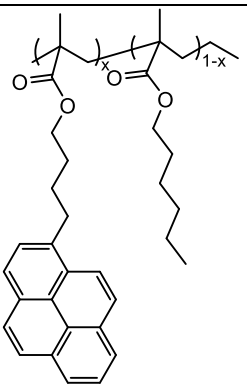
Poly(methyl methacrylate)	Poly(butyl methacrylate)	Poly(hexyl methacrylate)
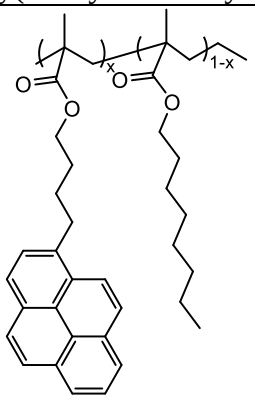	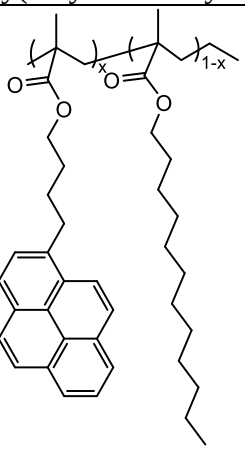	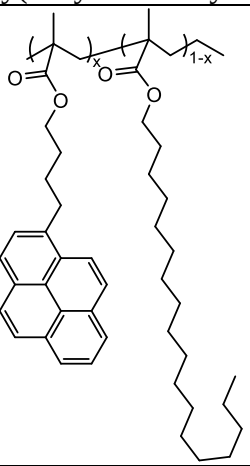
Poly(octyl methacrylate)	Poly(lauryl methacrylate)	Poly(stearyl methacrylate)

Figure 1.7. Chemical structure of the Py-PAMA samples used in the study described in Ref. #40

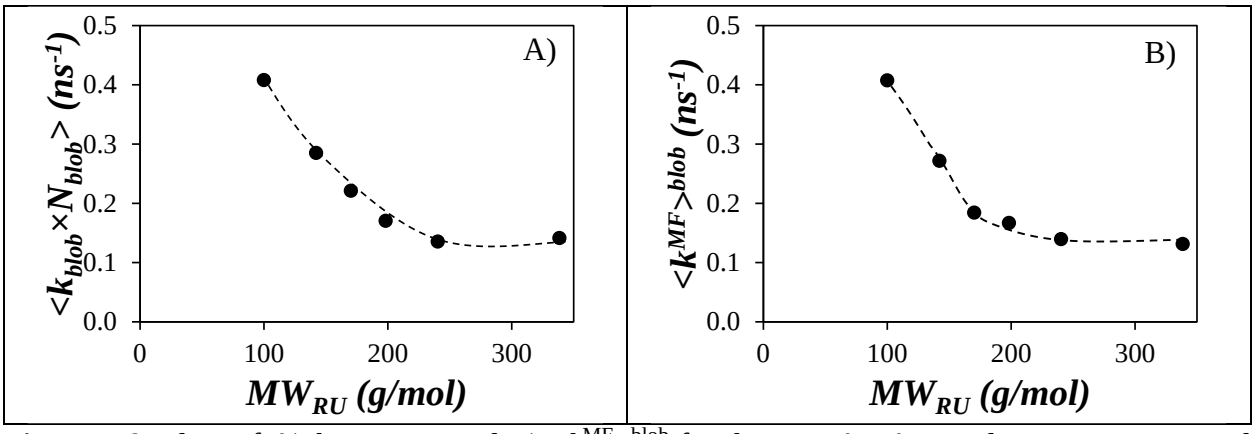

Figure 1.8. Plots of A) $k_{\text{blob}}\times N_{\text{blob}}$ and B) $<k^{\text{MF}}>^{\text{blob}}$ for the Py-PAMA samples in THF retrieved from the FBM and MFA, respectively. Adapted with permission from "Farhangi, S.; Weiss, H.; Duhamel, J. Effect of Side-Chain Length on the Polymer Chain Dynamics of Poly(Alkyl Methacrylate)s in Solution. *Macromolecules* **2013**, *46* (24), 9738–9747." copyright 2013 American Chemical Society and "Farhangi, S.; Casier, R.; Li, L.; Thoma, J. L.; Duhamel, J. Characterization of the Long-Range Internal Dynamics of Pyrene-Labeled Macromolecules by Pyrene Excimer Fluorescence. *Macromolecules* **2016**, *49*, 9597–9604." copyright 2016 American Chemical Society.

More interestingly, the trends obtained with $k_{\text{blob}}\times N_{\text{blob}}$ and $<k^{\text{MF}}>^{\text{blob}}$ as a function of MW_{RU} have been used as a calibration curve against which the LRBD of other polymers possessing different side chains[40] or backbones[40,48,49] can be compared. For instance, $k_{\text{blob}}\times N_{\text{blob}}$ or $<k^{\text{MF}}>^{\text{blob}}$ were plotted in Figure 1.9B for the polymers, whose chemical structure is presented in Figure 1.9A, along with the trend obtained for the Py-PAMA benchmark. The comparison of $k_{\text{blob}}\times N_{\text{blob}}$ or $<k^{\text{MF}}>^{\text{blob}}$ obtained for the polymers in Figure 1.9A against the same parameters obtained for the Py-PAMA benchmark led to the conclusion that increasing the steric hindrance of the side chain by changing the side chain from *n*-butyl or *n*-hexyl to *t*-butyl or *cyclo*-hexyl diminishes Ω_{SU} as reported by $k_{\text{blob}}\times N_{\text{blob}}$. Likewise, the greater flexibility of poly(methyl acrylate) or

poly(dimethyl siloxane) results in an increase in Ω_{SU}, while the rigid maleic anhydride groups in the alternating co-polymer poly(isobutylene-*alt*-maleic anhydride) yield a significant decrease of Ω_{SU}.

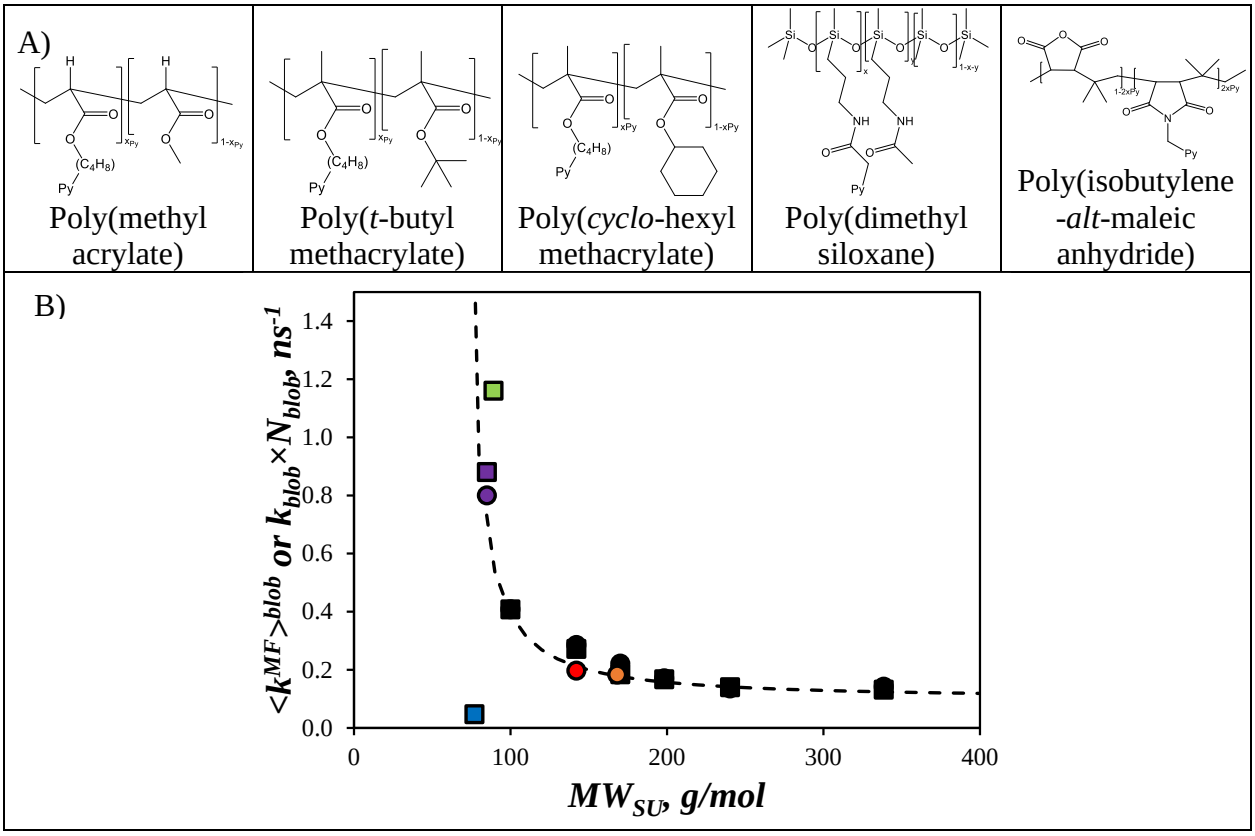

Figure 1.9. (A) Chemical structure of several pyrene-labeled polymers, whose Ω_{SU} was compared to that of the Py-PAMA benchmark. (B) plot of the encounter frequency described by (circles) $k_{blob}\times N_{blob}$ or (squares) $<k^{MF}>^{blob}$ for the (●■) poly(*n*-alkyl methacrylate)s,[40,51] (●■) poly(methyl acrylate),[40,51] (●) poly(*t*-butyl methacrylate),[40] (●) poly(cyclo-hexyl methacrylate),[40] (■) poly(dimethyl siloxane),[49] and (■) poly(isobutylene-*alt*-maleic anhydride).[48] Equation used to describe trendline previously reported in Reference #49 as $< k^{MF} >^{blob} = 0.1 + 21.5\left(MW_{SU} - 65\right)^{-1.21}$.

While the trends obtained for the Py-PAMA benchmark can be used as a calibration curve against which the LRBD of other polymers, such as those described in Figure 1.9A, could be compared, these polymers were all soluble in THF, the same solvent used to dissolve the Py-PAMA samples. Since the Py-PAMA samples were hardly soluble in organic solvents more polar than THF, the limited solubility of the Py-PAMA samples represented an important limitation for the trends obtained in Figure 1.8, since they could only be applied to other polymers, that were also soluble in THF. Unfortunately, many polar polymers such as polyacrylamides,[52] polysaccharides,[53] or polypeptides[54] require a more polar solvent such as DMSO or DMF to dissolve.[53,54] While the parameters describing the LRBD of these polymers have been determined in various solvents,[39,50] they cannot be easily compared to those obtained with the Py-PAMA samples, since these samples are mostly insoluble in polar solvents. This is regrettable as the characterization of the LRBD of these polymers would be of great interest to better understand how and on which time scale they deform in solution. For instance, the ability of polyacrylamides to act as flocculants in water treatment depends on their spring like behavior to connect and bring together solid particulate dispersed in the medium;[55,56] polysaccharides are often modified in solution where their accessibility to reagents is governed by their flexibility;[57–59] and the folding of polypeptides into three-dimensional structures to make enzymes, which are necessary for life, depends on their specific flexibility.[60]

Although these applications are important to many branches of chemistry, understanding the dynamics of these polymers cannot be done in isolation. A more universal calibration curve would allow researchers to compare different families of polymers under the same conditions to a known benchmark. To address this situation, more calibration curves should be generated using pyrene-labeled polymers soluble in polar solvents and their fluorescent decays characterized with

both the FBM and MFA. This would provide an experimental means to compare the LRBD of polymers prepared with different side and main chains to each other in solution by fluorescence.

1.6 THESIS OUTLINE

The primary goal of this project was to probe the LRBD of polymers in solvents of various polarities and viscosities to prepare calibration curves against which the parameters describing the LRBD of other polymers could be compared. Chapter 1 summarized background material on polymer dynamics, fluorescence quenching, and the calibration curve describing the LRBD of the Py-PAMA samples in THF. In Chapter 2, a series of 41 Py-PEG$_n$MAs were prepared and characterized, their fluorescence decays were acquired and analyzed using the FBM to retrieve the parameters N_{blob} and $k_{blob}\times N_{blob}$, which were plotted as a function of MW_{SU} in different solvents. The N_{blob}- and $k_{blob}\times N_{blob}$-*vs*-MW_{SU} trends were parametrized in terms of the MW_{SU} and solvent viscosity resulting in equations from which the N_{blob} and $k_{blob}\times N_{blob}$ could be predicted for any MW_{SU} and solvent viscosity. Furthermore, application of the Kratky-Porod equation to N_{blob} yielded the persistence length, while the equations obtained to parametrize $k_{blob}\times N_{blob}$ were used to generate calibration curves in different solvents against which the LRBD of other polymers could be compared. The fluorescence decays acquired for the same 41 polymers were analyzed according to the MFA in Chapter 3. The parameters retrieved from the MFA were found to match those obtained with the FBM in Chapter 3 demonstrating that both models probe PEF in the same manner, even though their mathematical derivation and analytical solutions are different. In particular, the parameter $<k^{MF}>^{blob}$ retrieved from the MFA equaled the product $k_{blob}\times N_{blob}$ obtained from the FBM and could be used in the same manner to build calibration curves to

compare the LRBD of polymers in different solvents. Finally, Chapter 4 summarizes the results presented in this thesis and outlines potential avenues for future investigations.

CHAPTER 2

BENCHMARKING LONG RANGE BACKBONE DYNAMICS WITH PYRENE-LABELED POLY(OLIGO(ETHYLENE GLYCOL) METHYL ETHER)S

2.0 SUMMARY

Following a study where the fluorescence response of a series of poly(alkyl methacrylate)s labeled with the dye pyrene (Py-PAMA) could be used as a calibration curve to characterize the long range backbone dynamics (LRBD) of other polymers, a series of pyrene-labeled poly(oligo(ethylene glycol) methyl ether methacrylate)s (Py-PEG_nMAs) of varying side-chain length was prepared by random radical copolymerization of 1-pyrenebutyl methacrylate and nine different EG_nMA monomers with *n* ranging from 0 to 19. Compared to the Py-PAMA samples, which did not dissolve well in organic solvents more polar than tetrahydrofuran (THF), the higher polarity of the side chains of the Py-PEG_nMA samples enabled their study in 4 solvents covering a broad polarity range, namely toluene, THF, *N*,*N*-dimethylformamide (DMF), and dimethylsulfoxide (DMSO). Analysis of the fluorescence decays of all Py-PEG_nMA samples acquired in the four solvents according to the fluorescence *blob* model (FBM) yielded the number N_{blob} of structural units (SUs) in the volume, referred to as a *blob*, probed by an excited pyrene and the rate constant k_{blob} for excimer formation between an excited and a ground-state pyrenyl label located inside a same *blob*. N_{blob} and k_{blob} remained constant within experimental error as a function of pyrene content for Py-PEG_nMA samples having a same EG_n side chain. After averaging over all pyrene contents for a same Py-PEG_nMA series, $<N_{blob}>$ and the product $<k_{blob} \times N_{blob}>$ were found to decrease with increasing side chain length reflecting a progressive decrease in the polymethacrylate backbone LRBD. $<N_{blob}>$ and $<k_{blob} \times N_{blob}>$ could be parametrized as a function of the molecular weight of an SU and the solvent viscosity. The parametrized form of $<N_{blob}>$ was applied to determine the persistence length of the PEG_nMA samples while the parametrized form of $<k_{blob} \times N_{blob}>$ was used as a calibration curve against which the LRBD of polypeptides and poly(methyl methacrylate) (PMMA) could be compared in DMSO.

2.1 INTRODUCTION

The mechanical properties of any polymeric material can be characterized by how much and how quickly the polymeric material can deform after application of a stress, since it is well established that the extent of deformation of a plastic depends on the time scale over which the deformation is being applied.[1–3] In turn, these properties experienced at the macroscopic level by the polymeric material are a reflection of the behavior of the polymer chains constituting the polymeric material at the molecular level.[2,3] These properties are represented by the ability of a chain to bend, described by its persistence length (l_p), and the frequency at which bending occurs, which can be defined as the frequency at which the structural units (SUs) of a chain segment encounter per unit time (Ω_{SU}), a measure of the long range backbone dynamics (LRBD) of the polymer. Traditionally, l_p has been determined by scattering techniques, which typically require polymer samples prepared with a narrow molecular weight distribution,[4–7] or conformation plots generated by gel chromatography (GPC),[8–10] which can handle polydisperse polymers but require careful calibration of the GPC instrument. A measure of Ω_{SU} can be obtained from the glass transition temperature (T_g)[2,3] or correlation times (τ_C)[11] of the polymer determined from a tensile test experiment for a solid polymer sample or ^{1}H NMR for a polymer solution, respectively.

Recent developments in the analysis of fluorescence decays acquired with solutions of polymers randomly labeled with pyrene have established that the product $k_{blob}\times N_{blob}$ also provides an accurate representation of Ω_{SU}.[12–14] The fluorescence decay analysis is based on the fluorescence blob model (FBM),[14,15] which recognizes that an excited pyrenyl label can only probe a limited volume called a *blob* within the polymer coil. N_{blob} represents the number of structural units constituting a *blob* and the rate constant describing the diffusive encounters between two

structural units bearing one excited and one ground state pyrene inside a same *blob* is given by k_{blob}.[14,15] N_{blob} and k_{blob} were determined in an earlier study for a series of pyrene-labeled poly(alkyl methacrylate)s (Py-PAMA) in tetrahydrofuran (THF), where the alkyl side chains were constituted of 1 to 18 carbons for poly(methyl methacrylate) to poly(stearyl methacrylate), respectively.[12] Both N_{blob} and the product $k_{blob}\times N_{blob}$ decreased with increasing molar mass of a structural unit (MW_{SU}), reflecting a decrease in the backbone flexibility and Ω_{SU} as the chain became more extended with increasing side chain length.[12,16] The product $k_{blob}\times N_{blob}$ was found to faithfully reflect Ω_{SU}, decreasing with increasing side chain stiffness or side chain length or increasing from poly(methyl methacrylate) to poly(methyl acrylate).[12]

While this preliminary study was informative, it suffered from two main limitations. First, the Py-PAMA samples did not dissolve in solvents that were more polar than THF, thus preventing the characterization of important families of polar polymers such as polypeptides or polysaccharides. Second, the decrease in N_{blob} with increasing side chain length was most likely related to the l_p of the polymer. Unfortunately, application of the Kratky-Porod equation[17] to the polymer segment encompassed inside a *blob* to determine l_p from N_{blob} required the average squared end-to-end distance ($\langle r_{EE}^2\rangle_{blob}$) of that polymer segment.[18,19] In turn, $\langle r_{EE}^2\rangle_{blob}$ could have been determined with a fully extended polymethacrylate chain, but longer side chains than that of the poly(stearyl methacrylate) used in the Py-PAMA study would have been needed to achieve the full extension of the main polymethacrylate chain.[18,19]

To address these limitations, the fluorescence of 9 pyrene-labeled poly(oligo(ethylene glycol) methyl ether methacrylate)s (Py-PEG$_n$MA with n = 0, 1, 2, 3, 4, 5, 9, 16, and 19) were characterized in the present study. Since the EG$_n$ side chain of the PEG$_n$MA samples were much more polar than the alkyl side chains of the PAMA samples, plots of $k_{blob}\times N_{blob}$ as a function of

MW_{SU} could be obtained in a broad range of solvents that included more viscous and polar solvents like DMF and DMSO. Furthermore, the much longer side chains of Py-PEG_{16}MA and Py-PEG_{19}-MA ensured that the N_{blob}-*vs*-MW_{SU} plots showed a continuous decrease with increasing MW_{SU} in all four solvents, reaching a plateau with an N_{blob} value of 12 (±2) for the Py-PEG_nMA series with n equal to 16 and 19, corresponding to the maximum chain extension. These trends reflected the stiffening of the PEG_nMA sample that occurred with increasing side chain length with the PEG_nMA chains becoming fully extended in solution for the two longer EG_n side chains. After parametrizing the N_{blob}-*vs*-MW_{SU} and $k_{blob}\times N_{blob}$-*vs*-MW_{SU} trends as a function of MW_{SU} and η, these trends were used, respectively, to determine the l_p of the PEG_nMA samples and as a calibration curve against which Ω_{SU} of other polymers could be compared. Consequently, this study establishes the use of PEF between pyrenyl labels covalently attached onto a polymer as a new means to characterize the two main physical characteristics of any polymer in solution, namely l_p and Ω_{SU} through N_{blob} and $k_{blob}\times N_{blob}$, respectively.

2.2 EXPERIMENTAL

2.2.1 Chemicals:

1-Pyrenebutanol, methacrylic anhydride, 4-(dimethylamino)pyridine (DMAP), 2,2'-azobisbutyrontrile (AIBN), dicyclohexylcarbodiimide (DCC), oligo(ethylene glycol) methyl ether methacrylate (EG_nMA with n equal to 1, 2, and 3), tetra and penta(ethylene glycol) methyl ether (EG_n with n = 4 and 5), EG_9MA with a number average molecular weight (M_n) of 500 g/mol, EG_{16} with an M_n of 750 g/mol, HPLC grade dimethyl formamide (DMF), dimethylsulfoxide (DMSO), diethyl ether, ethyl acetate, and dichloromethane (DCM) were purchased from Sigma Aldrich. Inhibitor-free THF that had been distilled into glass was supplied by Fisher Scientific. Toluene

that had been distilled into glass was purchased from Caledon. Nitrogen gas was provided by Praxair. AIBN was recrystallized from ethanol and DCM was distilled before use. All other reagents were used as received. The Py-PEG$_0$MA and Py-PEG$_{19}$MA samples were prepared by Drs. Shiva Farhangi and Janine Thoma, respectively.[12,18]

2.2.2 Methacrylation of 1-pyrenebutanol, EG$_4$, EG$_5$, and EG$_{16}$:

1-Pyrenebutyl methacrylate (PyBMA) and the EG$_n$MA samples with n = 4, 5, and 16 were prepared in the same manner. The procedure is described in detail for the synthesis of PyBMA, which was conducted according to the reaction scheme shown in Figure 2.1.

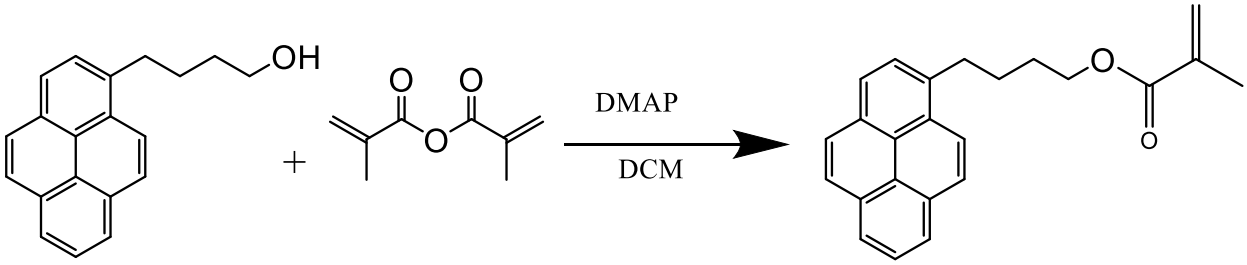

Figure 2.1. Reaction scheme for the methacrylation of 1-pyrenebutanol

Freshly distilled dichloromethane (DCM, 25 mL) was placed in a 50 mL round-bottom flask (RBF) equipped with a magnetic stir bar was chilled in an ice-water bath and placed under a nitrogen atmosphere. 1-Pyrenebutanol (0.5 g, 1.8 mmol, 1.0 molar equivalent (meq)) and DMAP (0.045 g, 0.3 mmol, 0.16 meq) were dissolved in the cold DCM with stirring. The 50 mL RBF was then sealed with a rubber septum and the contents of the flask were allowed to mix under the inert atmosphere for fifteen minutes before 0.43 mL (2.8 mmol, 1.5 meq) of methacrylic anhydride was introduced to the flask dropwise using a 1 mL syringe. The flask was covered with aluminum foil to prevent the photo-degradation of pyrene and the mixture was left to react overnight.

The next day, the flask was unsealed, and the reaction mixture was washed three times with a solution of 1 M sodium hydroxide before being dried over anhydrous sodium sulphate. The DCM was decanted and evaporated under a stream of nitrogen. The reaction product was further purified by column chromatography with DCM as the eluent and it was obtained in 71% yield. The purity of the final product was confirmed by both ^{1}H NMR and time-resolved fluorescence (TRF). The ^{1}H NMR spectrum of the purified PyBMA monomer is shown in Figure S2.1 in the supporting information (SI) and the integration of the assigned peak matched the expected chemical composition of PyBMA. For the fluorescence measurement, a 2.5×10^{-6} M solution of the PyBMA monomer in THF was prepared and its TRF decay was acquired. The decay was fitted with a biexponential function whose 210 ns long-lived component contributed > 90 % of the total pre-exponential weight. Since it corresponded to the expected lifetime (τ_M) of PyBMA, the monomer was deemed sufficiently pure to prepare the Py-PEG$_n$MA samples.

The only difference between the syntheses of the PyBMA and EG$_n$MA (n = 4,5) monomers was the use of ethyl acetate as eluent during the last purification step by column chromatography. The purity of the final products was confirmed by NMR. The ^{1}H NMR spectrum of EG$_5$MA is shown in Figure S2.2 as an example. The final yields were 5.5 g (74%) and 4.5 g (65%) for OEG$_4$MA and OEG$_5$MA, respectively.

The EG$_{16}$MA monomer was found to stick to the silica gel of the column, which prevented it from eluting. EG$_{16}$MA was purified by 3 washes with a 1 M aqueous solution of sodium hydroxide and one wash with saturated sodium chloride. The sample was dried over anhydrous sodium sulphate before being collected by rotary evaporation. This washing was completed twice and afforded 5.3 g of the product in a 75% yield.

2.2.3 Synthesis of Py(x)PEG$_n$MA:

The poly(oligo(ethylene glycol) methyl ether methacrylate)s, where a molar percentage x of structural units bore a pyrenyl label (Py(x)-PEGnMA) were prepared according to the reaction scheme shown in Figure 2.2. The synthesis of Py-PEG1MA is described in detail hereafter. The stabilizer present in the EG1MA monomer was removed by conducting three extractions from the monomer dissolved in DCM with a 1 M aqueous solution of NaOH. The organic phase was dried over anhydrous sodium sulphate and the OEG1MA monomer was recovered by evaporating the DCM under a gentle stream of air.

The copolymerization was carried out in a Schlenk tube, which was dried overnight in a 100 °C oven. OEG_1MA (0.5 g, 3.5 mmol, 1 meq) was dissolved in 1.5 mL of distilled in glass THF and the solution was placed in the dried tube, followed by the addition of 1.5 mL of THF with PyBMA (2.4 mg, 0.17 mmol, 0.05 meq). The Schlenk tube was then placed in an ice bath and 0.3 mL of a THF solution of AIBN (19 mg, 0.12 mmol) was added. To prepare copolymers with different pyrene contents, the ratio of PyBMA-to-EG_nMA was varied while the initiator concentration remained constant for each polymerization.

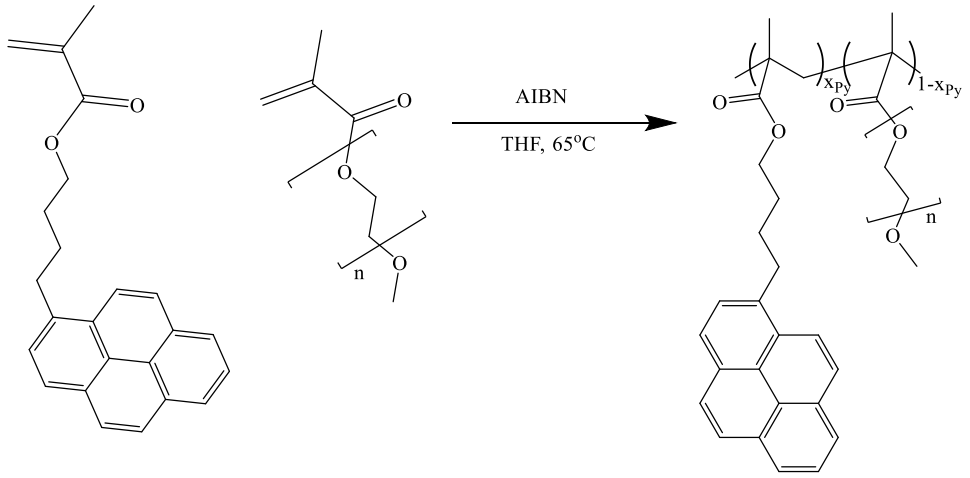

Figure 2.2. Reaction scheme for the preparation of Py-PEG_nMAs

Following the initiator addition, the Schlenk tube was partially sealed and degassed by bubbling a gentle stream of nitrogen through the solution for 30 minutes. The tube was then fully sealed and transferred to an oil bath held at 65 ℃. The extent of polymerization was monitored by ^{1}H NMR and stopped at a conversion of less than 20% to minimize composition drift. Termination of the polymerization was executed by opening the Schlenk tube to the air. The polymer mixture was then precipitated into cold diethyl ether and collected by centrifugation. The pellet was re-dissolved in THF, reprecipitated into diethyl ether, and collected by centrifugation. This cycle was repeated 4-5 times to ensure that any unreacted monomer had been removed. The final polymer was isolated from the solvent and then dried under vacuum overnight before being stored in a −20 °C freezer.

2.2.4 Polymer Characterization:

The molecular weight of the Py-PEG$_n$MA samples was determined by gel permeation chromatography (GPC) using a TOSOH GPC-WS instrument equipped with two TSKgel Alpha-M 13 μm mixed bed columns, a refractive index and viscosity detectors, and in conjunction with a Wyatt DAWN HELEOS multiangle light-scattering detector. The instrument used DMSO as the eluent and was operated at 70 °C.

The pyrene content (λ_{Py}) expressed in μmol of pyrene per gram of polymer was obtained by determining the absorbance of a solution prepared by dissolving a known mass (m) of a Py-PEG$_n$MA sample in a given volume (V) of THF. The corresponding pyrene concentration [Py] of the solution was determined by applying Beer-Lambert law to the absorbance of the solution at 344 nm measured with a Cary 100 UV-Visible spectrophotometer and using the molar extinction

coefficient of 42,250 $M^{-1}\cdot cm^{-1}$ for 1-pyrenebutanol in THF at 344 nm.[20] λ_{Py} could then be calculated according to Equation 2.1.

$$\lambda_{Py} = [Py] \times V / m \tag{2.1}$$

λ_{Py} was then used to determine the molar fraction of pyrene-labeled repeating-units (x_{Py}) according to Equation 2.2, where M_o is the molar mass of the unlabeled repeating unit equal to 100, 144, 186, 232, 276, 320, 500, 805, and 950 g/mol for EG_nMA with n = 0, 1, 2, 3, 4, 5, 9, 16, and 19, respectively. M_{Py} is the molar mass of the pyrene-labeled repeating unit equal to 342 g/mol.

$$x_{Py} = \frac{M_o}{M_o - M_{Py} - \lambda_{Py}^{-1}} \tag{2.2}$$

2.2.5 Fluorescence Measurements:

All fluorescence experiments were conducted with Py-PEG_nMA solutions having an absorbance of 0.1 at 344 nm, corresponding to a pyrene concentration of 2.4×10^{-6} M, low enough to prevent intermolecular PEF. The Py-PEG_nMA solution was then introduced into a quartz degassing cell. Nitrogen gas (Praxair, 4.8-T, 99.998%) was bubbled through the solution for 30 minutes for solutions in THF and toluene, or 45 minutes for solutions in DMF and DMSO to remove dissolved oxygen, which is a quencher of pyrene.

Steady-state fluorescence (SSF) spectra were acquired with a HORIBA QM-400 spectrofluorometer equipped with a xenon arc-lamp as an excitation source. The monochromator

slits were set to 1 nm for all experiments. The solutions were excited at 344 nm and the fluorescence spectra were acquired from 350 to 600 nm using the front face geometry. The fluorescence intensity of the monomer (I_M) and excimer (I_E) were calculated by integrating the area under the spectrum from 377–381 nm and 500 to 530 nm for the monomer and excimer, respectively. The ratio I_E/I_M could then be used to quantify the PEF efficiency.

The TRF decays were acquired with an IBH Ltd. time-resolved fluorometer equipped with an IBH 340 nm NanoLED as an excitation source. Samples were excited at 344 nm while the monomer and excimer emission were measured as a function of time at 375 nm and 510 nm, respectively. Cut-off filters at 370 and 495 nm were placed between the sample and the emission monochromator to prevent scattered light from reaching the detector during acquisition of the fluorescence decays for the monomer and excimer, respectively. The fluorescence decays were obtained with the conventional right-angle geometry, accumulating 20,000 counts at the maximum of the monomer and excimer decays, and using a time-per-channel of either 2.04 or 1.02 ns/ch as required.

2.2.6 TRF Decay Analysis:

The TRF decays of the Py-PEG$_n$MA samples were analyzed globally according to the FBM. The FBM assumes that PEF occurs in a sequential fashion.[14,15] The motion of an excited pyrene Py_{diff}* in solution is controlled by the SU it is attached to and the rate constant k_{blob} describes the rate at which the SUs bearing pyrenyl labels encounter inside the polymer coil. Upon encounter of a structural units bearing Py_{diff}* with a structural unit bearing a ground-state pyrene, Py_{diff}* turns into the species Py_{k2}*, which rearranges rapidly with a rate constant k_2 to form an excimer $E0$* or D* constituted of two pyrenyl moieties that are either well or poorly stacked, respectively. Finally, pyrenyl species located in pyrene-poor domains of the Py-PEG$_n$MA sample cannot form excimer.

Since they emit as if they were free in solution, they are referred to as Py_{free}*. The species Py_{diff}*, Py_{k2}*, and Py_{free}* emit with the lifetime τ_M of the pyrene monomer while *E*0* and *D** emit with a lifetime τ_{E0} and τ_D, respectively. Beside k_{blob} and k_2, the FBM analysis of the fluorescence decays also yields the average number <*n*> of pyrenyl labels per *blob* and the product $k_e \times$[*blob*] equal to the product of the rate constant k_e describing the exchange of ground-state pyrenes among *blobs* and the local *blob* concentration inside the polymer coil.[14,15] The molar fractions f_{Mdiff}, f_{Mk2}, and f_{Mfree} describe the pyrene species Py_{diff}*, Py_{k2}*, and Py_{free}* detected in the monomer fluorescence decays, respectively, and the molar fractions f_{Ediff}, f_{Ek2}, f_{EE0}, and f_{EEL} represent the pyrenyl species Py_{diff}*, Py_{k2}*, *E*0*, and *D** detected in the excimer decays, respectively. The molar fractions specific to the monomer and excimer decays can be combined into the molar fractions f_{diff}, f_{k2}, f_{free}, and f_{E0}, and f_D representing the molar fractions of all pyrenyl species detected in solution, namely Py_{diff}*, Py_{k2}*, Py_{free}*, *E*0*, and *D**, respectively. The molar fractions f_{E0} and f_D are summed to yield f_{agg} (= f_{E0} + f_D), which represent the molar fraction of aggregated pyrenyl labels in solution. All monomer and excimer fluorescence decays for a series of Py-PEG$_n$MA of a given side-chain length in a same solvent were analyzed first according to the FBM using the *globmis90gbg* program where the value of k_2 was optimized in the analysis.[21,22] Once this was accomplished, the value of k_2 was averaged over all the Py-PEG$_n$MA samples of a given *n*-series to yield <k_2>. The same decays of the Py-PEG$_n$MA series were then re-fit using the program *globmis90bbg* using the value <k_2>, which was fixed in the analysis. A good fit was indicated by a χ^2 value smaller than 1.3 and a random distribution of the residuals and autocorrelation of the residuals around zero. The fluorescence decay analysis yielded all the parameters described above including <*n*>, which was used to calculate N_{blob} according to Equation 2.3.

$$N_{blob} = \frac{1 - f_{Mfree}}{x_{Py}} < n > \qquad (2.3)$$

2.3 RESULTS

2.3.1 Polymer characterization:

A series of Py-PEG$_n$MAs were prepared by radical copolymerization of PyBMA and oligo(ethylene glycol) methyl ether methacrylate (EG$_n$MA with n = 0, 1, 2, 3, 4, 5, 9, 16, and 19). PyBMA was selected in these experiments because the 4-atom butyl linker connecting pyrene to the methacrylate monomer is short enough to ensure that the motion of pyrene reflects polymer backbone motion.[23] The chemical structure of the Py-PEG$_n$MA samples synthesized for this study is provided in Table 2.1.

Table 2.1. Chemical structure of the Py-PEG$_n$MA samples.

Py-PEG$_0$MA	Py-PEG$_1$MA	Py-PEG$_2$MA	Py-PEG$_3$MA	Py-PEG$_4$MA
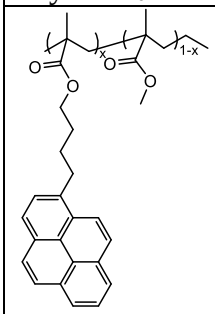	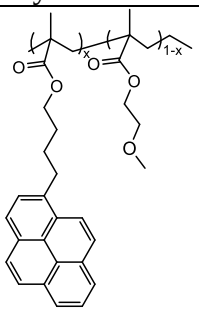	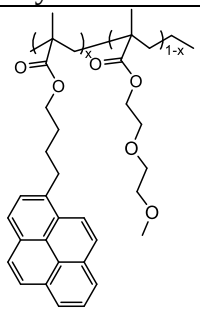	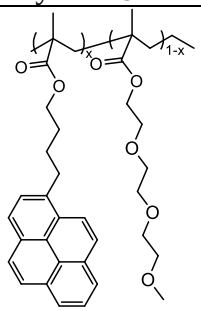	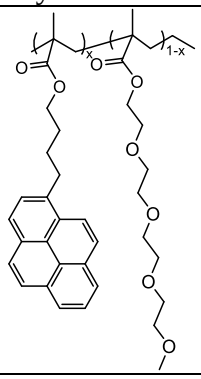
Py-PEG$_5$MA	**Py-PEG$_9$MA**	**Py-PEG$_{16}$MA**	**Py-PEG$_{19}$MA**	
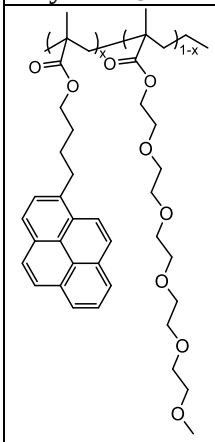	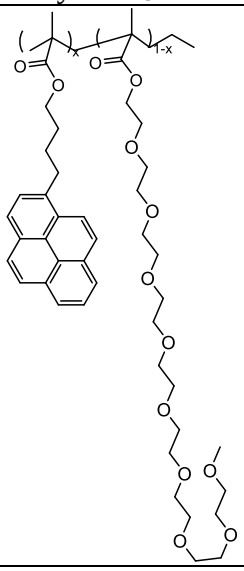	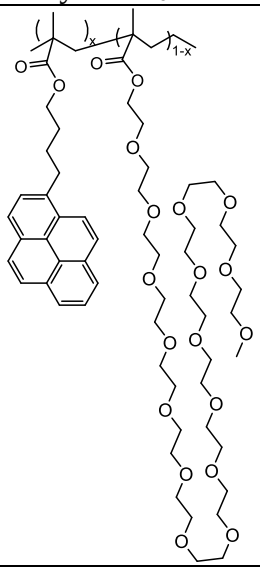	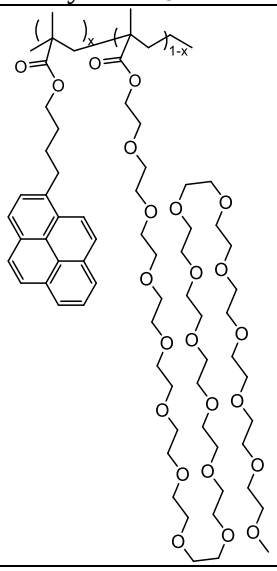	

These polymers were characterized by both GPC and UV-Visible spectroscopy to determine their number (M_n) and weight (M_w) average molecular weight, polydispersity ($Đ$), and pyrene content, which are listed in Table 2.2. The degree of polymerization of all samples was at least 4 times larger than N_{blob}, thus ensuring that a polymer coil could be represented by a large number of *blobs* enabling the application of the FBM. The number of atoms in the side chain (N_S) of the Py-PEG$_n$MA samples was calculated as $N_S = 3n + 3$. N_S accounted for the three non-hydrogen atoms that made up an ethylene glycol unit as well as the terminal methyl group and the two atoms of the ester bond connecting the side chain to the polymethacrylate backbone.

The SSF spectra of all Py-PEG$_n$MA samples were acquired in THF, toluene, DMF, and DMSO and are presented in Figures S2.3-S2.11. The spectra obtained for Py-PEG$_3$MA are presented in Figure 2.3, after being normalized at the first peak of the pyrene monomer corresponding to the 0-0 transition of pyrene. In a same solvent, the SSF spectra show a gradual increase in the amount of excimer formed with increasing fraction x_{Py} of pyrene-labeled SUs in the Py-PEG$_3$MA samples. This is reasonable since a larger x_{Py} results in more pyrene-pyrene encounters and higher PEF. Furthermore, the PEF efficiency decreases with increasing solvent viscosity, since PEF is a diffusion-controlled process. This effect is more easily visualized by plotting the I_E/I_M ratio as a function of pyrene content as shown in Figure 2.4A for Py-PEG$_3$MA as an example. I_E/I_M was found to increase linearly with increasing pyrene content and the slope ($m(I_E/I_M)$) of each I_E/I_M-*vs*-x_{Py} line in Figure 2.4A represented the PEF efficiency for a given Py-PEG$_n$MA series in a given solvent. The $m(I_E/I_M)$ slopes could then be plotted as a function of the molecular weight of a structural unit (MW_{SU}) in Figure 2.4B to assess the effect that solvent viscosity and side chain length have on the PEF efficiency. Increasing the side chain length of the PEG$_n$MA samples results in an extension of the main chain, which can no longer fold back onto itself. This process hinders PEF between two pyrenyl labels and reduces $m(I_E/I_M)$.

Table 2.2. Polymers used in this study

Py-PEG$_0$MA[a]			Py-PEG$_1$MA			Py-PEG$_2$MA		
N_s = 3			N_s = 6			N_s = 9		
Pyrene content (mol%)	M_n (g/mol)	$Đ$	Pyrene content (mol%)	M_n (g/mol)	$Đ$	Pyrene content (mol%)	M_n (g/mol)	$Đ$
0.3	134,000	1.7	0.1	445,000	1.7	0.3	147,000	1.5
4.0	135,000	1.6	3.1	509,000	1.4	3.4	433,00	1.5
5.2	206,000	1.7	3.5	482,000	1.3	5.1	166,00	1.4
5.3	101,000	2.1	3.8	600,000	1.4	6.1	149,00	1.2
5.6	170,000	1.6	5.3	621,000	1.2	6.9	286,00	1.3
7.3	176,000	1.8	7.5	686,000	1.2	-/-	-/-	-/-
Py-PEG$_3$MA			Py-PEG$_4$MA			Py-PEG$_5$MA		
N_s = 12			N_s = 15			N_s = 18		
Pyrene content (mol%)	M_n (g/mol)	$Đ$	Pyrene content (mol%)	M_n (g/mol)	$Đ$	Pyrene content (mol%)	M_n (g/mol)	$Đ$
1.2	974,000	1.3	0.8	575,000	1.3	1.0	164,000	1.4
4.6	233,000	1.4	2.4	451,000	1.4	4.7	206,000	1.6
6.3	870,000	2.1	5.4	894,000	1.4	6.1	172,000	1.4
8.3	356,000	1.5	6.5	193,000	1.8	6.2	588,000	1.5
9.2	334,000	1.2	7.3	220,000	1.7	6.6	554,000	1.4
12.3	345,000	1.6	-/-	-/-	-/-	-/-	-/-	-/-
Py-PEG$_9$MA			Py-PEG$_{16}$MA			Py-PEG$_{19}$MA[b]		
N_s = 30			N_s = 51			N_s = 60		
Pyrene content (mol%)	M_n (g/mol)	$Đ$	Pyrene content (mol%)	M_n (g/mol)	$Đ$	Pyrene content (mol%)	M_n (g/mol)	$Đ$
0.7	492000	1.8	1.3	34,800	1.4	1.0	69,200	1.1
5.8	97,900	1.4	4.5	40,300	1.3	7.4	62,300	1.4
6.8	493,000	1.3	6.3	37,500	1.5	7.6	96,700	1.3
7.2	245,000	1.3	8.8	112,000	1.9	10.2	148,000	1.3
9.3	240,000	1.4	11.2	107,000	1.3	12.4	64,200	1.5
10.9	194,000	1.4	-/-	-/-	-/-	14.7	66,800	1.1

a) Polymers prepared by Dr. Shiva Farhangi
b) Polymers prepared by Dr. Janine Thoma

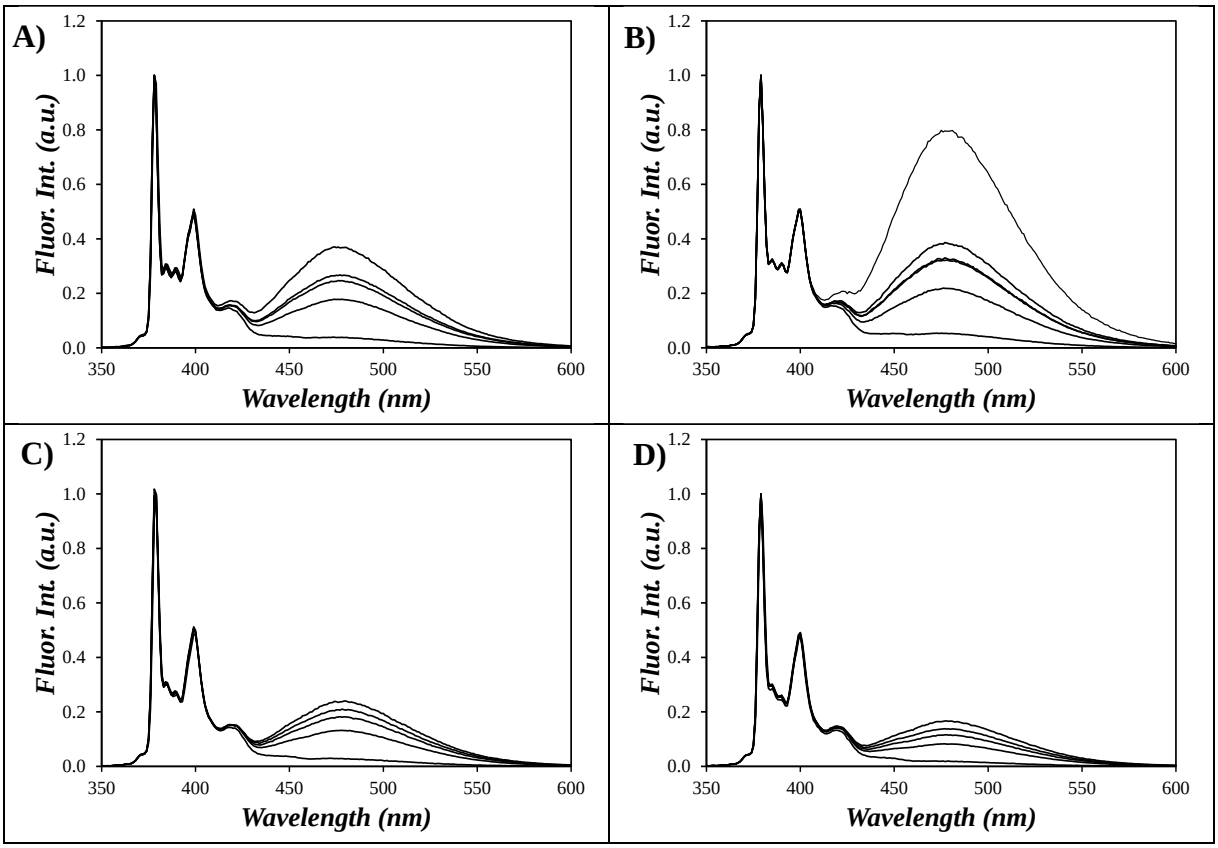

Figure 2.3. Steady-state fluorescence spectra of the Py(x)-PEG$_3$MA samples in (A) THF (η(25 °C) = 0.46 mPa·s), (B) toluene (η(25 °C) = 0.56 mPa·s), (C) DMF (η(25 °C) = 0.79 mPa·s), and (D) DMSO (η(25 °C) = 1.99 mPa·s). x_{Py} = 0.01 to 0.12.

For a same solvent, little change in $m(I_E/I_M)$ was observed in Figure 2.4B for MW_{SU} larger than 232 g/mol corresponding to a side chain with 3 EG units. For PEG$_n$MA samples with n > 3, the main chain seems to be fully extended as $m(I_E/I_M)$ remains constant. $m(I_E/I_M)$ decreases with increasing viscosity from THF (0.46 mPa·s) and toluene (0.56 mPa·s), which have similar solvent viscosities and thus yield similar $m(I_E/I_M)$, to DMF (0.79 mPa·s) and finally to DMSO (1.99 mPa·s), which was the most viscous solvent used in this study. This behaviour is expected since PEF for the Py-PEG$_n$MA samples in organic solvents is a diffusion-controlled process.

Consequently, the trends shown in Figure 2.4B suggest that PEF in the PEG$_n$MA samples is controlled by the side chain length and solvent viscosity.

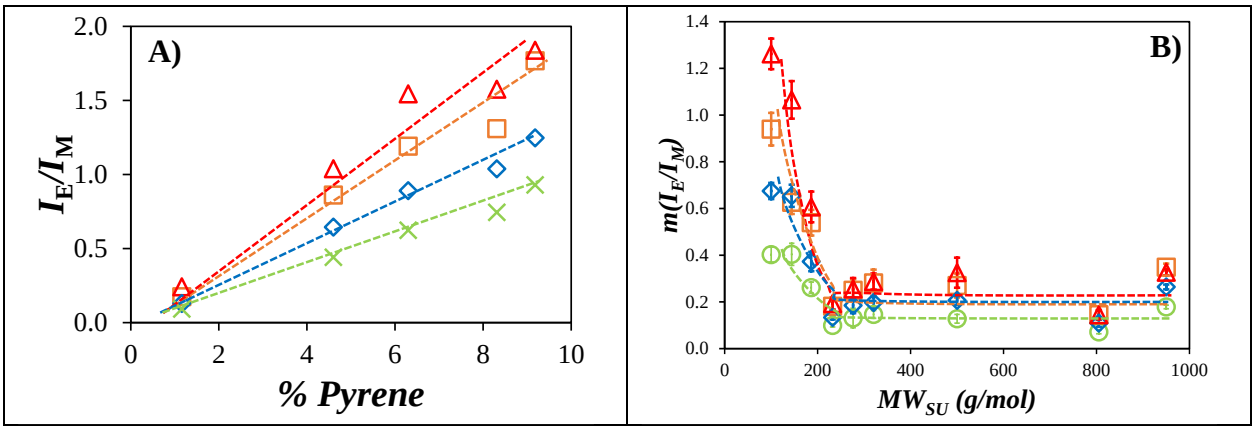

Figure 2.4. Plot of A) the I_E/I_M ratios obtained for Py-PEG$_3$MA as a function of pyrene content and B) the slopes of the I_E/I_M-*vs*-x_{Py} plots obtained for the different Py-PEG$_n$MA series as a function of MW_{SU} in (□) THF, (△) toluene, (◇) DMF, and (○) DMSO.

2.3.2 Fluorescence Blob Model:

One problem associated with the analysis of the SSF spectra is that the I_E/I_M ratio depends on the probability (p) of forming an excimer upon encounter between an excited and a ground-state pyrene.[12,14,24] Since p depends on the solvent properties, such as its polarity, the I_E/I_M ratio depends on both p and η so that the $m(I_E/I_M)$ slopes do not solely depend on η. This might be why the $m(I_E/I_M)$ values for toluene were larger than those for THF, despite the viscosity of THF being smaller than that of toluene. These problems can be circumvented by applying the FBM analysis to the TRF decays acquired with the Py-PEG$_n$MA solutions, since the FBM separates the process of PEF described by the rate constant k_2 from the diffusive motion of the SUs, which is represented by the parameters N_{blob} and k_{blob}. Consequently, the fluorescence decays of the Py-PEG$_n$MA samples in THF, toluene, DMF, and DMSO were analyzed according to the FBM to yield k_{blob} and

N_{blob}, calculated according to Equation 2.3 and assess the effect of the solvent viscosity on N_{blob}, k_{blob}, and the product $k_{blob}\times N_{blob}$. Example fits of the fluorescence decays of the monomer and excimer are presented in Figure S2.12 for each of the four solvents.

As can be seen in Figures S2.13–14 in SI, k_{blob} and N_{blob} took similar values within experimental error for a same Py-PEG$_n$MA sample and organic solvent regardless of pyrene content. Consequently, k_{blob} and N_{blob} were averaged over all the pyrene contents of a given Py-PEG$_n$MA sample to yield $<k_{blob}>$ and $<N_{blob}>$, which were plotted as a function of MW_{SU} in Figures 2.5A and B, respectively. $<k_{blob}>$ did not change much with MW_{SU} and solvent viscosity, taking an average value of 8.1 (±1.3) μs^{-1}. By definition, k_{blob} equals the product $k_{diff}\times(1/V_{blob})$, where k_{diff} is the bimolecular rate constant for diffusive encounters between two SUs bearing a pyrenyl label inside a same *blob* and $1/V_{blob}$ represents the concentration equivalent to one ground-state pyrene inside a *blob*.[25,26] Since k_{diff} is inversely proportional to the solvent viscosity, the constancy of $<k_{blob}>$ implies that V_{blob} decreases with increasing solvent viscosity. This conclusion is reasonable since a more viscous solvent hinders the mobility of the backbone, which constrains an excited pyrenyl label to probe a smaller V_{blob}. The constancy of $<k_{blob}>$ as a function of MW_{SU} and solvent viscosity in Figure 2.5A also suggests that in a same organic solvent, all the Py-PEG$_n$MA share a same V_{blob}.

When plotted as a function of MW_{SU} in Figure 2.5A, $<N_{blob}>$ decreased with increasing side chain length in all solvents. This behavior matches that observed earlier with the Py-PAMA samples in THF and it reflects the extension of the polymethacrylate backbone resulting from enhanced steric hindrance between the side chains as their length increases. This trend is general and was also observed for the $<N_{blob}>$ values obtained with the Py-PAMA samples in THF, which overlapped nicely the $<N_{blob}>$ values obtained for the Py-PEG$_n$MA samples in THF in Figure S2.15

in SI. Contrary to the Py-PAMA study, where the longest side chain had an N_S of only 20 non-hydrogen atoms, the longer side chains used for Py-PEG$_{16}$MA and Py-PEG$_{19}$MA with, respectively, N_S equal to 51 and 60 clearly indicate that N_{blob} reaches a plateau reflecting a full extension of the polymethacrylate backbone for these longer side chains. At this point, $<N_{blob}>$ became independent of MW_{SU}. The two low viscosity solvents, namely THF and toluene, shared similarly large $<N_{blob}>$ values. As the viscosity of the solvent increased to 0.79 mPa.s for DMF and 1.99 mPa.s for DMSO, a pronounced decrease in $<N_{blob}>$ was observed in these two solvents. As was already discussed for $<k_{blob}>$ in Figure 2.5A, an increase in solvent viscosity led to a decrease in V_{blob} and thus N_{blob}, since N_{blob} is the number of SU's in V_{blob}.

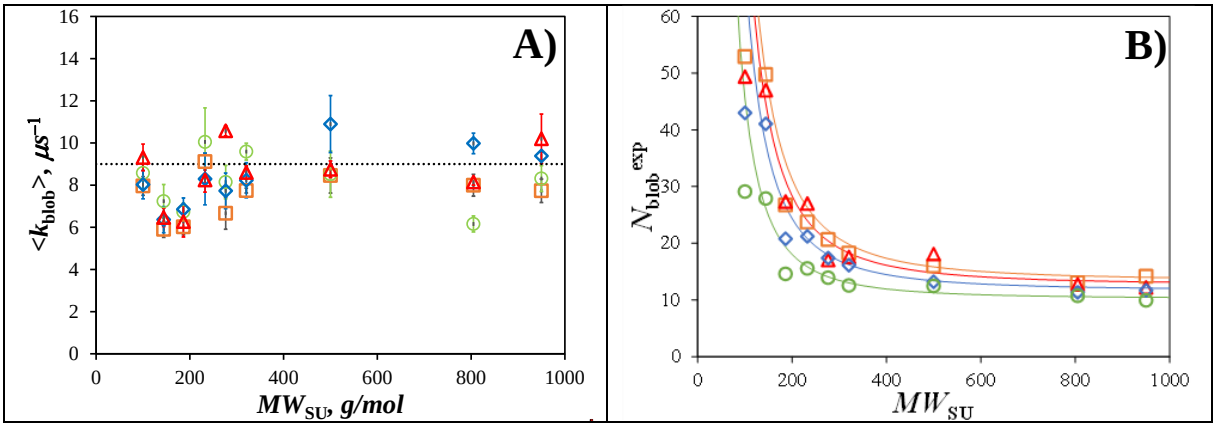

Figure 2.5. Plot of (A) $<k_{blob}>$, with the dashed horizontal line representing $<k_{blob}>$ averaged over all Py-PEG$_n$MA samples and organic solvents, and (B) $<N_{blob}>$ as a function of MW_{SU} with the lines representing the scaling law given in Equation 2.4. (□) THF, (△) toluene, (◇) DMF, and (○) DMSO.

The $<N_{blob}>$ values in the plateau region of Figure 2.5B took an average value of 12 (±2) for the Py-PEG$_{16}$MA and Py-PEG$_{19}$MA in all solvents. This indicated that upon full extension of the polymer main chain for larger side chains, the solvent became a weaker factor to define the

volume probed by an excited pyrene and a similar $<N_{blob}>$ value was obtained. That the $<N_{blob}>$ value of 12 (±2) obtained in the plateau region of Figure 2.5B would represent the N_{blob} value for a fully extended polymethacrylate backbone was supported by molecular mechanics optimizations (MMOs) carried out with HyperChem on an extended PMMA chain made of 80 methyl methacrylate monomers, which had been generated in an earlier publication.[27] A SU was selected along the backbone with the random number generator in MS Excel to randomly select a SU located at a position between the 10th and 70th SU of the PMMA construct. Although the PMMA chain was prepared with 80 methyl methacrylate units,[27] these boundaries were chosen during the random selection of a SU to ensure that the selected SU was sufficiently distant from the chain ends.[24] The methyl group of the selected methyl methacrylate unit was replaced by a 1-pyrenebutyl side chain and this pyrene-labeled SU was taken as reference and referred to as the zero-position (i = 0). A second methyl group was replaced by another 1-pyrenebutyl side chain on the adjacent monomer corresponding to the position i = 1. This pyrenyl label was viewed as the secondary pyrene. Allowing the 1-pyrenylbutyl side chains to move down to the carbonyl carbon but leaving the polymethacrylate backbone immobile, the planes of the two pyrenyl labels were induced to come within 0.34 nm of each other. The number of carbon atoms (n_C) from the reference pyrene overlapping the frame of the second pyrene were counted. Successful excimer formation was reflected by an n_C value larger than 7, corresponding to an overlap of 43% between the two pyrene labels, which has been reported as the minimum overlap necessary for PEF.[28] The secondary pyrene was then moved to the next adjacent monomer corresponding to position i = 2 along the polymethacrylate backbone, and the procedure was repeated to obtain n_C at this position. The secondary pyrene was moved along the polymethacrylate backbone one SU at a time and at each position i, n_C was determined. The process was repeated until three consecutive positions yielded

no overlap between the pyrenyl labels ($n_C = 0$). At this point, the pyrenyl labels were too far apart and could no longer overlap. The reference pyrene was then moved to another position that was selected randomly and its overlap with a secondary pyrene was monitored as a function of the position of the secondary pyrene with respect to the reference pyrene along the backbone. The results of these molecular mechanics optimizations are shown in Figure 2.6 for 4 different reference pyrenes. The maximum number N_o of SUs separating the reference and the secondary pyrene on one side of the reference pyrene was used to calculate the theoretical N_{blob} obtained by MMOs, N_{blob}^{MMO}, taken as $2N_o + 1$ to account for the symmetry of the backbone with respect to the reference pyrene and 1 was added to account for the reference pyrene. Based on the trends shown in Figure 2.7, N_{blob}^{MMO} was found to equal 12 (±1), which is in good agreement with the $<N_{blob}>$ value of 12 (±2) for Py-PEG$_{19}$MA in all solvents. Since N_{blob}^{MMO} was obtained for an extended polymethacrylate backbone, the agreement between N_{blob}^{MMO} and the experimental $<N_{blob}>$ suggests that the PEG$_{19}$MA backbone is extended in solution.

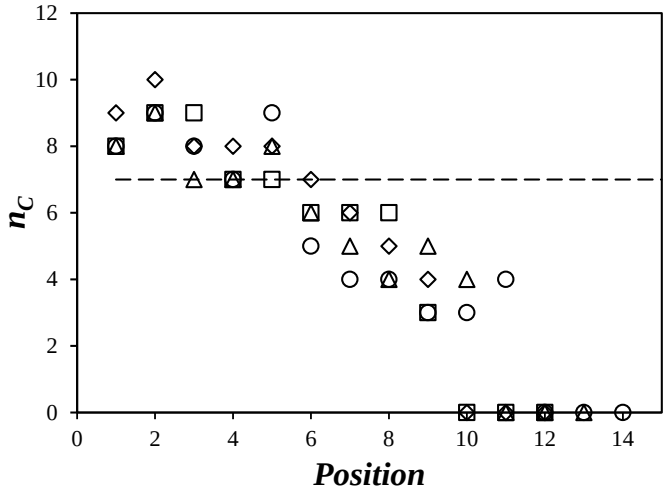

Figure 2.6. Plots of the number of overlapping carbons (n_C) as a function of the position of the secondary pyrene along the polymethacrylate backbone with respect to the reference pyrene. The dashed line represents the cut-off for $n_c = 7$ below which PEF is not expected to occur.

The products $\langle k_{blob} \times N_{blob} \rangle$ were calculated for the Py-PEG$_n$MA samples in the different solvents and were plotted as a function of MW_{SU} in Figure 2.7. The product $\langle k_{blob} \times N_{blob} \rangle$ has been found to provide a quantitative measure of the LRBD of a polymer in solution. All $\langle k_{blob} \times N_{blob} \rangle$-*vs*-$MW_{SU}$ trends in Figure 2.7 showed a same behavior, with $\langle k_{blob} \times N_{blob} \rangle$ decreasing with increasing MW_{SU} and reaching a plateau value in each solvent for the Py-PEG$_{16}$MA and Py-PEG$_{19}$MA samples with the longest side chains. An increase in MW_{SU} resulted in a dampening of the LRBD for the Py-PEG$_n$MA samples characterized in the present study. This behavior is reasonable as a larger MW_{SU} slows down the LRBD of a polymer chain with both effect resulting in more energy being required to move a SU. Interestingly, the $\langle k_{blob} \times N_{blob} \rangle$-*vs*-$MW_{SU}$ trends obtained in THF, toluene, and DMF were fairly clustered within experimental error and only that obtained in DMSO yielded significantly lower $\langle k_{blob} \times N_{blob} \rangle$ values. Since $\langle k_{blob} \times N_{blob} \rangle$ represents the frequency of SU encounters (Ω_{SU}), this result suggests that low viscosity solvents like THF, toluene, and DMF do not affect Ω_{SU} and that the LRBD in these solvents are controlled by the polymer and not the solvent, but that a viscosity threshold must be reached beyond which higher viscosity solvents like DMSO control Ω_{SU}.

2.4 DISCUSSION

2.4.1 Parametrization of $\langle N_{blob} \rangle$ and $\langle k_{blob} \times N_{blob} \rangle$ versus MW_{SU} trends:

The $\langle N_{blob} \rangle$-*vs*-MW_{SU} and $\langle N_{blob} \times k_{blob} \rangle$-*vs*-$MW_{SU}$ trends shown in Figures 2.5A and 2.7 suggest that $\langle N_{blob} \rangle$ and $\langle N_{blob} \times k_{blob} \rangle$ could be simple functions of MW_{SU} and η. If an empirical equation could be established, it would allow one to predict the value of $\langle N_{blob} \rangle$ *and* $\langle k_{blob} \times N_{blob} \rangle$ for a

Py-PEG$_n$MA samples of any n and in any organic solvent. A same mathematical procedure was applied to determine these functions and the process was applied to $<N_{blob}>$ first. The N_{blob} values obtained for PyBu-PEG$_0$MA (= PyBu-PMMA) corresponding to an MW_{SU} = 100 g/mol were excluded from this process as they were found to scale differently than the PyBu-PEG$_n$MA samples with $n > 0$.

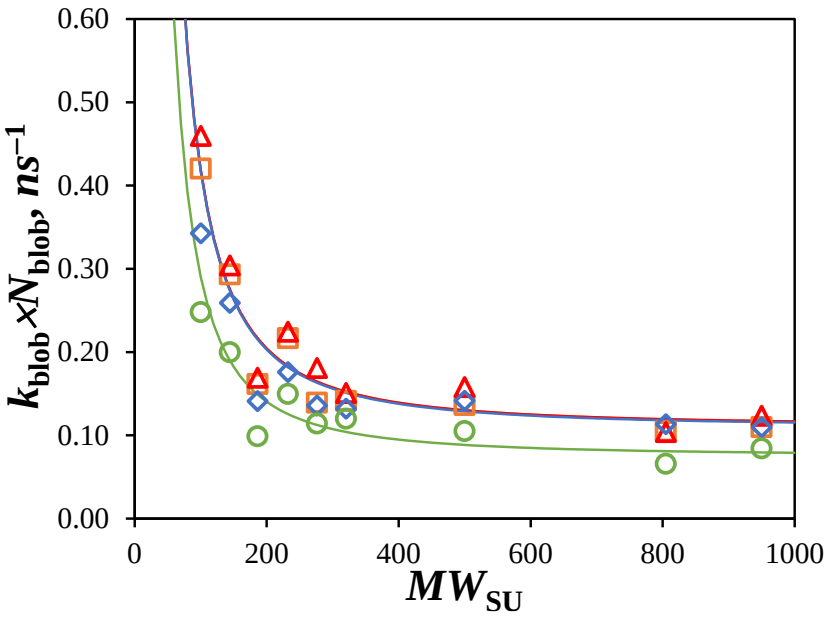

Figure 2.7. Plot of $<k_{blob} \times N_{blob}>$ as a function of MW_{SU} in (□) THF, (△) toluene, (◇) DMF, and (○) DMSO. Lines represent the scaling law given in Equation 2.11.

First, the dependency of N_{blob}^{∞}, representing the $<N_{blob}>$ values in the plateau region of Figure 2.5B, on the solvent viscosity was investigated. Plotting N_{blob}^{∞} as a function of η^{-1} in Figure 2.8A yielded a straight line with a small dependency on solvent viscosity, whose expression is given in Equation 2.4. Equation 2.4 represented the effect of solvent viscosity on N_{blob}^{∞} for a fully extended polymethacrylate chain. The larger $<N_{blob}>$ values obtained for the Py-PEG$_n$MA with

shorter side chains having n < 16 reflected increased bending of the Py-PEG$_n$MA chain. The bending of the chain was represented by the bending function $f_{b1}(MW_{SU},\eta)$, whose expression is given in Equation 2.5. $f_{b1}(MW_{SU},\eta)$ equaled unity at infinite MW_{SU} and η. Its expression was determined by finding the exponents a and b and the pre-factor c yielding the best agreement between $f_{b1}(MW_{SU},\eta) - 1 = \langle N_{blob}\rangle / N_{blob}^{\infty} - 1$ and the function $c \times MW_{SU}^{a} \times \eta^{b}$. The function $N_{blob}^{theo}(MW_{SU},\eta)$ that would best represent the $\langle N_{blob}\rangle$ values was then obtained by applying Equation 2.6. Plotting $\langle N_{blob}\rangle$ as a function of N_{blob}^{theo} yielded a cloud of data points that clustered around the diagonal indicating a good agreement between the two quantities and suggesting that Equation 2.6 could be applied to represent $\langle N_{blob}\rangle$ for any solvent viscosity and any Py-PEG$_n$MA sample with $n > 0$.

$$N_{blob}^{\infty}(\eta) = 9.243 + \frac{1.909}{\eta} \tag{2.4}$$

$$f_{b1}(MW_{SU},\eta) = 1.01 \times 10^{6} \times MW_{SU}^{-2.175} \times \eta^{-0.378} + 1 \tag{2.5}$$

$$N_{blob}^{theo}(MW_{SU},\eta) = N_{blob}^{\infty}(\eta) \times f_{b}(MW_{SU},\eta) \tag{2.6}$$

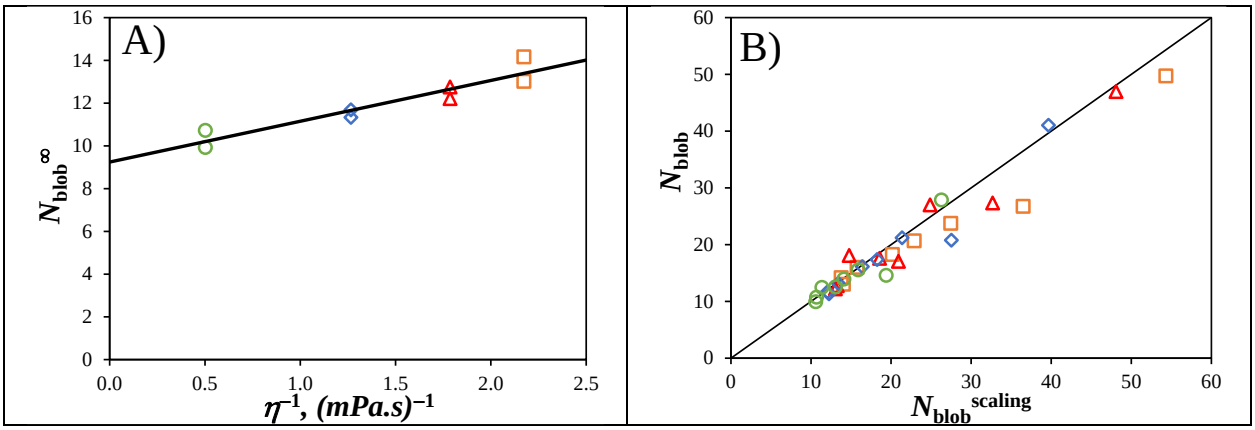

Figure 2.8. Plots for the PyBu-PEG$_n$MA samples with $n > 0$ of A) N_{blob}^{∞} as a function of η^{-1} and B) N_{blob} as a function of N_{blob}^{theo} with the black line indicating the diagonal. (□, η = 0.46 mPa.s) THF, (△, η = 0.56 mPa.s) toluene, (◇, η = 0.79 mPa.s) DMF, and (○, η = 1.99 mPa.s) DMSO.

A similar procedure was applied to find the expression of the function $(k_{blob}\times N_{blob})^{theo}$ expected to describe $\langle k_{blob}\times N_{blob}\rangle$ as a function of MW_{SU} and η. First, the behavior of the $\langle k_{blob}\times N_{blob}\rangle$ values obtained in the plateau region in Figure 2.7 for Py-PEG$_{16}$MA and Py-PEG$_{19}$MA could be well represented by Equation 2.9. Equation 2.9 captures the constancy of $\langle k_{blob}\times N_{blob}\rangle$ for solvent viscosity lower than that of DMF. The larger $\langle k_{blob}\times N_{blob}\rangle$ values obtained for the Py-PEG$_n$MA with $n < 16$ reflected the increased LRBD experienced by these samples. These increased dynamics were represented mathematically by the function $f_{b2}(MW_{SU},\eta)$, whose expression is given in Equation 2.10. As for f_{b1}, the function f_{b2} was determined by finding the exponents a and b and the pre-factor c yielding the best agreement between $f_{b2}(MW_{SU},\eta) - 1 = \langle k_{blob}\times N_{blob}\rangle/(k_{blob}\times N_{blob})^{\infty} - 1$ and the function $c\times MW_{SU}^{a}\times\eta^{b}$. Interestingly, the b exponent for the function f_{b2} was small and equal to –0.025 suggesting that f_{b2} depended little on solvent viscosity and was mainly defined by MW_{SU}. Finally the theoretical $(k_{blob}\times N_{blob})^{theo}$ function could simply be obtained by multiplying $(k_{blob}\times N_{blob})^{\infty}$ and $f_{b2}(MW_{SU},\eta)$ as shown in Equation 2.11.

Plotting $k_{blob}\times N_{blob}$ as a function of $(k_{blob}\times N_{blob})^{theo}$ in Figure 2.8B resulted in data points that clustered around the diagonal indicating that Equation 2.11 could satisfyingly describe the experimental $k_{blob}\times N_{blob}$ values as shown in Figure 2.7 where the solid lines pass through most of the data points.

$$(k_{blob}\times N_{blob})^{\infty} = 0.0522 + 0.0453/\eta \quad \text{if } \eta > 0.79 \text{ mPa.s} \qquad (2.9)$$

$$0.1108 \quad \text{if } \eta < 0.79 \text{ mPa.s}$$

$$f_{b2}(MW_{SU},\eta) = 7857\times MW_{SU}^{-1.72}\times\eta^{-0.025}+1 \qquad (2.10)$$

$$(k_{blob}\times N_{blob})^{theo}(MW_{SU},\eta) = (k_{blob}\times N_{blob})^{\infty}\times f_{b2}(MW_{SU},\eta) \qquad (2.11)$$

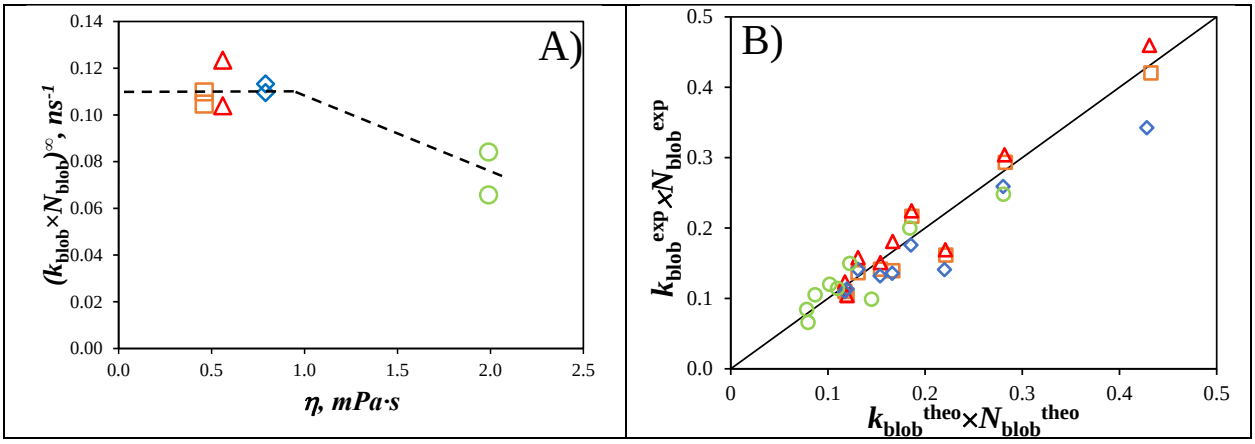

Figure 2.9. Plots for the PyBu-PEG$_n$MA samples of A) $(k_{blob}\times N_{blob})^{\infty}$ as a function of η and B) $k_{blob}\times N_{blob}$ as a function of $(k_{blob}\times N_{blob})^{theo}$ with the black line indicating the diagonal. (□, η = 0.46 mPa.s) THF, (△, η = 0.56 mPa.s) toluene, (◇, η = 0.79 mPa.s) DMF, and (○, η = 1.99 mPa.s) DMSO.

2.4.2 Persistence Length:

The $<N_{blob}>$-*vs*-MW_{SU} trends shown in Figure 2.5B indicate that $<N_{blob}>$ responds to the flexibility of the PEG$_n$MA backbone. Since the flexibility of a polymer chain is defined by its persistence length (l_p), the behavior uncovered in Figure 2.5B could indicate that$<N_{blob}>$ is related to l_p and that l_p could be determined from $<N_{blob}>$. For a monodisperse chain, l_p is determined by applying the Kratky-Porod equation,[17] which relates the average squared end-to-end distance ($<r_{EE}^2>$) of the chain to its contour length and l_p. However, the present FBM study does not characterize the entire chain of the Py-PEG$_n$MA samples, but rather the chain segment made of $<N_{blob}>$ SUs that is encompassed inside a *blob*. Consequently, the Kratky-Porod equation needs to be adjusted to describe the chain segment inside a *blob* as done in Equation 2.12.

$$< r_{EE}^2 >_{blob} = 2l_p(b \times < N_{blob} >) - 2l_p^2\left[1 - \exp\left(-\frac{b \times < N_{blob} >}{l_p}\right)\right] \qquad (2.12)$$

In Equation 2.12, $<r_{EE}^2>_{blob}$ is the average squared end-to-end distance of the polymer segment contained within a *blob* and *b* is the length of a methacrylate SU taken to be 0.25 nm, corresponding to an alkyl-chain in the *trans* conformation.[5,18,29] Since *b* and $<N_{blob}>$ are known, extracting l_p from Equation 2.12 requires determining $<r_{EE}^2>_{blob}$. $<r_{EE}^2>_{blob}$ was determined by using the fact that V_{blob} does not change much with MW_{SU} based on the constancy of $<k_{blob}>$ in Figure 2.5A. This result is a consequence of having all the Py-PEG$_n$MA samples labeled with the same 1-pyrenbutyl derivative, thus providing the same reach for a pyrenyl label, which probe a same volume V_{blob}. Since V_{blob} is the same for all the Py-PEG$_n$MA samples in a given solvent, $<r_{EE}^2>_{blob}$ will be constant for all the Py-PEG$_n$MA samples, including the Py-PEG$_{16}$MA and Py-

$PEG_{19}MA$ samples, which were found to be fully extended and for which $\langle r_{EE}^2 \rangle_{blob}$ simply equals $(N_{blob}^{\infty} \times b)^2$.

Having determined $\langle r_{EE}^2 \rangle_{blob}$, Equation 2.6 could be applied to calculate N_{blob}^{theo} for Py-PEG_nMA samples having any MW_{SU} and in solvents having any viscosity, and l_p could then be determined by solving Equation 2.7. The result of these calculations is shown in Figure 2.10, where l_p was determined for MW_{RU} values between 100 and 1,000 g/mol and plotting l_p as a function of N_s^2.[30] The l_p-*vs*-N_S^2 trends in Figure 2.10 indicate that l_p scales as N_S^2 for N_S values between 14 and 32. This scaling behavior matches theoretical expectations about the effect of the side chain length on l_p.[30] However, all the trends show a dependency on solvent viscosity. This outcome is not unreasonable since the l_p values in Figure 2.10 were obtained from data based on PEF, which is a diffusion-controlled process. Since a larger solvent viscosity reduces the PEF efficiency in Figures 2.4 and $\langle N_{blob} \rangle$ in Figure 2.5B, solvent viscosity has the same effect as MW_{SU}, namely a depression of $\langle N_{blob} \rangle$ and an increase in l_p at high viscosities. Since backbone flexibility and solvent viscosity combine to yield l_p values that depend on solvent viscosity in Figure 2.11, conditions should be identified where the effect of the solvent viscosity on the l_p-*vs*-N_S^2 trends is eliminated. Such conditions could be found by noting that the N_{blob}^{∞} value of 12 calculated from MMO simulations in Figure 2.6 was unaffected by solvent viscosity. Using $N_{blob}^{\infty} = 12$ in Equation 2.4 resulted in a solvent viscosity of 0.69 mPa·s. The l_p-*vs*-N_S^2 trend obtained with this viscosity is shown as the black line in Figure 2.10.

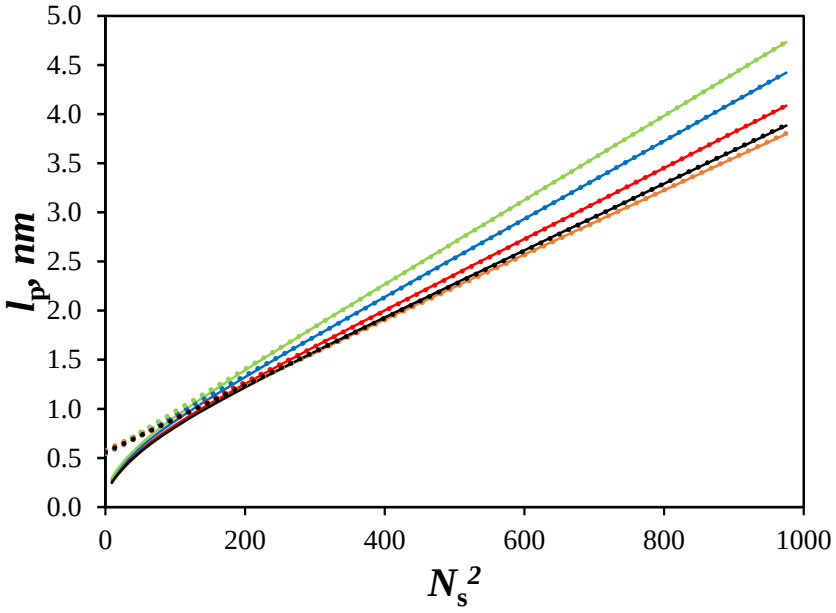

Figure 2.10. Plot of l_p as a function of N_S^2 for PyBu-PEG$_n$MA samples for solvent viscosities equal to ( ) 0.5 mPa.s, ( ) 0.69 mPa.s, ( ) 1.0 mPa.s, ( ) 1.5 mPa.s, and ( ) 2.0 mPa.s. Dashed lines represent the fit of the linear portion of the plot for N_S^2 values between 200 and 1,000 corresponding to N_S values between 14 and 32.

Though l_p deviated from linearity for short sidechains and small values of N_s^2 due to the failure to accurately describe the Py-PEG$_0$MAs, the linear section of the trend using an η = 0.69 mPa·s was used to derive Equation 2.13.

$$l_p = 0.557 + 3.42\times10^{-3}\times N_S^2 \qquad (2.13)$$

Equation 2.13 could be used to calculate the expected l_p of any polymer with a polymethylmethacrylate backbone with a side chain having N_S < 32. Using an N_s = 3, corresponding to PMMA, yielded l_p = 0.59 nm, which agrees with the l_p of 0.53 nm reported for

PMMA by Norisuye et al.[31] This good agreement found for the l_p of PMMA and the increase in l_p with N_S^2 found in Figure 2.10, that matches theoretical expectations,[30,32,33] suggests that the methodology developed in this study for determining l_p from $<N_{blob}>$ yields reasonable l_p values.

2.4.3 Calibration Curves:

One appealing feature of the $<k_{blob}\times N_{blob}>$-*vs*-$MW_{SU}$ trends shown in Figure 2.7 is that they can be used as calibration curves against which the Ω_{SU} of other polymers can be compared. Such a calibration curve was established in THF earlier for a series of PAMA.[12,34,35] Unfortunately, the PAMA samples were insoluble in organic solvents, that were more polar than THF, thus limiting its application to apolar polymers. As a result, the effect of solvent on the LRPD probed by PEF was never investigated with the PAMA samples. This is unfortunate since the present study establishes that solvent viscosity has a strong effect on the Ω_{SU} of the Py-PEG$_n$MA samples. Consequently, the Ω_{SU} of biomacromolecules like polypeptides and polysaccharides, which are only soluble in more polar, and also more viscous, solvents such as DMF or DMSO, could not be easily compared with those of the Py-PAMA samples in THF.

The $<k_{blob}\times N_{blob}>$-*vs*-$MW_{SU}$ trend obtained for the Py-PEG$_n$MA samples in DMSO was used in Figure 2.13 to compare the Ω_{SU} of several pyrene-labeled poly(glycine-*co*-D,L-glutamic acid) (PGlyGlu),[16] poly(D,L-alanine-*co*-D,L-glutamic acid) (PAlaGlu),[16] and poly(methyl acrylate)[36] in DMSO. The chemical structure of these polymers is shown below in Figure 2.11. Since the SU of these polymers contributed a number (N_{bb}) of two for PEG$_n$MA and PMA or three for PGlyGlu and PAlaGlu non-hydrogen backbone atoms to the polymer chain, their respective contribution was accounted for by multiplying $<k_{blob}\times N_{blob}>$ by N_{bb} and dividing MW_{SU} by N_{bb} in Figure 2.12.

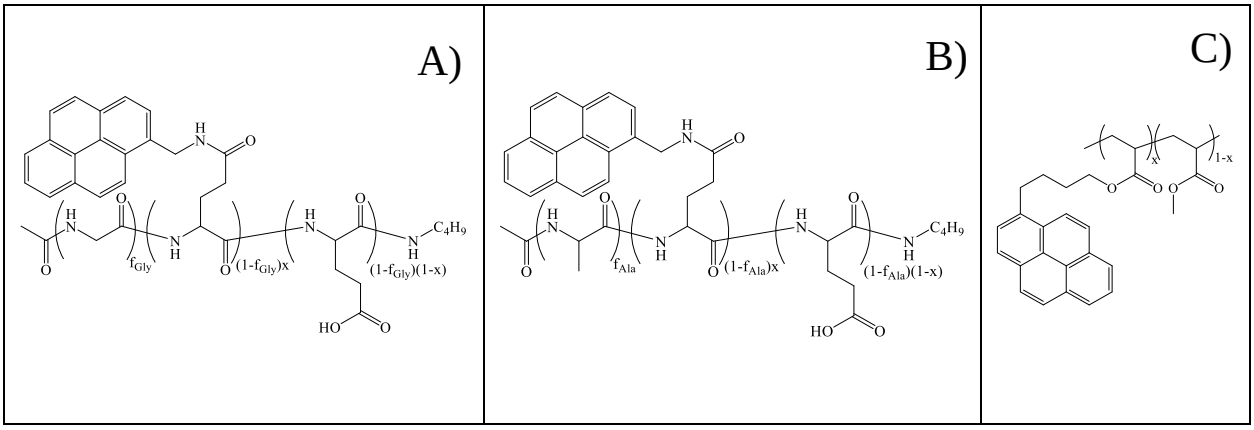

Figure 2.11. Chemical structure of pyrene-labeled (A) poly(glycine-*co*-glutamic acid) with f_{Gly} = 0.14, 0.40, and 0.54, (B) poly(alanine-*co*-glutamic acid) with f_{Ala} = 0.24, 0.41, and 0.58, prepared in Reference #16, and (C) poly(methyl acrylate) prepared in Reference #36.

Figure 2.12 nicely illustrates the effect of the chemical structure of different polymers on Ω_{SU}. Five out of the six polypeptides described in Figure 2.11 have $\langle k_{blob} \times N_{blob} \rangle \times N_{bb}$ values that range between those of PEG_0MA and PEG_1MA, but with a MW_{SU}/N_{bb}, that is 30-to-50 % smaller than that of the two polymethacrylate samples. Consequently, these polypeptides should exhibit faster LRBD than those observed experimentally. Instead, all the polypeptides, whose peptide bonds have a partially double bond character that reduces LRBD, yield smaller $\langle k_{blob} \times N_{blob} \rangle \times N_{bb}$ than the PEG_nMA samples of equivalent MW_{SU}. The mobility of the polypeptide backbone is thus more hindered than that of the polymethacrylate backbone. Similarly, PMA without its α–methyl substituent, and whose polyacrylate backbone is much less sterically hindered, and thus more dynamic, than the polymethacrylate backbone, yields a larger $\langle k_{blob} \times N_{blob} \rangle \times N_{bb}$ value. The effects observed for the PGlyGlu, PAlaGlu, PEG_nMA, and PMA samples are reasonable based on their chemical structure shown in Figure 2.11. Consequently, the $\langle k_{blob} \times N_{blob} \rangle \times N_{bb}$-*vs*-$MW_{SU}/N_{bb}$ trend

obtained with the PEG$_n$MA samples yields a calibration curve against which the Ω_{SU} of different polymers can be compared.

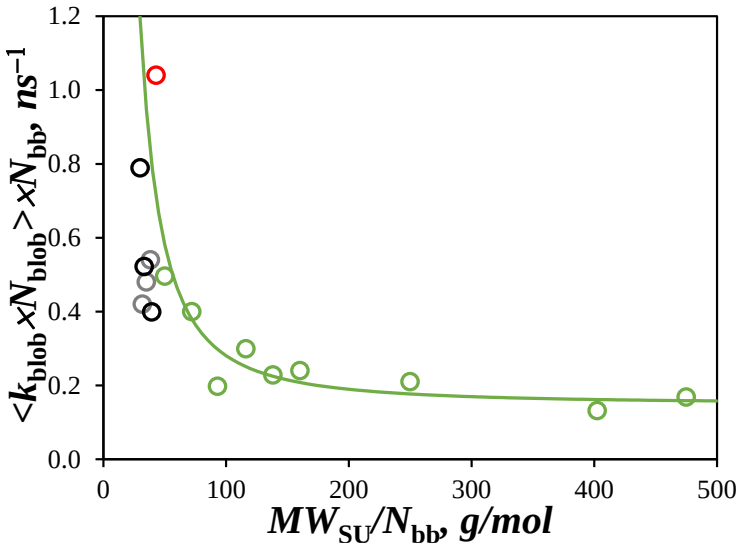

Figure 2.12. Comparison of $<k_{blob} \times N_{blob}> \times N_{bb}$ for samples of (O) Py-PEG$_n$MA, (O) Py-PMA, (O) Py-PGlyGlu, and (O) Py-PAlaGlu. Solid green line obtained with Equation 2.11.

2.4.4 Advantages and disadvantages:

Compared to scattering techniques, which can characterize a macromolecule without any chemical modification, the main disadvantage of the PEF-based methodology introduced in this report is that the macromolecules of interest must be fluorescently labeled, which implies some chemical workup. Fortunately, this complication is somewhat alleviated by the large number of pyrene derivatives that are commercially available with various functionalities, which usually enables the ready labeling of many macromolecules. A second disadvantage is the limited reach of the 1-pyrenebutyl labels, which probe a small *blob* with a diameter of about 3.0 nm (= $N_{blob}^{\infty} \times b$ with $N_{blob}^{\infty} \sim 12$ and $b = 0.25$ nm). Consequently, only fairly flexible backbones like that of PEG$_n$MA

can be probed by PEF since the backbone must show some curvature within 3.0 nm to determine its l_p. Stiffer polymeric backbones showing little curvature over 3.0 nm would appear fully extended on the length scale probed by pyrene. Larger *blobs* could be probed if a longer linker was selected to connect pyrene to the polymer backbone, but such studies remain to be conducted. Beside these important disadvantages, the methodology counts numerous advantages. First and foremost, the polydispersity of the macromolecule is irrelevant in a fluorescence decay analysis according to the FBM. Like any other *blob* model, the *blob* in the FBM becomes the focus of the study and a small or large macromolecule will be described by few or many identical *blobs* so that polydispersity becomes irrelevant. This feature was particularly useful for the characterization of the PEG_nMA samples, which are typically difficult to obtain in a monodisperse form,[37] a major disadvantage for the determination of their l_p through diffusion techniques, which are negatively affected by polydispersity. Second, the sensitivity of fluorescence in general and PEF in particular enables the study of pyrene-labeled macromolecules at concentrations lower than 5 mg/L, so dilute that macromolecular aggregation is minimized and individual macromolecules are being probed in solution. Third, the $<n>$ and k_{blob} parameters are absolute values from which $<N_{blob}>$ and $<k_{blob} \times N_{blob}>$ are determined. Consequently, a FBM analysis requires no calibration contrary to gel permeation chromatography from which conformation plots are generated to obtain l_p. While recognizing that the fluorescent labeling of a macromolecule represents a disadvantage, the three important advantages described above are expected to offset this disadvantage to make the PEF-based methodology appealing to characterize the flexibility and dynamics of polymers.

2.5 CONCLUSIONS

A methodology, which was based on PEF and the FBM analysis of fluorescence decays, was applied for the first time to determine both l_p and Ω_{SU} for polymers in solution. The study involved the preparation of a series of 9 Py-PEG$_n$MA samples with n ranging from 0 to 19. The EG$_n$ side chains ensured that the polymers would be soluble in organic solvents displaying a broad range of polarity and viscosity from toluene to DMF and DMSO and the use of EG$_{16}$ and EG$_{19}$ provided a means to generate fully extended polymethacrylate backbones in solution. These conditions enabled the application of the FBM to determine the parameters N_{blob} and $k_{blob}\times N_{blob}$ and assess how they would vary as a function of MW_{SU} and solvent viscosity. By extracting l_p from N_{blob} with the Kratky-Porod equation and using $k_{blob}\times N_{blob}$ as a measure of Ω_{SU}, the flexibility and LRBD of the PEG$_n$MA samples could be determined. Both l_p and Ω_{SU} are important parameters in the characterization of macromolecules. The PEF-based methodology introduced in this report to determine l_p and Ω_{SU} is general and could be further extended to other polymeric backbones.

CHAPTER 3

VALIDATING THE USE OF THE MODEL FREE ANALYSIS THOUGH COMPARISON WITH THE FLUORESCENCE BLOB MODEL

3.0 SUMMARY

The model free analysis (MFA) was applied to a series of 41 pyrene-labeled poly(oligo(ethylene glycol) methyl ether methacrylate)s (Py-PEG$_n$MA with n = 0, 1, 2, 3, 4, 5, 9, 16, and 19). Since these polymers were randomly labeled, their fluorescence decays had been shown to be well described by the fluorescence blob model (FBM). The FBM assumes that a macromolecule randomly labeled with pyrene can be viewed as a cluster of *blobs*, defined as the volume probed by an excited pyrene, among which the pyrenyl labels distribute themselves randomly according to a Poisson distribution. The most important FBM parameters are the average number $<n>$ of ground-state pyrenes inside a *blob*, the rate constant k_{blob} describing the diffusive encounters between two structural units (SU) bearing an excited and a ground-state pyrene inside a *blob*, and the number N_{blob} of SUs inside a *blob*. Since the MFA makes no assumption about the nature of the dye distribution in the macromolecule, the Py-PEG$_n$MA samples provided a valuable set of fluorescence decays, which were subject to the MFA and the FBM to gauge how the parameters retrieved from the MFA are related to those obtained with the FBM. Even though the equations used in the MFA and FBM take very different forms, a finite sum of 2-to-3 exponentials for the former and an infinite sum of exponentials for the latter, the average rate constant $<k>$ for pyrene excimer formation (PEF) between an excited and a ground-state pyrene determined by the MFA was found to match the product $k_{blob}\times<n>$, as theoretically predicted by the fundamental principles of the FBM and MFA. The normalized rate constant $<k^{MF}>^{blob}$ obtained through the re-arrangement of $<k>$ was found to equal the product $k_{blob}\times N_{blob}$, which is a direct measure of the frequency of encounters (Ω_{SU}) between SU. Consequently, $<k^{MF}>^{blob}$ could also be used to compare Ω_{SU} of different polymers with the Ω_{SU} of the Py-PEG$_n$MA samples used as a benchmark.

3.1 INTRODUCTION

Fluorescence dynamic quenching (FDQ) experiments conducted with a dye and a quencher covalently attached onto a macromolecule are routinely applied to characterize the long-range backbone dynamics (LRBD) of macromolecules.[1–4] As a quenching event marks an encounter between the two structural units of the macromolecule bearing the dye and quencher, a stiff macromolecule with slow LRBD generates fewer quenching events compared to a flexible macromolecule with fast LRBD. [5–7] Information about the LRBD of a fluorescently labeled macromolecule is obtained from FDQ experiments by retrieving the pseudo-unimolecular rate constant for FDQ taken as the product $k_{diff}\times[Q]_{loc}$, where k_{diff} is the bimolecular rate constant of diffusive encounters between dye and quencher and $[Q]_{loc}$ is the local concentration of quenchers covalently attached to the macromolecule.[8–10] While the product $k_{diff}\times[Q]_{loc}$ is obtained experimentally, the encounter frequency Ω_{SU} is better represented by the product $k_{diff}\times N$ with N being the number of polymer structural units (SUs) in the volume (V_{blob}) of the polymer coil, often referred to as a *blob*, probed by the excited dye.[11,12] The product $k_{diff}\times N$ reflects the encounter frequency between the N structural units, whereas $[Q]_{loc}$ describes the distribution of the quenchers within the macromolecule,[10,13] which in turn provides a measure of N equal to $[Q]_{loc}\times V_{blob}/x$, where x is the molar fraction of SUs labeled with a quencher. Consequently, drawing conclusions about the LRBD of a macromolecule from the product $k_{diff}\times[Q]_{loc}$ requires that $[Q]_{loc}$ be carefully considered. Furthermore, the nature of $[Q]_{loc}$ dictates the type of models that must be applied for the fluorescence decay analysis yielding the product $k_{diff}\times[Q]_{loc}$.[3,13–17] Because numerous FDQ experiments aiming to characterize LRBD are conducted with macromolecules that are labeled with the dye pyrene, due to its ability to form an excimer upon encounter between an excited and

a ground-state pyrene,[3,12,18] the following discussion focuses on pyrene-labeled macromolecules (PyLM). In this case, $[Q]_{loc}$ is replaced by the local pyrene concentration $[Py]_{loc}$.

By and large, the simplest macromolecular design for a FDQ experiment consists in labeling a macromolecule with a pyrene derivative at two specific positions, typically the chain ends of a monodisperse linear polymer.[1,2,19,20] Pyrene excimer formation (PEF) occurs via a single rate constant (k_{cy}) for end-to-end cyclization, as theoretically predicted for a monodisperse chain,[2,19,21,22] which is equal to $k_{diff}\times[Py]_{loc}$. In this case, $[Py]_{loc}$ equals $1/V_{coil}$ since there is one ground-state pyrene inside the polymer coil. V_{coil} scales as $N^{3\nu}$ with N being the total number of bonds separating the dye from the quencher, equal to the degree of polymerization (DP) times the number of backbone atoms per SU, and ν being the Flory exponent, which varies between 0.5 and 0.6 for a θ– and good solvent for the polymer, respectively.[2,19,23] A scaling relationship is obtained between k_{cy} and N, with k_{cy} scaling as $N^{-3\nu}$ and the scaling factor reflecting the LRBD.[2,3,23] The main disadvantage of pyrene end-labeled linear chains is that $[Py]_{loc}$ decreases very quickly with increasing DP to the point that no quenching event can be recorded.[1,2,11,19,23] Consequently, these experiments are limited to the study of oligomers with a DP smaller than 100.[23] The study of real polymers with a DP greater than 100 requires that the polymers be randomly labeled with pyrenyl groups and their decays fitted with the fluorescence *blob* model (FBM).[11,13] In this case, an excited pyrene probes a finite volume inside the polymer coil called a *blob* and this unit volume is used to compartmentalize the polymer into a cluster of *blobs* among which the pyrenyl labels are randomly distributed. The FBM yields the parameters N_{blob} and k_{blob}, where N_{blob} is the number of SUs in the polymer segment occupying a *blob* and k_{blob} equals the product $k_{diff}\times(1/V_{blob})$, where $(1/V_{blob})$ represents the concentration equivalent to one ground-state pyrene inside a *blob*.[13] The product

$k_{blob}\times N_{blob}$ provides information about the LRBD in the same manner as the product $k_{cy}\times N$ does for a pyrene end-labeled linear chain.[11,24]

While many macromolecules can be labeled randomly or at two specific positions (and two only), some cannot. Dendrimers are a case in point. The terminal ends of dendrimers are highly reactive and constitute ideal targets for the covalent attachment of a pyrenyl derivative. However, a pyrene end-labeled dendrimer represents an example where the pyrenyl labels are not randomly distributed throughout the macromolecule and are attached at more than two specific positions. It is for cases like these that the model free analysis (MFA) was introduced.[17,25] The MFA yields the average rate constant for PEF ($<k>$), which is assumed to equal the product $k_{diff}\times[Py]_{loc}$ regardless of the type of macromolecular architecture and pyrene-labeling scheme being considered.[17,25,26] The relationship between $<k>$ and $[Py]_{loc}$ has been observed to date for a series of eight dendrimers with a bis(hydroxymethyl)propionic acid backbone that were end-labeled with 1-pyrenebutyric acid[9,10] and it was employed to determine the conformation of the side chains of polymeric bottle brushes.[27]

In the present study, the validity of the equality between $<k>$ and $k_{diff}\times[Py]_{loc}$ is expanded by applying the MFA to a series of nine poly(oligo(ethylene glycol) methyl ether methacrylate)s randomly labeled with pyrene (Py-PEG$_n$MAs with n = 0, 1, 2, 3, 4, 5, 9, 16, and 19) in four different solvents, namely tetrahydrofuran (THF), toluene, *N*,*N*,-dimethylformamide (DMF), and dimethylsulfoxide (DMSO). The goal is to assess how $<k>$ obtained from the MFA, which makes no assumption about the distribution of pyrenyl labels in a PyLM, is related to the parameters k_{blob}, the average number $<n>$ of pyrenyl labels per *blob*, and N_{blob}, which were obtained earlier through the FBM analysis of their fluorescence decays. In particular, $<k>$ was modified to yield $<k^{MF}>^{blob}$, which was found to match very closely the product $<k_{blob}\times N_{blob}>$ within experimental error. The

agreement found between the trends obtained with the parameters retrieved through the MFA and FBM analysis of the fluorescence decays demonstrates that the equality between $<k>$ and $k_{diff}\times[Py]_{loc}$ also holds for the Py-PEG$_n$MA samples. It further confirms that $<k>$ obtained through the MFA of fluorescence decays acquired with PyLM is related to both their internal dynamics and $[Py]_{loc}$. Furthermore, the trends of $<k^{MFA}>^{blob}$ as a function of the molar mass of a structural unit (MW_{SU}) obtained for the Py-PEG$_n$MA samples in different solvents offer an experimental means to gauge the LRBD of a given polymer against that of another in the same manner as the $<k_{blob}\times N_{blob}>$-*vs*-$MW_{SU}$ trends presented in Chapter 2 do. Such comparisons established in four different organic solvents take advantage of the solubility of the Py-PEG$_n$MA samples in a broad range of solvent viscosity and polarity, a feature which should enable the direct comparison of the LRBD of many other polymers in solution.

3.2 EXPERIMENTAL

3.2.1 Materials:

The synthesis and characterization of the 41 Py-PEG$_n$MA samples used in this study, along with the acquisition of their fluorescence spectra and decays was presented in Chapter 2, Section 2.2.

3.2.2 Global Analysis of the fluorescence decays according to the MFA:

The fluorescence decays of the Py-PEG$_n$MA solutions were analyzed globally according to the MFA using the program *sumegs17bg*, which was written in-house. The MFA fits the monomer and excimer decays globally using the sum of exponentials given in Equations S3.1 and S3.2 in the SI, where the parameters are optimized by the Marquardt-Levenburg algorithm.[11] A χ^2 smaller than 1.3 and the random distribution around zero of the residuals and the autocorrelation of the residuals indicated a good fit. The decay times (τ_i) and pre-exponential factors (a_i) retrieved from

the MFA were used to determine the number average lifetime ($<\tau>$) of the monomer decay excluding the contribution of pyrenyl labels, that did not form excimer. $<\tau>$ was combined with the natural lifetime of the pyrene monomer (τ_M)[17,28] in Equation 3.1 to yield the average rate constant ($<k>$) for PEF.[17,28]

$$< k >= \frac{\sum_{i=1}^{n} a_i}{\sum_{i=1}^{n} \tau_i a_i} - \frac{1}{\tau_M} = \frac{1}{< \tau >} - \frac{1}{\tau_M} \tag{3.1}$$

Beside τ_i and a_i, the MFA also retrieves the molar fractions for the different pyrenyl species present in solution. These pyrenyl labels are those that form excimer by diffusion (Py_{diff}*), are isolated, do not form excimer, and emit as if they were free in solution (Py_{free}*), and are aggregated and form excimer instantaneously upon direct excitation of a pyrene dimer (Py_{agg}*).[12] A short- and longer-lived excimer referred to as *E*0* and *D** are often detected during the decay analysis with lifetimes equal to τ_{E0} (between 30 and 50 ns) and τ_D (between 50 and 80 ns), depending on whether they are constituted of two well-stacked or two poorly stacked pyrene moieties, respectively.[12] The pyrene species Py_{free}* and Py_{diff}* forming *E0** and *D** are detected in the monomer decays, which yield their molar fractions f_{Mfree}, $f_{MdiffE0}$, and f_{MdiffD}, respectively.[12] Similarly, the pyrene species detected in the excimer decays are Py_{diff}*, that form excimer *E0** and *D** by diffusion, and the pyrene species *E0** and *D**, that form excimer upon direct excitation of a pyrene dimer, and their molar fractions are given as $f_{EdiffE0}$, f_{EdiffD}, f_{EE0}, and f_{ED}, respectively.[12] In turn, these molar fractions for the pyrene species observed in either the monomer or excimer decay can be combined to yield the overall molar fractions $f_{free,}$ $f_{diffE0,}$ $f_{diffD,}$ f_{E0}, and f_D of the pyrene species Py_{free}*, Py_{diffE0}*, Py_{diffD},

*E0**, and *D**, respectively.[12] The sum of $f_{diffE0}+f_{diffD}$ yields f_{diff} and that of $f_{E0} + f_{D}$ yields f_{agg} representative of Py_{diff}* and Py_{agg}*, respectively. The molar fraction (x_{Py}) of pyrene-labeled SUs in the Py-PEG$_n$MA samples, $<k>$, and f_{Mfree} were used to calculate the rate constant $<k^{MF}>^{blob}$ with Equation 3.2. $<k^{MF}>^{blob}$ was compared to the product $k_{blob}\times N_{blob}$, which has been found to describe the LRBD of a polymer.[3,5]

$$< k^{MF} >^{blob} = \frac{1- f_{Mfree}}{x_{Py}} < k > \tag{3.2}$$

The equations used to calculate the molar fractions of the different pyrenyl species are provided in SI.

3.3 RESULTS

3.3.1 Validity of the parameters retrieved from the MFA:

In two studies conducted by the Duhamel laboratory in 2012[26] and 2016,[28] the MFA was applied to 74 pyrene-labeled macromolecules, which included pyrene end-labeled poly(ethylene glycol)[18] and polystyrene,[11] a series of poly(alkyl methacrylate)s,[5] amylose, and amylopectin that were randomly labeled with pyrene,[29] and two series of pyrene end-labeled dendrimers.[9,10,25] The nature of the polymeric constructs investigated in these two studies meant that different polymers were soluble in different solvents, with the polysaccharides being soluble in DMF and DMSO, but not in THF and toluene, and the vast majority of Py-PAMA samples being insoluble in DMF and DMSO. In contrast, the MFA was applied herein to the 41 Py-PEG$_n$MA samples, which represent a novel family of PyLMs and were soluble in all four solvents, thus providing consistency to the study.

One major advantage of the MFA is its ability to retrieve the molar fractions f_{diffE0}, f_{diffD}, f_{E0}, and f_D of the pyrene species Py_{diffE0}*, Py_{diffD}*, *E0**, and *D**, respectively, and the lifetimes τ_{E0} and τ_D for *E0** and *D**, respectively. In turn, these parameters can be combined with $<\tau>$ and $<k>$ calculated from Equation 3.1 to yield Equation 3.3. Equation 3.3 provides the expression of the absolute fluorescence intensity ratio $(I_E/I_M)^{SPC}(f_{free}=0)$, that would be obtained after excluding the contribution from Py_{free}*.[26,28] If little excimer is formed by direct excitation of pyrene dimers (i.e. $f_{E0} \sim f_D \sim 0$), which was the case for the Py-PEG$_n$MA samples, $(I_E/I_M)^{SPC}(f_{free}=0)$ should increase linearly with $<k>$ with a slope that should be related to the excimer lifetime. The $(I_E/I_M)^{SPC}(f_{free}=0)$-*vs*-$<k>$ trend was found earlier to be well-described by the function $\tau_{E0}\times<k>^{\alpha}$ over three orders of magnitude, where τ_{E0} took values between 43 ns in DMSO and 53 ns in DMF, which are reasonable for a pyrene excimer in organic solvents, and α ranged between 0.94 and 0.98, which are values close to unity.[28]

$$(I_E / I_M)^{SPC}(f_{free} = 0) = \frac{(f_{diffE0} \times \tau_{E0} + f_{diffD} \times \tau_D) \times < k > \times < \tau > + f_{E0} \times \tau_{E0} + f_D \times \tau_D}{f_{diff} \times < \tau >} \qquad (3.3)$$

A log-log plot of $(I_E/I_M)^{SPC}(f_{free}=0)$ as a function of $<k>$ yielded a straight line in Figure 3.1 for THF, toluene, DMF, and DMSO with the data obtained for the 41 Py-PEG$_n$MA samples clustering around the master lines that were established earlier.[26,28] The good agreement obtained for the $(I_E/I_M)^{SPC}(f_{free}=0)$-*vs*-$<k>$ plots in Figure 3.1 and Equation 3.1 for the 41 additional Py-PEG$_n$MA samples in four different solvents further confirms the generality of these plots, which are expected to hold for any PyLM in any solvent, where the macromolecules and the pyrenyl labels are both soluble. Finally, since the $(I_E/I_M)^{SPC}(f_{free}=0)$-*vs*-$<k>$ trends shown in Figure 3.1 are

combinations of the parameters retrieved from the MFA of the Py-PEG$_n$MA fluorescence decays, the good agreement also confirms the validity of the MFA parameters, which yield results that are internally consistent.

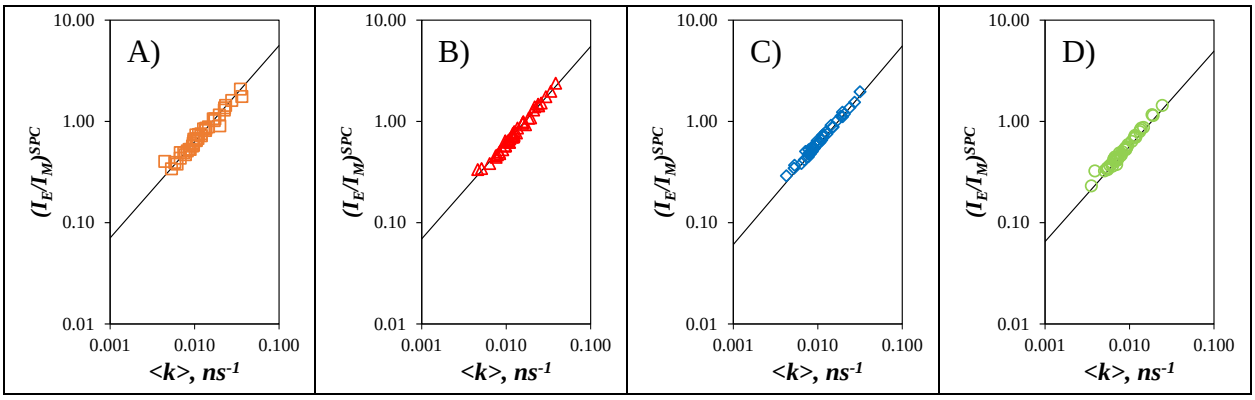

Figure 3.1. Plot of $(I_E/I_M)^{SPC}$-*vs*-<*k*> for the Py-PEG$_n$MA samples in A) (□, η = 0.46 mPa.s) THF, B) (△, η = 0.56 mPa.s) toluene, C) (◇, η = 0.79 mPa.s) DMF, and D) (○, η = 1.99 mPa.s) DMSO. The black line represents the predicted scaling law in each solvent as described in Ref #28.

3.3.2 Comparing the MFA and FBM parameters:

According to the MFA, <*k*> equals $k_{diff}\times[Py]_{loc}$. k_{blob} in the FBM equals $k_{diff}\times(1/V_{blob})$ and <*n*> is the average number of ground-state pyrenes per *blob*. Consequently, the product $k_{blob}\times$<*n*> equals $k_{diff}\times(<n>/V_{blob}) = k_{diff}\times[Py]_{loc} =$ <*k*>. The validity of this statement was tested by plotting <*k*> and $k_{diff}\times$<*n*> obtained from the MFA and the FBM as a function of pyrene content (x_{Py}) in Figure 3.2A, D, G, and J for solutions in THF, toluene, DMF, and DMSO, respectively. Though only four different side-chain lengths were selected to ensure that the plots remained legible, they remain representative of the overall trends. Within experimental error, the two quantities <*k*> and $k_{diff}\times$<*n*> were indistinguishable for all Py-PEG$_n$MA samples in the four solvents investigated. Interestingly, the <*k*>- and $k_{diff}\times$<*n*>-*vs*-x_{Py} plots in Figure 3.2 did not exhibit a linear trend as

would be expected if $[Py]_{loc}$ were proportional to x_{Py}. Instead, the trends seem to tend to a positive non-zero intercept at low pyrene contents. This observation is a consequence of the inherent compartmentalization of the pyrenyl labels into *blobs*. At low pyrene contents, most *blobs* are empty but excimer occurs with a rate constant $<k>$ in those *blobs* that have more than one pyrenyl label. As a result, while the overall $[Py]_{loc}$ is low on average for low pyrene contents, as defined by x_{Py}, the few *blobs* that generate excimer have a much larger $[Py]_{loc}$ from which PEF occurs with a larger than expected $<k>$. This effect is demonstrated by the plots of f_{free}-*vs*-x_{Py} presented in Figure 3.2B, E, H, and K, where the amount of pyrene isolated within a *blob*, emitting as a monomer, increases with decreasing pyrene content. Furthermore, the more flexible polymers with shorter side chains like Py-PEG$_0$MA form excimer more easily and yield lower f_{free} values than the stiffer polymers with longer side chains like Py-PEG$_{19}$MA.

In order to normalize for the effect of the *blobs* containing only one pyrene and the different pyrene contents, both $<k>$ and $k_{blob}\times<n>$ were multiplied by $(1-f_{free})/x_{Py}$, resulting in the expression first given in Equation 3.2 for $<k^{MF}>^{blob}$ for the former, and in $k_{blob}\times<n>\times(1-f_{free})/x_{Py} = k_{blob}\times N_{blob}$ for the latter. $<k^{MF}>^{blob}$ and the product $k_{blob}\times N_{blob}$ were plotted as a function of pyrene content in Figure 3.2C, F, I and L. Both remained constant with pyrene content and were equivalent within experimental error. The equivalence between the key parameters derived from the FBM, which assumes that the pyrene labels are distributed randomly in a macromolecule according to a Poisson distribution, and the MFA, which makes no assumption about the pyrene-labeling scheme, is quite remarkable as both models seem to capture the main features of PEF in PyLMs. It underlines the universality of the MFA, which is applicable to any PyLM, and the analytical power of the FBM, that separates the dynamics and structural components of a macromolecule through the parameters k_{blob} and N_{blob}, respectively.

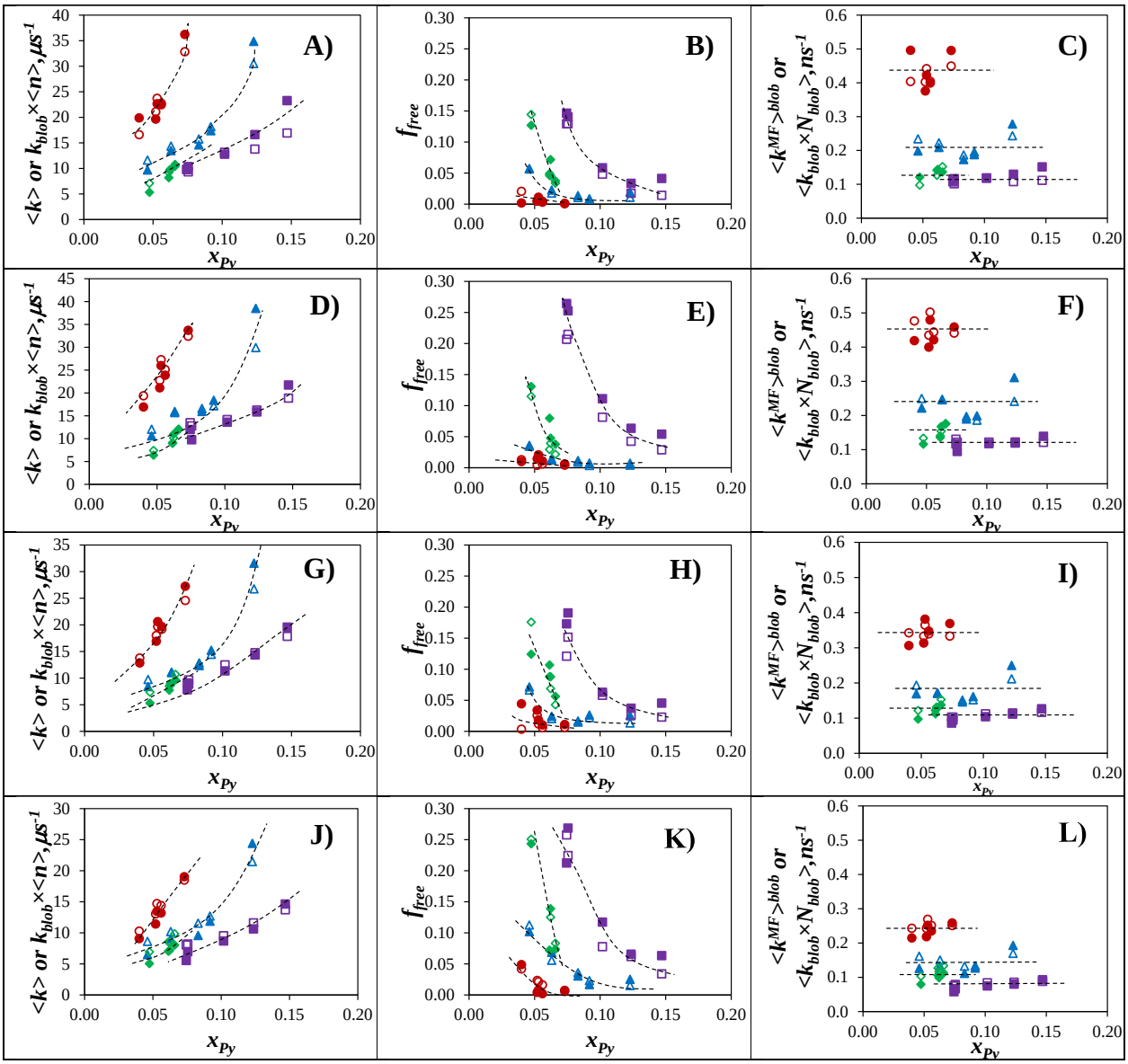

Figure 3.2. The (filled symbols) MFA parameters and (hollow symbols) FBM parameters (A, D, G, J) $\langle k \rangle$ and $k_{blob}\langle n \rangle$, (B, E, H, K) f_{free}, and (C, F, I, L) $\langle k^{MF} \rangle_{blob}$ and $k_{blob} \times N_{blob}$ as a function of x_{Py}. For clarity, only the parameters for the polymers (○,●) Py-PEG$_0$MA, (△,▲) Py-PEG$_3$MA, (◇,◆) Py-PEG$_5$MA, and (□,■) Py-PEG$_{19}$MA were plotted. Dashed lines were added to guide the eye. From top to bottom row: THF, toluene, DMF, and DMSO.

3.3.3 Calibration curve for the LRBD of Polymers Based on $<k^{MF}>^{blob}$:

The equivalence illustrated in Figure 3.3 between the parameters $<k^{MF}>^{blob}$ and $<k_{blob}\times N_{blob}>$ implies that both parameters can be used interchangeably. Consequently, since $<k_{blob}\times N_{blob}>$ has been found to describe the LRBD of polymers based on a calibration curve established with a series of Py-PAMAs in THF, so should $<k^{MF}>^{blob}$. The main difference between the former Py-PAMA study and that on Py-PEG_nMA is that the Py-PAMA samples were only probed in THF, the Py-PEG_nMA samples were characterized in four different organic solvents. To this end, $<k^{MF}>^{blob}$ was plotted as a function of MW_{SU} in Figure 3.3 to yield a series of calibration curves against which the $<k^{MF}>^{blob}$ of other polymers or macromolecules can be compared. An increase in MW_{SU} results in a decrease in the LRBD of the polymethacrylate backbone, which is associated with a decrease in $<k^{MF}>^{blob}$ in Figure 3.3. $<k^{MF}>^{blob}$ decreases rapidly with MW_{SU} up to an MW_{SU} of 500 g/mol, above which it remained constant. The plateau region observed in Figure 3.3 for high MW_{SU} indicates that any further increase in side chain length no longer has an effect on the polymethacrylate backbone suggesting that the main chain is locally extended on the length scale probed by an excited pyrenyl label. As with the $<k_{blob}\times N_{blob}>$-*vs*-$MW_{SU}$ trends presented in Chapter 2 of this thesis, similar $<k^{MF}>^{blob}$ trends were obtained in the lower viscosity solvents, namely THF, toluene, and DMF, with DMSO yielding lower $<k^{MF}>^{blob}$ due to its higher viscosity. The difference in behavior observed between the low and high viscosity solvents seems to reflect a change in regime depending on whether the polymer or the solvent controls the encounter frequency, Ω_{SU}, between SU. A high viscosity solvent might control the mobility of the polymethacrylate backbone probed by PEF whereas the backbone motions would control PEF in low viscosity solvents.

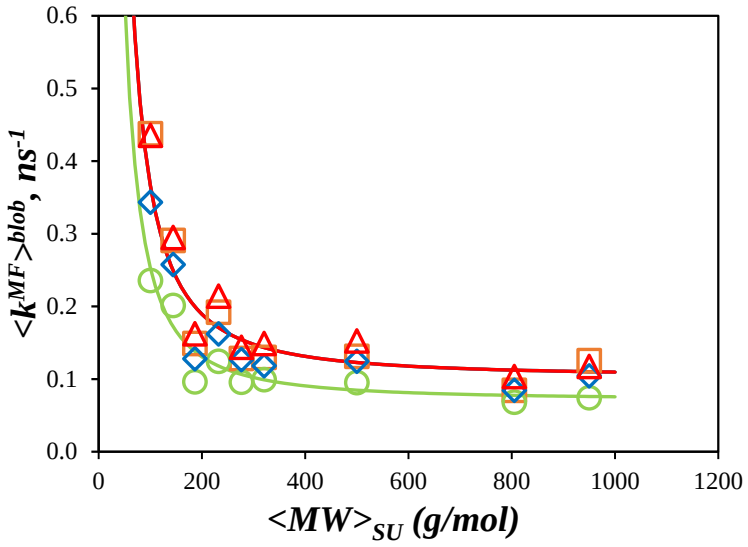

Figure 3.3 Plot of $\langle k^{MF}\rangle^{blob}$ as a function of MW_{SU} in (□) THF, (△) toluene, (◇) DMF, and (○) DMSO. Lines correspond to the scaling laws presented in Equations 3.4-3.6.

3.4 DISCUSSION

3.4.1 Parameterization of $\langle k^{MF}\rangle^{blob}$-vs-$MW_{SU}$:

As with the parameterization of the $k_{blob}\times N_{blob}$-*vs*-MW_{SU} trends presented in Chapter 2, $\langle k^{MF}\rangle^{blob}$ was assumed to be a function of MW_{SU} and the solvent viscosity, η. The $\langle k^{MF}\rangle^{blob}$ values obtained for Py-PEG$_{16}$MA and Py-PEG$_{19}$MA were taken as the $\langle k^{MF}\rangle^{blob,\infty}$ values for a polymer with a fully extended backbone, for which MW_{SU} did not have an effect. $\langle k^{MF}\rangle^{blob,\infty}$ was well described by Equation 3.4, where $\langle k^{MF}\rangle^{blob,\infty}$ decreased from a constant value as the viscosity increased beyond 0.79 mPa·s as shown in Figure 3.4A, where $\langle k^{MF}\rangle^{blob,\infty}$ was plotted as a function of η.

$$\langle k^{MF}\rangle^{blob,\infty} = \begin{cases} 0.056 + 0.0304/\eta & \text{if } \eta > 0.79 \text{ mPa·s} \\ 0.1033 & \text{if } \eta < 0.79 \text{ mPa·s} \end{cases} \quad (3.4)$$

The polymers with side-chains shorter than 16 ethylene glycol could be represented by the bending function, $f_{b3} = c \times MW_{SU}^{a} \times \eta^{b} + 1$, where the scaling exponents a and b along with the pre-factor c were optimized through chi-square minimization until the functions $f_{b3}(MW_{SU}, \eta)$ and $<k^{MF}>^{blob}/<k^{MF}>^{blob,\infty}$ would show a good match. The b exponent was found to equal −0.001, indicating that $<k^{MF}>^{blob}$ depended even less on viscosity than $k_{blob} \times N_{blob}$ and was primarily dependent on MW_{SU}. Equation 3.5 describes the bending function. The theoretical value of $<k^{MF}>^{blob}$, $<k^{MF}>^{theo}$, could then be determined as the product of $<k^{MF}>^{blob,\infty}$ and $f_{b3}(MW_{SU}, \eta)$ as shown in Equation 3.6. The plot of $<k^{MF}>^{blob}$-*vs*-$<k^{MF}>^{theo}$ in Figure 3.4B confirmed that Equations 3.4 – 3.6 described the experimental $<k^{MF}>^{blob}$ values well, with most points falling on or close to the diagonal.

$$f_{b3} = 4378 \times MW_{SU}^{-1.617} \times \eta^{-0.001} + 1 \tag{3.5}$$

$$< k^{MF} >^{theo} (MW_{SU}, \eta) = < k^{MF} >^{blob,\infty} \times f_{b3}(MW_{SU}, \eta) \tag{3.6}$$

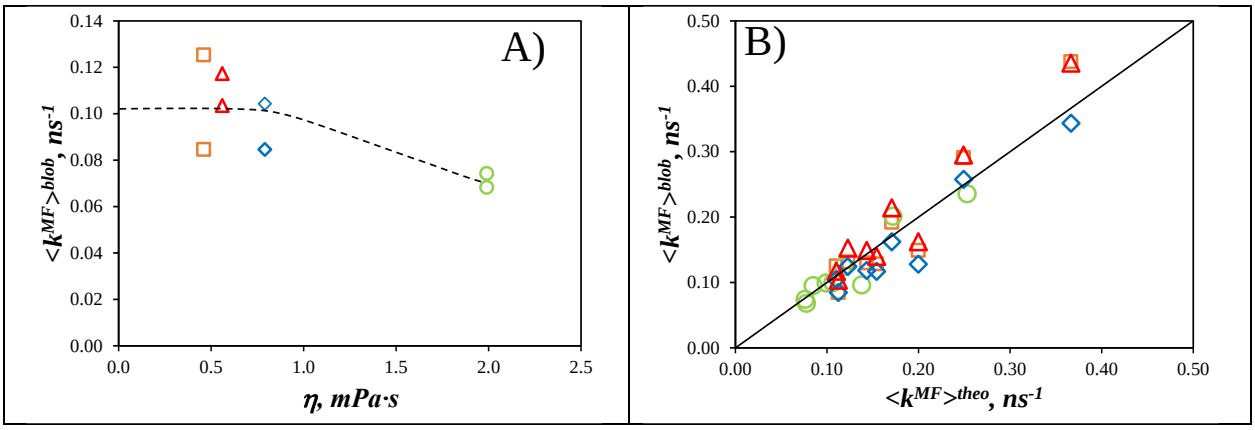

Figure 3.4. Plots for the Py-PEG$_n$MA samples of A) $\langle k^{MF}\rangle_{blob,\infty}$ as a function of η and B) $\langle k^{MF}\rangle_{blob}$ as a function of $\langle k^{MF}\rangle_{theo}$ with the black line indicating the diagonal. (□, η = 0.46 mPa.s) THF, (△, η = 0.56 mPa.s) toluene, (◇, η = 0.79 mPa.s) DMF, and (○, η = 1.99 mPa.s) DMSO.

3.4.2 Calibration Curves:

As with the plot of $k_{blob}\times N_{blob}$-*vs*-MW_{SU} presented in Chapter 2 of this thesis, an appealing feature of the $\langle k^{MF}\rangle_{blob}$-*vs*-$MW_{SU}$ plots shown in Figure 3.3 is its potential application as a calibration curve for Ω_{SU}. Indeed, the $\langle k^{MF}\rangle_{blob}$-*vs*-$MW_{SU}$ calibration curves could be viewed as a characterization tool that is even more universal than the $k_{blob}\times N_{blob}$-*vs*-MW_{SU} calibration curves generated with polymers randomly labeled with pyrene; while both calibration curves can be used in several organic solvents, only the MFA and the $\langle k^{MF}\rangle_{blob}$-*vs*-$MW_{SU}$ calibration curve can be applied to any PyLM.

The $\langle k^{MF}\rangle_{blob}$-*vs*-$MW_{SU}$ trend for THF in Figure 3.3 was used to compare the dynamics of a series of poly(methyl acrylate) (PMA),[5] polystyrene (PS),[11] poly(dimethyl siloxane) (PDMS),[7] and poly(isobutylene-alt-maleic anhydride) (PIMA) samples in THF.[6] The chemical structures of the polymers are shown in Figure 3.5. Both $\langle k^{MF}\rangle_{blob}$ and MW_{SU} were normalized by multiplying or dividing them by the number N_{bb} of backbone atoms per SU, respectfully. While PMA, PS, and

PDMS all had N_{bb} values of 2, the N_{bb} for PIMA equaled 4 since the SU of this alternating copolymer was comprised of a succinic anhydride and an isobutylene monomer representing a total of four backbone atoms.

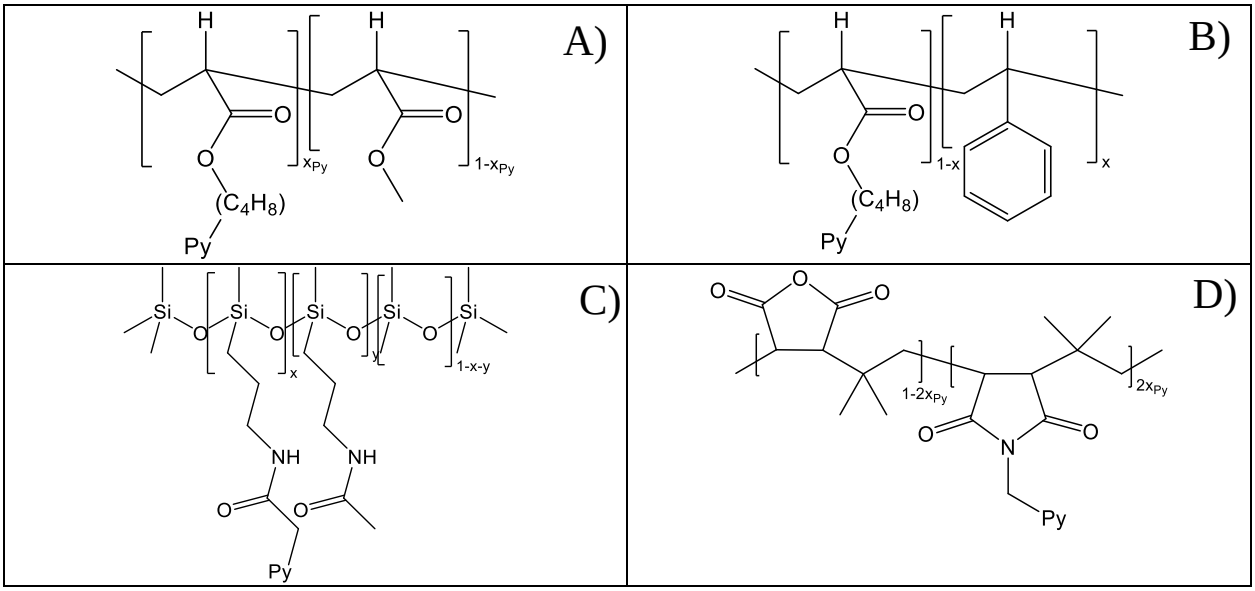

Figure 3.5. Chemical structure of (A) poly(methyl acrylate), (B) polystyrene, (C) poly(dimethyl siloxane), and (D) poly(isobutylene-*alt*-maleic anhydride).

Figure 3.6 neatly shows the effect of the chemical structure of the polymer on $\langle k^{MF} \rangle^{blob}$. Compared to the polymethacrylates, PMA is more flexible due to the lack of the α–methyl group on the backbone, while PDMS experiences much faster LRBD, and thus greater Ω_{SU}, due to the greater Si-O-Si bond angle compared to the O-Si-O bond angle, resulting in a more coiled polymer.[7] Interestingly, the $\langle k^{MF} \rangle^{blob}$ values retrieved for PS and PEG_0MA indicate that both polymers exhibit similar LRBD. This result is quite satisfying since these polymers share similar T_g values reported to equal 100 °C and 105 °C for PS[7,23] and PEG_0MA,[30] respectively. This good agreement between the Ω_{SU} measure in solution by PEF and in the bulk by calorimetry or viscoelastic measurements confirms the validity of the PEF-methodology described in this thesis.

Finally, and unsurprisingly, PIMA shows the most hindered dynamics due to the rigid anhydride ring which involves two out of four backbone atoms.

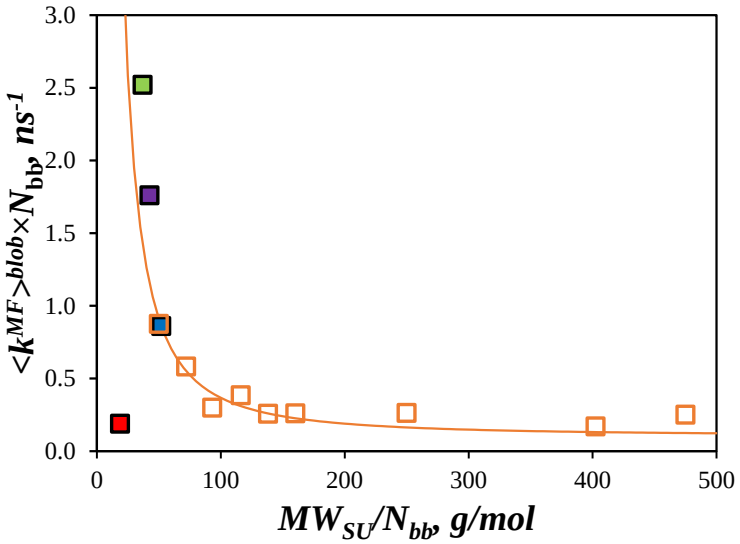

Figure 3.6. Comparison of $<k^{MF}>^{blob} \times N_{bb}$ for samples of (□) Py-PEG$_n$MA, (■) poly(methyl acrylate,[5] (■) polystyrene,[11] (■) poly(dimethyl siloxane),[7] and (■) poly(isobutylene-*alt*-maleic anhydride).[6]

3.4.3 Comparison between the FBM and MFA:

Both $<k^{MF}>^{blob}$ and $<k_{blob} \times N_{blob}>$ can be used interchangeably to report on the encounter frequency, Ω_{SU}, between SUs since they were found to yield similar values in Figures 3.2C, F, I, and L Stronger support for this statement is provided in Figure 3.7A where all 41 $<k^{MF}>^{blob}$ values were plotted as a function of the 41 $k_{blob} \times N_{blob}$ values reported in Chapter 2. All the values clustered around the diagonal, indicating excellent agreement between the two parameters. Since k_{blob} was shown to remain relatively constant in Chapter 2, regardless of solvent type and Py-PEG$_n$MA sample, the equivalence between $<k^{MF}>^{blob}$ and $k_{blob} \times N_{blob}$ suggests that N_{blob} should be proportional to $<k^{MF}>^{blob}$. Figure 3.7B demonstrates that this is indeed the case as N_{blob} was found

to increase linearly with increasing $<k^{MF}>^{blob}$ according to Equation 3.7. Referring to the N_{blob} value calculated with Equation 3.7 as N_{blob}^{MF}, a 1:1 correspondence was found between N_{blob}^{MF} and N_{blob} in Figure 3.7C since all data points aligned along the diagonal.

$$N_{blob} = 144(\pm 4) \times < k^{MF} >^{blob} \tag{3.7}$$

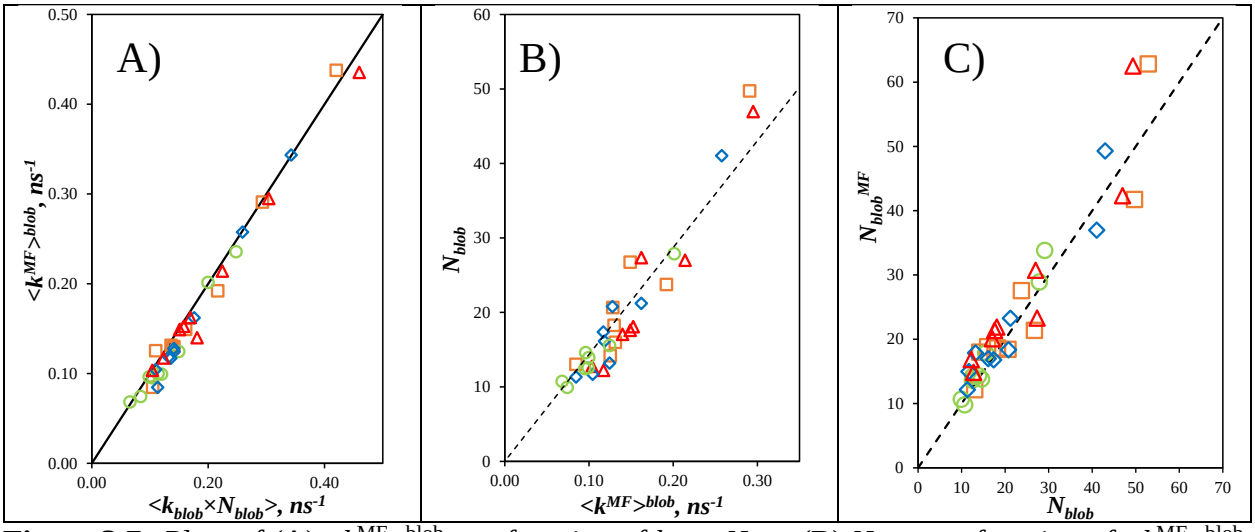

Figure 3.7. Plots of (A) $<k^{MF}>^{blob}$ as a function of $k_{blob} \times N_{blob}$. (B) N_{blob} as a function of $<k^{MF}>^{blob}$, and (C) N_{blob}^{MF} as a function of N_{blob}. (□) THF, (△) toluene, (◇) DMF, and (○) DMSO.

Taking the inverse of the slope of Equation 3.7 yielded $k^{MF,blob}$ found to equal 6.9 $(\pm 0.2) \times 10^6$ s^{-1}, similar in magnitude to the k_{blob} value of 8.1 $(\pm 1.3) \times 10^6$ s^{-1} reported in Chapter 2 for the Py-PEG$_n$MA samples and that of 6.9 $(\pm 1.2) \times 10^6$ s^{-1} reported for the Py-PAMA samples.[5] The similar values taken by $k^{MF,blob}$ from the MFA and k_{blob} from the FBM for the 41 Py-PEG$_n$MA samples might indicate that a universal k_{blob} value might exist, at least for the polymethacrylate backbone. If this were the case, the simpler MFA could be used to obtain $<k^{MF}>^{blob}$ as a measure

of Ω_{SU} and N_{blob}^{MF} as $<k^{MF}>^{blob}/k^{MF,blob}$ to measure the persistence length as was done in Chapter 2.

3.4.3 Advantages and disadvantages:

Many of the advantages and disadvantages of the PEF-based methodologies developed in the Duhamel laboratory have already been reviewed in Chapter 2 and are still relevant here. One advantage not previously discussed and specific to the MFA is the ability to analyze the fluorescence decays acquired with PyLMs, where covalent attachment of the pyrenyl labels does not need to adhere to pre-existing labeling protocols requiring specific models. This study has illustrated the relationships existing between the parameters retrieved with the FBM or the MFA. Not surprisingly, since PEF in polymers randomly labeled with pyrene occurs within *blobs*, the MFA parameters mimicked those obtained by the FBM, even though no assumption was made about how PEF occurred when the Py-PEG$_n$MA samples were characterized according to the MFA. As a matter of fact, the MFA parameters could be re-arranged to yield N_{blob}^{MF} and $<k^{MF}>^{blob}$, which were found to be excellent representation of N_{blob} and the product $k_{blob}\times N_{blob}$ obtained with the FBM. Another advantage is the computational simplicity of the MFA compared to the FBM, which involves an infinite sum of exponentials versus a sum of three exponentials at most to fit the monomer fluorescence decays with the MFA. Yet despite these mathematical and computational differences, the parameters retrieved from the MFA and FBM are tightly connected since they all reflect the product $k_{diff}\times[Py]_{loc}$, thus reflecting the universal character of PEF in PyLMs.

The primary disadvantage of the MFA is its inherent inability to separate the dynamic and structural components describing a PyLM from $<k^{MF}>^{blob}$ without additional information. In the

case of the Py-PEG$_n$MA samples, the FBM analysis of the fluorescence decays indicated that k_{blob} did not depend on solvent and Py-PEG$_n$MA sample. From this external knowledge, Equation 3.7 could be derived, which resulted in N_{blob}^{MF} values that matched fairly well the N_{blob} values obtained with the FBM. In fact, the N_{blob}^{MF} values determined with Equation 3.7 for the Py-PAMA samples studied earlier showed an excellent correlation with their N_{blob} values determined with the FBM.[5] A 1:1 correspondence was observed upon plotting N_{blob}^{MF} as a function of N_{blob} determined in the original study[5] in Figure 3.8 indicating excellent agreement between the two analyses for the polymethacrylate samples. However, N_{blob}^{MF} was found to equal 126 (±13), when it was obtained through Equation 3.7 for pyrene-labeled poly(methyl acrylate) in THF, which was twice larger than the N_{blob} value of 59 (±10) obtained with the FBM.[5] The reason for this discrepancy was attributed to k_{blob}, which was twice larger for poly(methyl methacrylate) than for Py-PEG$_0$MA.[5] In the case of poly(methyl acrylate), an excited pyrenyl label is limited in its mobility by the polyacrylate backbone, which constrains its motion to a *blob* made of only 59 SU, similar to the 60 SU found for PEG$_0$MA. The difference between the two backbones is Ω_{SU} which is twice larger for poly(methyl acrylate) than for PEG$_0$MA, as reflected by the twice larger $<k^{MF}>^{blob}$ value obtained in Figure 3.6. Without external knowledge that k_{blob} determined with the FBM is twice larger for poly(methyl methacrylate), usage of Equation 3.7 to determine N_{blob}^{MF} assuming a constant k_{blob} value of 6.9 (±0.2)×10^6 s^{-1} leads to an erroneous N_{blob}^{MF} value in Figure 3.8. The inability to properly separate the dynamic and structural components of a PyLM through the MFA of the fluorescence decays highlights an important disadvantage of the MFA compared to the FBM.

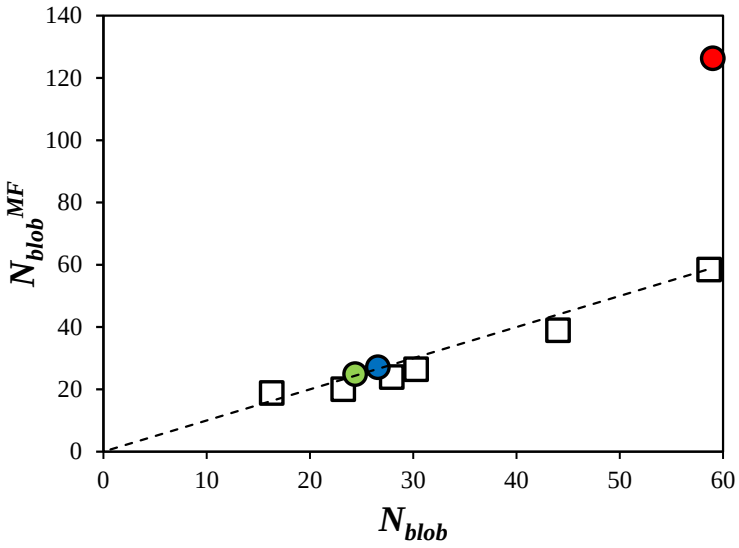

Figure 3.8. Plot of N_{blob}^{MF} as a function of N_{blob} for the (□) *n*-alkyl, (●) *t*-butyl, (●) *cyclo*-hexyl polymethacrylates, and (●) poly(methyl acrylate) in THF. N_{blob} values were taken from Ref. #5. Equation 3.7 was applied to determine N_{blob}^{MF} from the $\langle k^{MF} \rangle^{blob}$ values taken from Ref. #28. Dashed line represents a 1:1 correspondence.

3.5 CONCLUSIONS

The MFA was applied to the fluorescence decays acquired with a series of Py-PEG$_n$MA samples with *n* ranging from 0 to 19. Since these samples were randomly labeled with pyrene, their decays were well described by the FBM, which assumes that the pyrenyl labels distribute themselves among *blobs* according to a Poisson distribution. Consequently, they offered a set of well-characterized fluorescence decays, that could be used to assess how well the MFA parameters would represent the main features of the Py-PEG$_n$MA samples described through the parameters N_{blob} and $k_{blob} \times N_{blob}$ obtained through the FBM decay analysis. Considering that the MFA makes no assumption about the conditions leading to PEF in a PyLM, a remarkably good agreement was obtained between $\langle k \rangle$ and the product $k_{blob} \times \langle n \rangle$. This agreement was much satisfying since both

quantities are expected to equal $k_{diff}\times[Py]_{loc}$ and are thus a direct measure of $[Py]_{loc}$. In turn, $\langle k\rangle$ could be re-arranged to yield $\langle k^{MF}\rangle^{blob}$ which was an excellent representation of the product $k_{blob}\times N_{blob}$ determined with the FBM. Similarly to $k_{blob}\times N_{blob}$, $\langle k^{MF}\rangle^{blob}$ obtained for the Py-PEG$_n$MA samples could be used as a benchmark against which $\langle k^{MF}\rangle^{blob}$ of other polymers could be compared. Furthermore, the constancy of k_{blob} established for the Py-PEG$_n$MA samples with the FBM led to a mathematical derivation allowing the determination of N_{blob}^{MF} from $\langle k^{MF}\rangle^{blob}$. N_{blob}^{MF} obtained with the MFA was found to satisfyingly represent N_{blob} obtained with the FBM for a wide variety of samples with a polymethacrylate backbone. However, the mathematical derivation to obtain N_{blob}^{MF} cannot be generalized to all PyLMs as the determination of N_{blob}^{MF} requires that k_{blob} be determined independently. Nevertheless, the ability of the MFA to characterize the LRBD of any PyLM through $\langle k^{MF}\rangle^{blob}$ without making any assumption about the labeling methodology represents a great advantage for the characterization of polymer dynamics in solution and this study has expanded its applicability to three additional solvents beyond THF, namely toluene, DMF, and DMSO.

Particular emphasis was placed on examining the relationship that exists between $\langle k\rangle$ and $k_{diff}\times[Py]_{loc}$. The equality $\langle k\rangle = k_{diff}\times[Py]_{loc} = k_{diff}\times(\langle n\rangle/V_{blob}) = k_{blob}\times\langle n\rangle$ was found to hold true within experimental error. This allowed for the extraction of k_{blob} and $\langle n\rangle$ from the $\langle k\rangle$ as determined by MFA. The ensuing parameters were used to determine the structural parameter N_{blob}^{MFA} which quantifies the ability of a polymer to bend, and is analogous to the parameter N_{blob} as retrieved from the FBM. This presents a great step forward as previously no such structural information could be extracted from the FMA parameters. However, much work still remains to be done to properly separate the effects of dynamics and structure from the MFA parameters.

Equation 3.7 provides an accurate picture of the structural parameter N_{blob}^{MFA}, so long as it is only applied to polymers with a methacrylate backbone.

CHAPTER 4

CONCLUSIONS AND FUTURE WORK

4.1 SUMMARY OF THESIS

The macroscopic properties of polymers in the bulk are dictated by the behavior of the individual polymer chains at the molecular level.[1–3] Their behavior is described by two parameters, namely the persistence length l_p, which describes the ability of a polymer chain to bend, and the frequency Ω_{SU} of encounters between structural units (SUs), which quantifies the bending dynamics. Stiffer polymers take larger l_p values, reflecting a lessened ability to bend,[4] and correspondingly take smaller Ω_{SU} values, representing a decreased frequency of encounter between SUs.[5,6] Among the methods applied to measure Ω_{SU}, the analysis of the fluorescence decays acquired with polymers labeled with the fluorophore pyrene possesses several advantages over other techniques as it fulfills three criteria not met by any other techniques, namely that it is capable of handling polymers of high polydispersity, is easily used in multiple solvents, and selectively reports on the backbone of the polymer as opposed to its side-chains.

The first goal of this thesis was to probe the l_p and Ω_{SU} of a series of 41 pyrene-labeled poly(oligo(ethylene glycol)methyl ether methacrylate)s (Py-PEG$_n$MA) in solution. A similar study had been conducted on a series of poly(alkyl methacrylates) in THF,[5] as they proved difficult to dissolve in more polar solvents. The more polar oligo(ethylene glycol) side-chains of the Py-PEG$_n$MA samples used in this study improved the solubility in polar solvents such as DMF and DMSO. The fluorescence decays of the pyrene monomer and excimer of the Py-PEG$_n$MA samples were analyzed globally using the fluorescence blob model (FBM), which retrieved the parameters k_{blob}, N_{blob}, and the product $k_{blob}\times N_{blob}$ in the solvents THF, toluene, DMF, and DMSO. N_{blob} and $k_{blob}\times N_{blob}$ were found to decrease with increasing molecular weight (MW_{SU}) of the structural units and solvent viscosity (η). In each solvent, N_{blob} and $k_{blob}\times N_{blob}$ decreased to a plateau value for infinitely large MW_{SU} and the plateau value was taken as N_{blob}^{∞} and $k_{blob}\times N_{blob}^{\infty}$, respectively,

corresponding to a fully extended backbone. N_{blob} and $k_{blob}\times N_{blob}$ could be parametrized as functions of MW_{SU} and η by introducing the bending function to model the deviation of N_{blob} and $k_{blob}\times N_{blob}$ from N_{blob}^{∞} and $k_{blob}\times N_{blob}^{\infty}$, respectively, yielding Equations 2.6 and 2.11.

Since N_{blob} was found to decrease with increasing stiffness of the PEG$_n$MA backbone, N_{blob} was believed to reflect the l_p of the polymer so that Equation 2.6, predicting N_{blob} for a polymer of any MW_{SU} in a solvent of any viscosity, was applied to extract l_p from N_{blob} using a modified version of the Kratky-Porod equation.[4,7] While l_p determined form N_{blob} was found to scale as N_S^2 for $N_S > 14$ as theoretically predicted,[8] it was also found to depend on η. Since the bending ability of a polymer is an intrinsic property of the polymer, its l_p should not depend on η. Upon review, this unexpected dependency was attributed to the fact that PEF is a diffusion controlled process with less excimer being formed in higher viscosity solvents. Since both an increase in MW_{SU} and η result in a decrease in N_{blob}, l_p values retrieved from N_{blob} also show a dependency on viscosity. To find conditions where η would not affect the determination of l_p, molecular mechanics optimizations (MMOs) were carried out on an extended conformation of the polymethacrylate backbone to determine a theoretical N_{blob}^{∞} unaffected by viscosity. The experimental N_{blob}^{∞} obtained by PEF was found to match the theoretical N_{blob}^{∞} obtained by MMOs for an η value of 0.69 mPa·s. Equation 2.6 was then applied to generate the N_{blob} curve for η = 0.69 mPa.s from which l_p could be extracted. The l_p values retrieved from that procedure were found to be reasonable based on the published l_p value of poly(methyl methacrylate)[9] and the expected dependency of l_p on N_S^2.[8]

Consequently, the methodology described to retrieve l_p from N_{blob} has fulfilled all three requirements stated earlier. First, it is impervious to polymer polydispersity, thanks to the inherent

ability of the FBM to characterize the chain segment within a *blob* instead of the entire chain;[10] second, it has expanded the range of solvents where these PEF studies on pyrene-labeled macromolecules can be carried out by including solvents that are more polar than THF; and finally, the short butyl linker connecting pyrene to the polymethacrylate backbone keeps the motion of the pyrene correlated to the backbone motion,[11] ensuring that the backbone, and not the side chains, is the focus of the study. The main disadvantage of this method is the dependence of N_{blob} on solvent viscosity, which needs to be accounted for when determining l_p.

Furthermore, since $k_{blob} \times N_{blob}$ reports on the parameter Ω_{SU}, it could be used as a calibration curve against which the long range backbone dynamics (LRBD) of other polymers could be compared. This comparison was done for pyrene-labeled poly(methyl acrylate)[12] and a series of pyrene-labeled polypeptides[6,13] in DMSO. As expected, the loss of the α-methyl group of PMA significantly increased its backbone flexibility. Conversely, the double-bond character of the peptide bond decreased the polypeptides flexibility, which was further diminished as more glutamic acid with a side chain, that was longer than the proton of glycine or methyl of alanine, was incorporated in the polypeptides. Such a comparison between different polymers and the PEG_nMA samples in DMSO could not have been made with the PAMA samples due to their poor solubility in DMSO.

The monomer and excimer decays of the 41 Py-PEG_nMA samples were then fitted according to the model free analyzed (MFA). Unlike the FBM, which deals with polymers randomly labeled with pyrene, where the excited pyrenyl labels are assumed to probe a finite volume known as a *blob*,[10,14] the MFA makes no assumptions about how excimer formation occurs, merely that PEF can be described by a sum of exponentials.[14,15] Despite the significant conceptual differences between the theoretical assumptions used to derive the mathematical

equations used to fit the fluorescence decays of the pyrene monomer and excimer according to the two models, excellent agreement was found between $<k>$ and $k_{blob}\times<n>$ retrieved from the MFA and FBM, respectively. This agreement between these two parameters was satisfying as both are expected to equal $k_{diff}\times[Py]_{loc}$.[10,14,15] By theoretically predicting $[Py]_{loc}$ for a given pyrene-labeled macromolecule (PyLM), the conformation of a PyLM of interest can be characterized through the relationship between $<k>$ and $[Py]_{loc}$. For instance, the conformation of the oligo(ethylene glycol) side chains of a series of PEG_nMA samples[16] and the crowding of the termini of a series of bis(hydroxymethyl)propanoic acid dendrimers[17,18] was obtained after equating $[Py]_{loc}$ with $<k>$. Consequently, the equivalence between $<k>$ and the product $k_{diff}\times[Py]_{loc}$ implies that $<k>$ can be used to retrieve structural information about PyLMs regardless of the type pyrene-labeling scheme applied to prepare the PyLM.

Normalizing $<k>$ to account for those pyrenyl labels, that were isolated along the polymer backbone and emitted as monomer, yielded the parameter $<k^{MF}>^{blob}$ which equaled the product $k_{blob}\times N_{blob}$ obtained with the FBM.[19] This in turn suggested that the calibration curve that had been established with $k_{blob}\times N_{blob}$ to compare the Ω_{SU} of other polymers could also be built with $<k^{MF}>^{blob}$. To this end, $<k^{MF}>^{blob}$ was parameterized in terms of MW_{SU} and η, yielding an equation which could describe the expected $<k^{MF}>^{blob}$ for any polymer in any solvent. This represented an important achievement, as this calibration curve could now be used with any polymers regardless of the type of pyrene labeling scheme, making this calibration curve more universal than the one prepared with the product $k_{blob}\times N_{blob}$.

The second consequence of the equivalence between $<k^{MF}>^{blob}$ and $k_{blob}\times N_{blob}$ was that $<k^{MF}>^{blob}$ was comprised of the same $k_{blob}{}^{MF}$ and $N_{blob}{}^{MF}$ parameters as k_{blob} and N_{blob} derived from the FBM. The fact that a plot of $<k^{MF}>^{blob}$ as a function of N_{blob} yielded a straight line suggested

that the slope of this straight line would represent k_{blob}^{MF} with N_{blob}^{MF} being equal to $\langle k^{MF} \rangle^{blob}/k_{blob}^{MF}$. Both k_{blob}^{MF} and N_{blob}^{MF} were found to agree well with both their analogous values, k_{blob} and N_{blob}, retrieved from the FBM with the Py-PEG$_n$MA samples in THF, toluene, DMF, and DMSO and with the PAMA samples in THF. Unfortunately, this derivation is currently limited in application to polymers with a polymethacrylate backbone and is not applicable yet to all PyLMs. This arises from the MFA inability to separate the dynamic from the structural components of a PyLM in the analysis, meaning that k_{blob} must be determined separately. However, this procedure should still serve as the basis for further experiments in retrieving N_{blob}^{MF} from $\langle k^{MF} \rangle^{blob}$.

4.2 FUTURE WORK

Much of the work described herein focused on characterizing the dynamics of polymers in polar solvents by establishing calibration curves that could be applied to solvents of varying polarities and viscosities. Despite widening the range of solvent viscosities and polarities that can be employed to characterize the LRBD of polymers in solution, this study has identified some complex nonlinear trends in the determination of $k_{blob} \times N_{blob}^{\infty}$ and $\langle k^{MF} \rangle^{blob,\infty}$ depending on whether η was greater or less than 0.79 mPa·s. To better understand the implications of these trends, the same experiments should be conducted in three more solvents as described below.

The first solvent should have a lower viscosity than THF. Acetone with a viscosity of 0.36 mPa·s would be ideal to further solidify the trend found for low viscosity solvents showing that the product $k_{blob} \times N_{blob}$ remain constant in the three solvents with viscosities $\leq$ 0.79 mPa·s. Acetone would thus serve to confirm or refute this assumption. Dioxane, with a viscosity of 1.2 mPa·s falls

nearly between DMF (0.79 mPa·s) and DMSO (1.99 mPa·s). Since $k_{blob}\times N_{blob}^{\infty}$ and $\langle k^{MF}\rangle^{blob,\infty}$ take different values in DMSO compared to the three other low-viscosity solvents used in this study, dioxane would provide more insight into how $k_{blob}\times N_{blob}^{\infty}$ and $\langle k^{MF}\rangle^{blob,\infty}$ change with solvent viscosity. Finally, since a mixture of 10 wt% PEG_{400} in DMSO has a viscosity of 5.1 mPa·s, it would provide a solvent with a viscosity, that is significantly higher than that of DMSO, and like dioxane would improve the understanding of how $k_{blob}\times N_{blob}^{\infty}$ and $\langle k^{MF}\rangle^{blob,\infty}$ are affected by solvent viscosity. If these experiments are unable to fully characterized the effect of viscosity on these parameters, calibration curves could be prepared using glycol ethers, or glymes, as solvent.[20] A series of glymes of increasing length would have very similar polarities, removing the effect of solvent polarity on the parameters $k_{blob}\times N_{blob}^{\infty}$ and $\langle k^{MF}\rangle^{blob,\infty}$, which would then solely depend on solvent viscosity.[20] This would afford a series of calibration curves free from the effect of solvent polarity and may improve the understanding of how viscosity affects $k_{blob}\times N_{blob}^{\infty}$ and $\langle k^{MF}\rangle^{blob,\infty}$ uncoupled from solvent polarity. Acquiring and analyzing the parameters retrieved from the fit of the fluorescence decays of the Py-PEG_nMA samples in these to solvents would lead to a better understanding of how high viscosity affects Ω_{SU}.

Undoubtably there are other situations where having a calibration curve would be useful to probe l_p and Ω_{SU}. The procedure outlined in this thesis should provide the basic steps necessary for the development of other calibration curves for different combinations of solvents and polymeric backbones of interest. One such situation would involve the preparation of calibration curves specific for macromolecules involved having biological functions. For instance, there are many classes of trans-membrane proteins which act as ion channels,[21–23] pigments,[21,24] receptors,[25] or enzymes[26] to name but a few examples. Since section(s) of every membrane bound protein is inserted inside the lipid bilayer, developing an understanding of the dynamics of biological

macromolecules bound to a lipid membrane would be most interesting. This could be accomplished by probing the LRBD of the Py-PAMA samples prepared earlier in a lipid membrane. Such a study would establish a calibration curve that would enable the characterization of other polymeric backbones, such as polypeptides, in a lipid membrane. In essence, these fluorescence studies could be expanded to heterogeneous systems, by taking advantage of the fluorescence emitted by the pyrenyl labels covalently attached onto the macromolecule of interest.

Another study would be to understand how the alkyl acrylates differ structurally and dynamically from their alkyl methacrylate counterparts. To this end, a series of pyrene-labeled poly(oligo(ethylene glycol) methyl ether acrylate)s (Py-PEG$_n$A) could be prepared to better understand the effect of the missing α-methyl group. Poly(methyl acrylate) was found to have the same N_{blob} as poly(methyl methacrylate) but the $k_{blob}\times N_{blob}$ product of the former sample was twice larger than the former.[5] The expectation would then be that the trend for N_{blob}-*vs*-MW_{SU} for the Py-PEG$_n$A samples would be the same as for Py-PEG$_n$MA, while the trends for $k_{blob}\times N_{blob}$-*vs*-MW_{SU} would be shifted to higher values.

Finally, while useful, Equations 2.6, 2.11, and 3.6 described PyLMs, where pyrene was connected to the polymer backbone via a 4-carbon butyl linker. Given the range of linker lengths accessible with different pyrene derivatives, the linker could also become another parameter that could be included in the parameterization of the N_{blob}-*vs*-MW_{SU} and $k_{blob}\times N_{blob}$-*vs*-MW_{SU} trends, which would then help the comparison of these parameters with those obtained from the study of other PyLMs. To do this, several additional series of Py-PEG$_n$MAs would need to be prepared with pyrene derivatives having different linker lengths. In the process, N_{blob} would scale up and down as a longer and shorter linker would result in a larger and smaller *blob*, respectively. These

trends would provide a means to include the linker length as one of the three parameters needed to describe the trends obtained with N_{blob} and $k_{blob} \times N_{blob}$, the two other parameters having been identified as MW_{SU} and η. When designing these experiments, the linker length should be kept lower than 9 atoms, which represents the linker length beyond which the motion of the pyrenyl labels becomes decorrelated from that of the polymer backbone.[11] For these longer linkers, PEF would no longer reflect Ω_{SU}.

REFERENCES

Chapter 1

(1) Mourey, T.; Le, K.; Bryan, T.; Zheng, S.; Bennett, G. Determining Persistence Length by Size-Exclusion Chromatography. *Polymer*. **2005**, *46*, 9033–9042.

(2) Kratky, O.; Porod, G. Röntgenuntersuchung Gelöster Fadenmoleküle. *Recl. Trav. Chim* **1949**, *68*, 1106–1122.

(3) Hokajo, T.; Terao, K.; Nakamura, Y.; Norisuye, T. Solution Properties of Polymacromonomers Consisting of Polystyrene V. Effect of Side Chain Length on Chain Stiffness. *Polym. J.* **2001**, *33*, 481–485.

(4) Terao, K.; Takeo, Y.; Tazaki, M.; Nakamura, Y.; Norisuye, T. Polymacromonomer Consisting of Polystyrene. Light Scattering Characterization in Cyclohexane. *Polym. J.* **1999**, *31*, 193–198.

(5) Sharp, P.; Bloomfield, V. A. Light Scattering from Wormlike Chains with Excluded Volume Effects. *Biopolymers* **1968**, *6*, 1201–1211.

(6) Murakami, H.; Norisuye, T.; Fujita, H. Dimensional and Hydrodynamic Properties of Poly(Hexyl Isocyanate) in Hexane. *Macromolecules* **1980**, *13*, 345–352.

(7) Matyjaszewski, K. Macromolecular Engineering by Controlled/Living Ionic and Radical Polymerizations. *Macromol. Symp.* **2001**, *174*, 51–68.

(8) Thoma, J. L. Characterizing Polymers with Complex Architecture Using Pyrene Excimer Fluorescence, University of Waterloo, 2021.

(9) Li, T.; Li, H.; Wang, H.; Lu, W.; Osa, M.; Wang, Y.; Mays, J.; Hong, K. Chain Flexibility and Glass Transition Temperatures of Poly(n-Alkyl (Meth)Acrylate)s: Implications of Tacticity and Chain Dynamics. *Polymer*. **2021**, *213*, 123207.

(10) Haidar Ahmad, I. A.; Striegel, A. M. Influence of Second Virial Coefficient and Persistence Length on Dilute Solution Polymer Conformation. *Anal. Bioanal. Chem.* **2011**, *399*, 1515–1521.

(11) Yamakawa, H.; Yoshizaki, T. Transport Coefficients of Helical Wormlike Chains. 3. Intrinsic Viscosity. *Macromolecules* **1980**, *13*, 633–643.

(12) Yamakawa, H.; Fujii, M. Intrinsic Viscosity of Wormlike Chains. Determination of the Shift Factor. *Macromolecules* **1974**, *7*, 128–135.

(13) Bohdanecky, M. New Method for Estimating the Parameters of the Wormlike Chain Model from the Intrinsic Viscosity of Stiff-Chain Polymers. *Macromolecules* **1983**, *16*, 1483–1492.

(14) Fox, T. G.; Flory, P. J. Second-Order Transition Temperatures and Related Properties of Polystyrene. I. Influence of Molecular Weight. *J. Appl. Phys.* **1950**, *21*, 581–591.

(15) Rogers, S. S.; Mandelkern, L. Glass Formation in Polymers. I. The Glass Transitions of the Poly-(*n*-Alkyl Methacrylates). *J. Phys. Chem.* **1957**, *61*, 985–990.

(16) Dais, P.; Spyros, A. 13C Nuclear Magnetic Relaxation and Local Dynamics of Synthetic Polymers in Dilute Solution and in the Bulk State. *Prog. Nucl. Magn. Reson. Spectrosc.* **1995**, *27*, 555–633.

(17) Zhuravleva, A.; Korzhnev, D. M. Protein Folding by NMR. *Prog. Nucl. Magn. Reson. Spectrosc.* **2017**, *100*, 52–77.

(18) Chatterjee, A.; Kumar, A.; Chugh, J.; Srivastava, S.; Bhavesh, N. S.; Hosur, R. V. NMR of Unfolded Proteins. *J. Chem. Sci* **2005**, *117*, 3–21.

(19) Dreydoppel, M.; Balbach, J.; Weininger, U. Monitoring Protein Unfolding Transitions by NMR-Spectroscopy. *J. Biomol. NMR* **2022**, *76*, 3–15.

(20) Mirau, P. A.; Heffner, S. A.; Koegler, G.; Bovey, F. A. 2D and 3D NMR for Polymer Characterization. *Polym. Int.* **1991**, *26*, 29–34.

(21) Duhamel, J. New Insights in the Study of Pyrene Excimer Fluorescence to Characterize Macromolecules and Their Supramolecular Assemblies in Solution. *Langmuir* **2012**, *28*, 6527–6538.

(22) Rubinstein, M.; Colby, R. H. Polymer Physics; Oxford University Press: New York, 2003.

(23) Kaszuba, M.; McKnight, D.; Connah, M. T.; McNeil-Watson, F. K.; Nobbmann, U. Measuring Sub Nanometre Sizes Using Dynamic Light Scattering. *J. Nanoparticle Res.* **2008**, *10*, 823–829.

(24) Duhamel, J.; Kanyo, J.; Dinter-Gottlieb, G.; Lu, P. Fluorescence Emission of Ethidium Bromide Intercalated in Defined DNA Duplexes: Evaluation of Hydrodynamics Components. *Biochemistry* **1996**, *35*, 16687–16697.

(25) Díaz, A. N.; García Sánchez, F.; López Guerrero, M. M. Modulated Anisotropy Fluorescence for Quantitative Determination of Carbaryl and Benomyl. *Talanta* **2003**, *60*, 629–634.

(26) Lakowicz, J. R. Principles of Fluorescence Spectroscopy, 3rd ed.; 2000.

(27) Winnik, M. A. End-to-End Cyclization of Polymer Chains. *Acc. Chem. Res.* **1985**, *18*, 73–79.

(28) Duhamel, J. Global Analysis of Fluorescence Decays to Probe the Internal Dynamics of Fluorescently Labeled Macromolecules. *Langmuir* **2014**, *30*, 2307–2324.

(29) Zachariasse, K. A.; Maçanita, A. L.; Kühnle, W. Chain Length Dependence of Intramolecular Excimer Formation with 1, n -Bis(1-Pyrenylcarboxy)Alkanes for n = 1−16, 22, and 32. *J. Phys. Chem. B* **1999**, *103*, 9356–9365.

(30) Neuweiler, H.; Löllmann, M.; Doose, S.; Sauer, M. Dynamics of Unfolded Polypeptide Chains in Crowded Environment Studied by Fluorescence Correlation Spectroscopy. *J. Mol. Biol.* **2007**, *365*, 856–869.

(31) Zachariasse, K.; Kühnle, W. Intramolecular Excimers with α , ω -Diarylalkanes. *Zeitschrift für Phys. Chemie* **1976**, *101*, 267–276.

(32) Ingratta, M.; Hollinger, J.; Duhamel, J. A Case for Using Randomly Labeled Polymers to Study Long-Range Polymer Chain Dynamics by Fluorescence. *J. Am. Chem. Soc.* **2008**, *130*, 9420–9428.

(33) Tassin, J. F.; Monnerie, L.; Fetters, L. J. Infrared Dichroism Study of the Relaxation of Selected Segments along a Stretched Polymer Chain and Comparison with Theoretical Models. *Macromolecules* **1988**, *21*, 2404–2412.

(34) Ellison, C. J.; Torkelson, J. M. The Distribution of Glass-Transition Temperatures in Nanoscopically Confined Glass Formers. *Nat. Mater.* **2003**, *2*, 695–700.

(35) Lee, S.; Winnik, M. A. Cyclization Rates for Two Points in the Interior of a Polymer Chain. *Macromolecules* **1997**, *30*, 2633–2641.

(36) Winnik, M. A.; Redpath, T.; Richards, D. H. The Dynamics of End-to-End Cyclization in Polystyrene Probed by Pyrene Excimer Formation. *Macromolecules* **1980**, *13*, 328–335.

(37) Nakajima, A. Fluorescence Spectra of Pyrene in Chlorinated Aromatic Solvents. *J. Lumin.* **1976**, *11*, 429–432.

(38) Kalyanasundaram, K.; Thomas, J. K. Environmental Effects on Vibronic Band Intensities in Pyrene Monomer Fluorescence and Their Application in Studies of Micellar Systems. *J. Am. Chem. Soc.* **1977**, *99*, 2039–2044.

(39) Casier, R.; Duhamel, J. The Effect of Amino Acid Size on the Internal Dynamics and Conformational Freedom of Polypeptides. *Macromolecules* **2020**, *53*, 9811–9822.

(40) Farhangi, S.; Weiss, H.; Duhamel, J. Effect of Side-Chain Length on the Polymer Chain Dynamics of Poly(Alkyl Methacrylate)s in Solution. *Macromolecules* **2013**, *46*, 9738–9747.

(41) Mathew, A. K.; Siu, H.; Duhamel, J. A Blob Model To Study Chain Folding by Fluorescence. *Macromolecules* **1999**, *32*, 7100–7108.

(42) Siu, H.; Duhamel, J. Comparison of the Association Level of a Pyrene-Labeled Associative Polymer Obtained from an Analysis Based on Two Different Models. *J. Phys. Chem. B* **2005**, *109*, 1770–1780.

(43) Duhamel, J.; Yekta, A.; Winnik, M. A.; Jao, T. C.; Mishra, M. K.; Rubin, I. D. A Blob Model To Study Polymer Chain Dynamics in Solution. *J. Phys. Chem* **1993**, *97*, 13708–13712.

(44) Duhamel, J. Internal Dynamics of Dendritic Molecules Probed by Pyrene Excimer Formation. *Polymers (Basel)*. **2012**, *4*, 211–239.

(45) Teertstra, S. J.; Lin, W. Y.; Gauthier, M.; Ingratta, M.; Duhamel, J. Comparison of the Long Range Polymer Chain Dynamics of Polystyrene and Cis-Polyisoprene Using Polymers Randomly Labeled with Pyrene. *Polymer*. **2009**, *50*, 5456–5466.

(46) Yip, J.; Duhamel, J.; Bahun, G. J.; Adronov, A. A Study of the Dynamics of the Branch Ends of a Series of Pyrene-Labeled Dendrimers Based on Pyrene Excimer Formation. *J. Phys. Chem. B* **2010**, *114*, 10254–10265.

(47) Fowler, M. A.; Duhamel, J.; Bahun, G. J.; Adronov, A.; Zaragoza-Galán, G.; Rivera, E. Studying Pyrene-Labeled Macromolecules with the Model-Free Analysis. *J. Phys. Chem. B* **2012**, *116*, 14689–14699.

(48) Thoma, J. L.; Duhamel, J.; Li, M. J.; Bertocchi, M. J.; Weiss, R. G. Long-Range, Polymer Chain Dynamics of a "Stiff" Polymer. Fluorescence from Poly(Isobutylene-Alt-Maleic Anhydride) with N-(1-Pyrenylmethyl)Succinimide Groups. *Macromolecules* **2017**, *50*, 3396–3403.

(49) Thoma, J.; Duhamel, J.; Bertocchi, M.; Weiss, R. Long Range Polymer Chain Dynamics of Highly Flexible Polysiloxane in Solution Probed by Pyrene Excimer Fluorescence. *Polymers (Basel)*. **2018**, *10*, 345.

(50) Li, L.; Duhamel, J. Conformation of Pyrene-Labeled Amylose in DMSO Characterized with the Fluorescence Blob Model. *Macromolecules* **2016**, *49*, 7965–7974.

(51) Farhangi, S.; Casier, R.; Li, L.; Thoma, J. L.; Duhamel, J. Characterization of the Long-Range Internal Dynamics of Pyrene-Labeled Macromolecules by Pyrene Excimer Fluorescence. *Macromolecules* **2016**, *49*, 9597–9604.

(52) “Solvents for Common Polymers.” In CRC Handbook of Chemistry & Physics, 101st Edition (Internet Version); Rumble, J. R., Ed.; CRC Press/Taylor & Francis: Boca Raton, FL.

(53) Xu, Y.; Ding, W.; Liu, J.; Li, Y.; Kennedy, J. F.; Gu, Q.; Shao, S. Preparation and Characterization of Organic-Soluble Acetylated Starch Nanocrystals. *Carbohydr. Polym.* **2010**, *80*, 1078–1084.

(54) Hall, T.; Whitton, G.; Casier, R.; Gauthier, M.; Duhamel, J. Arborescent Poly(L-Glutamic Acid)s as Standards To Study the Dense Interior of Polypeptide Mesoglobules by Pyrene Excimer Fluorescence. *Macromolecules* **2018**, *51*, 7914–7923.

(55) Wang, D.; Liu, X.; Zeng, G.; Zhao, J.; Liu, Y.; Wang, Q.; Chen, F.; Li, X.; Yang, Q. Understanding the Impact of Cationic Polyacrylamide on Anaerobic Digestion of Waste Activated Sludge. *Water Res.* **2018**, *130*, 281–290.

(56) Ma, J.; Shi, J.; Ding, H.; Zhu, G.; Fu, K.; Fu, X. Synthesis of Cationic Polyacrylamide by Low-Pressure UV Initiation for Turbidity Water Flocculation. *Chem. Eng. J.* **2017**, *312*, 20–29.

(57) Ellis, R. P.; Cochrane, P.; Finlay, M.; Dale, B.; Duþus, C. M.; Lynn, A.; Morrison, I. M.; Derek, R.; Prentice, M.; Swanston1, J. S.; Tiller1, S. A. Starch Production and Industrial Use. *J Sci. Food Agric.* **1998**, *77*, 289–311.

(58) Khlestkin, V. K.; Peltek, S. E.; Kolchanov, N. A. Review of Direct Chemical and Biochemical Transformations of Starch. *Carbohydr. Polym.* **2018**, *181*, 460–476.

(59) Kim, H. Y.; Park, S. S.; Lim, S. T. Preparation, Characterization and Utilization of Starch Nanoparticles. *Colloids Surfaces B Biointerfaces* **2015**, *126*, 607–620.

(60) Voet, D.; Voet, J. G. Biochemistry, 4th ed.; John Wiley & Sons, inc.: Hoboken, NJ, 2011.

Chapter 2

(1) Rudin, A. The Elements of Polymer Science & Engineering; Elsevier Science & Technology Books, 1998.

(2) Fox, T. G.; Flory, P. J. Second-Order Transition Temperatures and Related Properties of Polystyrene. I. Influence of Molecular Weight. *J. Appl. Phys.* **1950**, *21*, 581–591.

(3) Rogers, S. S.; Mandelkern, L. Glass Formation in Polymers. I. The Glass Transitions of the Poly-(n-Alkyl Methacrylates). *J. Phys. Chem.* **1957**, *61*, 985–990.

(4) Hokajo, T.; Terao, K.; Nakamura, Y.; Norisuye, T. Solution Properties of Polymacromonomers Consisting of Polystyrene V. Effect of Side Chain Length on Chain Stiffness. *Polym. J.* **2001**, *33*, 481–485.

(5) Terao, K.; Takeo, Y.; Tazaki, M.; Nakamura, Y.; Norisuye, T. Polymacromonomer Consisting of Polystyrene. Light Scattering Characterization in Cyclohexane. *Polym. J.* **1999**, *31*, 193–198.

(6) Sharp, P.; Bloomfield, V. A. Light Scattering from Wormlike Chains with Excluded Volume Effects. *Biopolymers* **1968**, *6*, 1201–1211.

(7) Murakami, H.; Norisuye, T.; Fujita, H. Dimensional and Hydrodynamic Properties of Poly(Hexyl Isocyanate) in Hexane. *Macromolecules* **1980**, *13*, 345–352.

(8) Mourey, T.; Le, K.; Bryan, T.; Zheng, S.; Bennett, G. Determining Persistence Length by Size-Exclusion Chromatography. *Polymer*. **2005**, *46*, 9033–9042.

(9) Li, T.; Li, H.; Wang, H.; Lu, W.; Osa, M.; Wang, Y.; Mays, J.; Hong, K. Chain Flexibility and Glass Transition Temperatures of Poly(n-Alkyl (Meth)Acrylate)s: Implications of Tacticity and Chain Dynamics. *Polymer.* **2021**, *213*, 123207.

(10) Haidar Ahmad, I. A.; Striegel, A. M. Influence of Second Virial Coefficient and Persistence Length on Dilute Solution Polymer Conformation. *Anal. Bioanal. Chem.* **2011**, *399*, 1515–1521.

(11) Dais, P.; Spyros, A. 13C Nuclear Magnetic Relaxation and Local Dynamics of Synthetic Polymers in Dilute Solution and in the Bulk State. *Prog. Nucl. Magn. Reson. Spectrosc.* **1995**, *27*, 555–633.

(12) Farhangi, S.; Weiss, H.; Duhamel, J. Effect of Side-Chain Length on the Polymer Chain Dynamics of Poly(Alkyl Methacrylate)s in Solution. *Macromolecules* **2013**, *46*, 9738–9747.

(13) Casier, R.; Duhamel, J. Blob-Based Predictions of Protein Folding Times from the Amino Acid-Dependent Conformation of Polypeptides in Solution. *Macromolecules* **2021**, *54*, 919–929.

(14) Duhamel, J. Global Analysis of Fluorescence Decays to Probe the Internal Dynamics of Fluorescently Labeled Macromolecules. *Langmuir* **2014**, *30*, 2307–2324.

(15) Mathew, A. K.; Siu, H.; Duhamel, J. A Blob Model To Study Chain Folding by Fluorescence. *Macromolecules* **1999**, *32*, 7100–7108.

(16) Casier, R.; Duhamel, J. The Effect of Amino Acid Size on the Internal Dynamics and Conformational Freedom of Polypeptides. *Macromolecules* **2020**, *53*, 9811–9822.

(17) Kratky, O.; Porod, G. Röntgenuntersuchung Gelöster Fadenmoleküle. *Recl. Trav. Chim* **1949**, *68*, 1106–1122.

(18) Thoma, J. L. Characterizing Polymers with Complex Architecture Using Pyrene Excimer Fluorescence, University of Waterloo, 2021.

(19) Rubinstein, M.; Colby, R. H. Polymer Physics; Oxford University Press: New York, 2003.

(20) Zaragoza-Galán, G.; Fowler, M. A.; Duhamel, J.; Rein, R.; Solladié, N.; Rivera, E. Synthesis and Characterization of Novel Pyrene-Dendronized Porphyrins Exhibiting Efficient Fluorescence Resonance Energy Transfer: Optical and Photophysical Properties. *Langmuir* **2012**, *28*, 11195–11205.

(21) Yip, J.; Duhamel, J.; Qiu, X. P.; Winnik, F. M. Long-Range Polymer Chain Dynamics of Pyrene-Labeled Poly(N-Isopropylacrylamide)s Studied by Fluorescence. *Macromolecules* **2011**, *44*, 5363–5372.

(22) Ingratta, M.; Mathew, M.; Duhamel, J. How Switching the Substituent of a Pyrene Derivative from a Methyl to a Butyl Affects the Fluorescence Response of Polystyrene Randomly Labeled with Pyrene. *Can. J. Chem.* **2010**, *88*, 217–227.

(23) Farhangi, S.; Duhamel, J. Probing Side Chain Dynamics of Branched Macromolecules by Pyrene Excimer Fluorescence. *Macromolecules* **2016**, *49*, 353–361.

(24) Hall, T.; Whitton, G.; Casier, R.; Gauthier, M.; Duhamel, J. Arborescent Poly(L-Glutamic Acid)s as Standards To Study the Dense Interior of Polypeptide Mesoglobules by Pyrene Excimer Fluorescence. *Macromolecules* **2018**, *51*, 7914–7923.

(25) Duhamel, J. New Insights in the Study of Pyrene Excimer Fluorescence to Characterize Macromolecules and Their Supramolecular Assemblies in Solution. *Langmuir* **2012**, *28*, 6527–6538.

(26) Ingratta, M.; Hollinger, J.; Duhamel, J. A Case for Using Randomly Labeled Polymers to Study Long-Range Polymer Chain Dynamics by Fluorescence. *J. Am. Chem. Soc.* **2008**, *130*, 9420–9428.

(27) Thoma, J. L.; Duhamel, J. Characterization of the Local Volume Probed by the Side-Chain Ends of Poly(Oligo(Ethylene Glycol) 1-Pyrenemethyl Ether Methacrylate) Bottle Brushes in Solution Using Pyrene Excimer Fluorescence. *Macromolecules* **2021**, *54*, 9341–9350.

(28) Ge, Y.; Wen, Y.; Liu, H.; Lu, T.; Yu, Y.; Zhang, X.; Li, B.; Zhang, S. T.; Li, W.; Yang, B. A Key Stacking Factor for the Effective Formation of Pyrene Excimer in Crystals: Degree of π-π Overlap. *J. Mater. Chem. C* **2020**, *8*, 11830–11838.

(29) Rathgeber, S.; Pakula, T.; Wilk, A.; Matyjaszewski, K.; Beers, K. L. On the Shape of Bottle-Brush Macromolecules: Systematic Variation of Architectural Parameters. *J. Chem. Phys.* **2005**, *122*, 164903.

(30) Fredrickson, G. H. Surfactant-Induced Lyotropic Behavior of Flexible Polymer Solutions. *Macromolecules* **1993**, *26*, 2825–2831.

(31) Norisuye, T.; Fujita, H. Excluded-Volume Effects in Dilute Polymer Solutions. XIII. Effects of Chain Stiffness. *Polym. J.* **1982**, *14*, 143–147.

(32) Pan, T.; Dutta, S.; Kamble, Y.; Patel, B. B.; Wade, M. A.; Rogers, S. A.; Diao, Y.; Guironnet, D.; Sing, C. E. Materials Design of Highly Branched Bottlebrush Polymers at

the Intersection of Modeling, Synthesis, Processing, and Characterization. *Chemistry of Materials* **2022**, *34*, 1990–2024.

(33) Subbotin, A.; Saariaho, M.; Ikkala, O.; ten Brinke, G. Elasticity of Comb Copolymer Cylindrical Brushes. *Macromolecules* **2000**, *33* (9), 3447–3452.

(34) Thoma, J. L.; Duhamel, J.; Li, M. J.; Bertocchi, M. J.; Weiss, R. G. Long-Range, Polymer Chain Dynamics of a "Stiff" Polymer. Fluorescence from Poly(Isobutylene-Alt-Maleic Anhydride) with N-(1-Pyrenylmethyl)Succinimide Groups. *Macromolecules* **2017**, *50*, 3396–3403.

(35) Thoma, J.; Duhamel, J.; Bertocchi, M.; Weiss, R. Long Range Polymer Chain Dynamics of Highly Flexible Polysiloxane in Solution Probed by Pyrene Excimer Fluorescence. *Polymers (Basel)*. **2018**, *10*, 345.

(36) Li, L.; Duhamel, J. Conformation of Pyrene-Labeled Amylose in DMSO Characterized with the Fluorescence Blob Model. *Macromolecules* **2016**, *49*, 7965–7974.

(37) Cho, H. Y.; Krys, P.; Szczešniak, K.; Schroeder, H.; Park, S.; Jurga, S.; Buback, M.; Matyjaszewski, K. Synthesis of Poly(OEOMA) Using Macromonomers via "Grafting-Through" ATRP. *Macromolecules* **2015**, *48*, 6385–6395.

Chapter 3

(1) Zachariasse, K. A.; Maçanita, A. L.; Kühnle, W. Chain Length Dependence of Intramolecular Excimer Formation with 1, n -Bis(1-Pyrenylcarboxy)Alkanes for n = 1−16, 22, and 32. *J. Phys. Chem. B* **1999**, *103*, 9356–9365.

(2) Winnik, M. A. End-to-End Cyclization of Polymer Chains. *Acc. Chem. Res.* **1985**, *18*, 73–

79.

(3) Duhamel, J. Global Analysis of Fluorescence Decays to Probe the Internal Dynamics of Fluorescently Labeled Macromolecules. *Langmuir* **2014**, *30*, 2307–2324.

(4) Neuweiler, H.; Löllmann, M.; Doose, S.; Sauer, M. Dynamics of Unfolded Polypeptide Chains in Crowded Environment Studied by Fluorescence Correlation Spectroscopy. *J. Mol. Biol.* **2007**, *365*, 856–869.

(5) Farhangi, S.; Weiss, H.; Duhamel, J. Effect of Side-Chain Length on the Polymer Chain Dynamics of Poly(Alkyl Methacrylate)s in Solution. *Macromolecules* **2013**, *46*, 9738–9747.

(6) Thoma, J. L.; Duhamel, J.; Li, M. J.; Bertocchi, M. J.; Weiss, R. G. Long-Range Polymer Chain Dynamics of a "Stiff" Polymer. Fluorescence from Poly(Isobutylene-Alt-Maleic Anhydride) with N-(1-Pyrenylmethyl)Succinimide Groups. *Macromolecules* **2017**, *50*, 3396–3403.

(7) Thoma, J.; Duhamel, J.; Bertocchi, M.; Weiss, R. Long Range Polymer Chain Dynamics of Highly Flexible Polysiloxane in Solution Probed by Pyrene Excimer Fluorescence. *Polymers (Basel)* **2018**, *10*, 345.

(8) Lakowicz, J. R. Principles of Fluorescence Spectroscopy, 3rd ed.; 2000.

(9) Thoma, J. L.; McNelles, S. A.; Adronov, A.; Duhamel, J. Direct Measure of the Local Concentration of Pyrenyl Groups in Pyrene-Labeled Dendrons Derived from the Rate of Fluorescence Collisional Quenching. *Polymers (Basel)* **2020**, *12*, 2919.

(10) McNelles, S. A.; Thoma, J. L.; Adronov, A.; Duhamel, J. Quantitative Characterization of the Molecular Dimensions of Flexible Dendritic Macromolecules in Solution by Pyrene Excimer Fluorescence. *Macromolecules* **2018**, *51*, 1586–1590.

(11) Ingratta, M.; Hollinger, J.; Duhamel, J. A Case for Using Randomly Labeled Polymers to Study Long-Range Polymer Chain Dynamics by Fluorescence. *J. Am. Chem. Soc.* **2008**, *130*, 9420–9428.

(12) Duhamel, J. New Insights in the Study of Pyrene Excimer Fluorescence to Characterize Macromolecules and Their Supramolecular Assemblies in Solution. *Langmuir* **2012**, *28*, 6527–6538.

(13) Mathew, A. K.; Siu, H.; Duhamel, J. A Blob Model to Study Chain Folding by Fluorescence. *Macromolecules* **1999**, *32*, 7100–7108.

(14) Winnik, M. A.; Egan, L. S.; Tencer, M.; Croucher, M. D. Luminescence Studies on Sterically Stabilized Polymer Colloid Particles: Pyrene Excimer Formation. *Polymer* **1987**, *28*, 1553–1560.

(15) Zachariasse, K. A.; Busse, R.; Duveneck, G.; Kühnle, W. Intramolecular Monomer and Excimer Fluorescence with Dipyrenylpropanes: Double-Exponential versus Triple-Exponential Decays. *J. Photochem.* **1985**, *28*, 237–253.

(16) Winnik, M. A.; Li, X. B.; Guillet, J. E. Cyclization Dynamics of Polymers. 13. Effects of Added Polymer on the Conformation and Dynamics of Polystyrene Containing Evenly Spaced Pyrene Groups. *Macromolecules* **1984**, *17*, 699–702.

(17) Siu, H.; Duhamel, J. Comparison of the Association Level of a Pyrene-Labeled Associative Polymer Obtained from an Analysis Based on Two Different Models. *J. Phys. Chem. B* **2005**, *109*, 1770–1780.

(18) Chen, S.; Duhamel, J.; Winnik, M. A. Probing End-to-End Cyclization beyond Willemski and Fixman. *J. Phys. Chem. B* **2011**, *115*, 3289–3302.

(19) Winnik, M. A.; Redpath, T.; Richards, D. H. The Dynamics of End-to-End Cyclization in

Polystyrene Probed by Pyrene Excimer Formation. *Macromolecules* **1980**, *13*, 328–335.

(20) Zachariasse, K.; Kühnle, W. Intramolecular Excimers with α, ω -Diarylalkanes. *Zeitschrift für Phys. Chemie* **1976**, *101*, 267–276.

(21) Wilemski, G.; Fixman, M. Diffusion-controlled Intrachain Reactions of Polymers. I Theory. *J. Chem. Phys.* **1974**, *60*, 866–877.

(22) Wilemski, G.; Fixman, M. Diffusion-controlled Intrachain Reactions of Polymers. II Results for a Pair of Terminal Reactive Groups. *J. Chem. Phys.* **1974**, *60*, 878–890.

(23) Farhangi, S.; Duhamel, J. Long Range Polymer Chain Dynamics Studied by Fluorescence Quenching. *Macromolecules* **2016**, *49*, 6149–6162.

(24) Yip, J.; Duhamel, J.; Qiu, X. P.; Winnik, F. M. Long-Range Polymer Chain Dynamics of Pyrene-Labeled Poly(N -Isopropylacrylamide)s Studied by Fluorescence. *Macromolecules* **2011**, *44*, 5363–5372.

(25) Yip, J.; Duhamel, J.; Bahun, G. J.; Adronov, A. A Study of the Dynamics of the Branch Ends of a Series of Pyrene-Labeled Dendrimers Based on Pyrene Excimer Formation. *J. Phys. Chem. B* **2010**, *114*, 10254–10265.

(26) Fowler, M. A.; Duhamel, J.; Bahun, G. J.; Adronov, A.; Zaragoza-Galán, G.; Rivera, E. Studying Pyrene-Labeled Macromolecules with the Model-Free Analysis. *J. Phys. Chem. B* **2012**, *116*, 14689–14699.

(27) Thoma, J. L.; Duhamel, J. Characterization of the Local Volume Probed by the Side-Chain Ends of Poly(Oligo(Ethylene Glycol) 1-Pyrenemethyl Ether Methacrylate) Bottle Brushes in Solution Using Pyrene Excimer Fluorescence. *Macromolecules* **2021**, *54*, 9341–9350.

(28) Farhangi, S.; Casier, R.; Li, L.; Thoma, J. L.; Duhamel, J. Characterization of the Long-Range Internal Dynamics of Pyrene-Labeled Macromolecules by Pyrene Excimer

Fluorescence. *Macromolecules* **2016**, *49*, 9597–9604.

(29) Li, L.; Duhamel, J. Conformation of Pyrene-Labeled Amylose in DMSO Characterized with the Fluorescence Blob Model. *Macromolecules* **2016**, *49*, 7965–7974.

(30) Rogers, S. S.; Mandelkern, L. Glass Formation in Polymers. I. The Glass Transitions of the Poly-(n-Alkyl Methacrylates). *J. Phys. Chem.* **1957**, *61*, 985–990.

Chapter 4

(1) Rudin, A. The Elements of Polymer Science & Engineering; Elsevier Science & Technology Books, 1998.

(2) Fox, T. G.; Flory, P. J. Second-Order Transition Temperatures and Related Properties of Polystyrene. I. Influence of Molecular Weight. *J. Appl. Phys.* **1950**, *21*, 581–591.

(3) Rogers, S. S.; Mandelkern, L. Glass Formation in Polymers. I. The Glass Transitions of the Poly-(*n*-Alkyl Methacrylates). *J. Phys. Chem.* **1957**, *61*, 985–990.

(4) Kratky, O.; Porod, G. Röntgenuntersuchung Gelöster Fadenmoleküle. *Recl. Trav. Chim* **1949**, *68*, 1106–1122.

(5) Farhangi, S.; Weiss, H.; Duhamel, J. Effect of Side-Chain Length on the Polymer Chain Dynamics of Poly(Alkyl Methacrylate)s in Solution. *Macromolecules* **2013**, *46*, 9738–9747.

(6) Casier, R.; Duhamel, J. The Effect of Amino Acid Size on the Internal Dynamics and Conformational Freedom of Polypeptides. *Macromolecules* **2020**, *53*, 9811–9822.

(7) Thoma, J. L. Characterizing Polymers with Complex Architecture Using Pyrene Excimer Fluorescence, University of Waterloo, 2021.

(8) Fredrickson, G. H. Surfactant-Induced Lyotropic Behavior of Flexible Polymer Solutions. *Macromolecules* **1993**, *26*, 2825–2831.

(9) Norisuye, T.; Fujita, H. Excluded-Volume Effects in Dilute Polymer Solutions. XIII. Effects of Chain Stiffness. *Polym. J.* **1982**, *14*, 143–147.

(10) Mathew, A. K.; Siu, H.; Duhamel, J. A Blob Model to Study Chain Folding by Fluorescence. *Macromolecules* **1999**, *32*, 7100–7108.

(11) Farhangi, S.; Duhamel, J. Probing Side Chain Dynamics of Branched Macromolecules by Pyrene Excimer Fluorescence. *Macromolecules* **2016**, *49*, 353–361.

(12) Li, L.; Duhamel, J. Conformation of Pyrene-Labeled Amylose in DMSO Characterized with the Fluorescence Blob Model. *Macromolecules* **2016**, *49*, 7965–7974.

(13) Casier, R.; Duhamel, J. Effects of Glycine on the Local Conformation and Internal Backbone Dynamics of Polypeptides. *Macromolecules* **2021**, *54*, 8904–8912.

(14) Tan, S.; Tan, H. T.; Chung, M. C. M. Membrane Proteins and Membrane Proteomics. *Proteomics* **2008**, *8*, 3924–3932.

(15) Boulton, S.; Akimoto, M.; Akbarizadeh, S.; Melacini, G. Free Energy Landscape Remodeling of the Cardiac Pacemaker Channel Explains the Molecular Basis of Familial Sinus Bradycardia. *J. Biol. Chem.* **2017**, *292*, 6414–6428.

(16) Boyd, C. M.; Bubeck, D. Advances in CryoEM and its Impact on b -Pore Forming Proteins. *Curr. Opin. Struct. Biol.* **2018**, *52*, 41–49.

(17) Ovchinnikov, Y. A. Structure of Rhodopsin and Bacteriorhodopsin. *Photochem. Photobiol.* **1987**, *45*, 909–914.

(18) Hedin, L. E.; Elofsson, A. An Introduction to Membrane Proteins. *J. Proteome Res* **2011**, *10*, 3324–3331.

(19) Fowler, M. A.; Duhamel, J.; Bahun, G. J.; Adronov, A.; Zaragoza-Galán, G.; Rivera, E. Studying Pyrene-Labeled Macromolecules with the Model-Free Analysis. *J. Phys. Chem. B* **2012**, *116*, 14689–14699.

(20) Carvalho, P. J.; Fonseca, C. H. G.; Moita, M.-L. C. J.; Santos, Â. F. S.; Coutinho, J. A. P. Thermophysical Properties of Glycols and Glymes. *J. Chem. Eng. Data* **2015**, *60*, 3721–3737.

(21) Tan, S.; Tan, H. T.; Chung, M. C. M. Membrane Proteins and Membrane Proteomics. *Proteomics* **2008**, *8*, 3924–3932.

(22) Boulton, S.; Akimoto, M.; Akbarizadeh, S.; Melacini, G. Free Energy Landscape Remodeling of the Cardiac Pacemaker Channel Explains the Molecular Basis of Familial Sinus Bradycardia. *J. Biol. Chem.* **2017**, *292*, 6414–6428.

(23) Boyd, C. M.; Bubeck, D. Advances in CryoEM and Its Impact on b -Pore Forming Proteins. *Curr. Opin. Struct. Biol.* **2018**, *52*, 41–49.

(24) Ovchinnikov, Y. A. Structure of Rhodopsin and Bacteriorhodopsin. *Photochem. Photobiol.* **1987**, *45*, 909–914.

(25) Hedin, L. E.; Elofsson, A. An Introduction to Membrane Proteins †. *J. Proteome Res* **2011**, *10*, 3324–3331.

APPENDICES

Appendix A Supporting Information for Chapter 2

A] ^{1}H NMR spectra

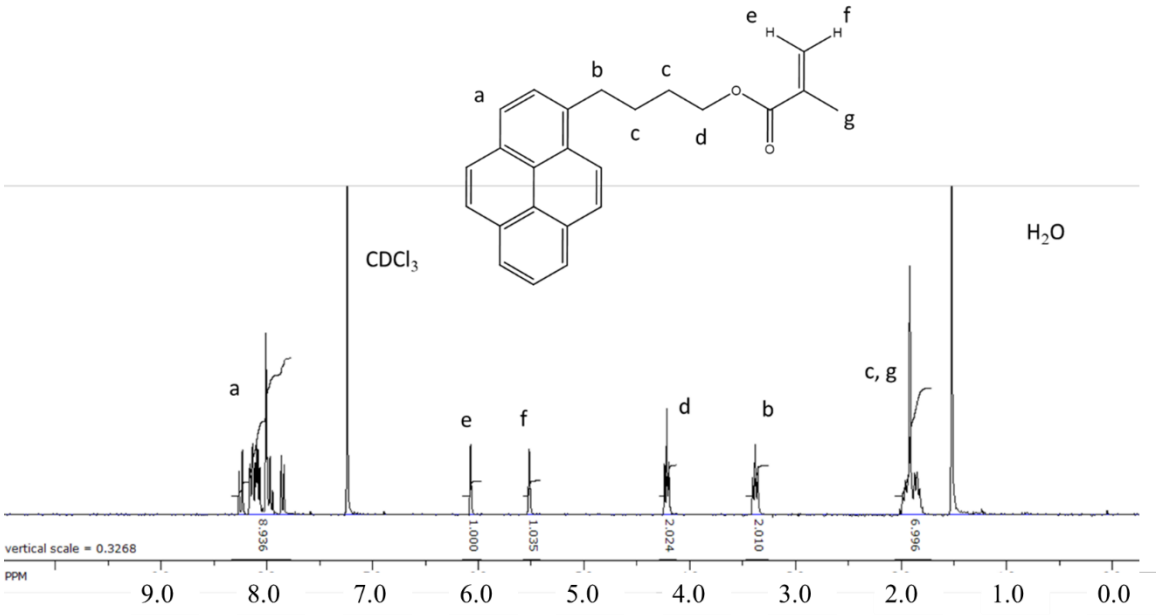

Figure S2.1. ^{1}H NMR spectrum of the 1-pyrenebutyl methacrylate in deuterated chloroform

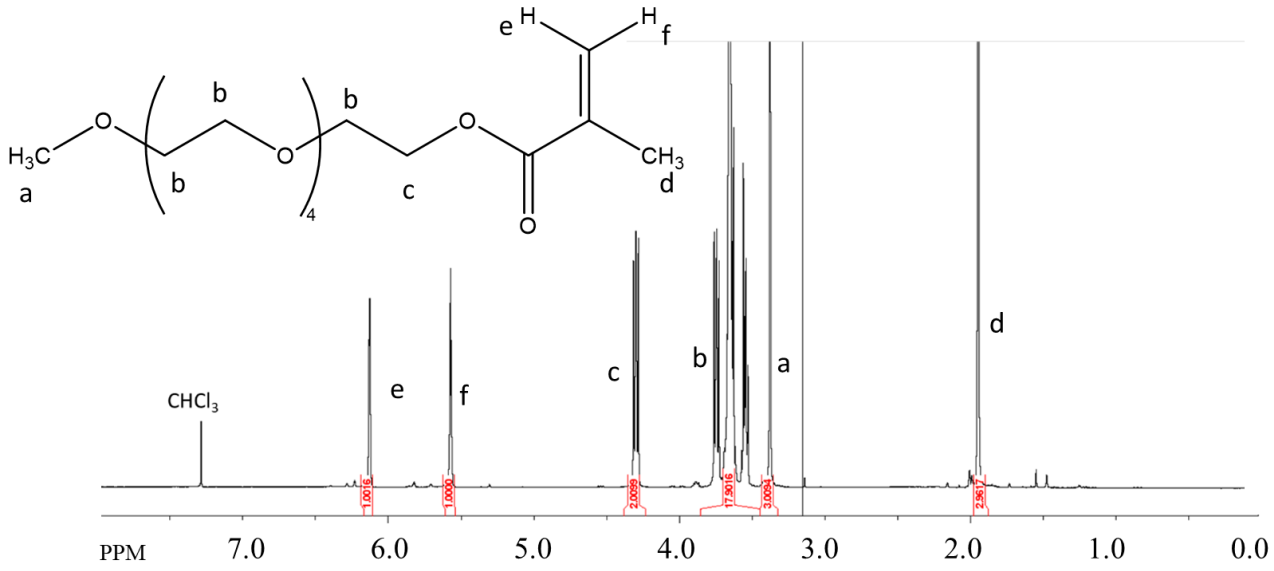

Figure S2.2. ^{1}H NMR spectrum of EG_5MA in deuterated chloroform

B] Equations describing the FBM

The following equations are used to fit the monomer (S2.1)

$$
\begin{aligned}
[Py^*] = &\left[Py^*_{diff}\right]_{t=0}\exp\left(-\left(A_2+\frac{1}{\tau_M}\right)t - A_3\left(1-\exp(-A_4 t)\right)\right)+\\
&\left([Py^*_{k2}]_{t=0}+\left[Py^*_{diff}\right]_{t=0}\exp(A_3)\sum_{i=0}^{\infty}\frac{A_3{}^i}{i!}\frac{A_2+iA_4}{A_2+iA_4-k_2}\right)\exp\left(-\left(k_2+\frac{1}{\tau_M}\right)t\right)\\
&-\left[Py^*_{diff}\right]_{t=0}\exp(A_3)\sum_{i=0}^{\infty}\frac{A_3{}^i}{i!}\frac{A_2+iA_4}{A_2+iA_4-k_2}\exp\left(-\left(A_2+iA_4+\frac{1}{\tau_M}\right)t\right)\\
&+[Py^*_{free}]_{t-0}\exp\left(-\frac{t}{\tau_M}\right)
\end{aligned}
\qquad \text{(S2.1)}
$$

and excimer (S2.2) decays of the pyrene-labelled polymers used in this study to the Fluorescence Blob Model.

$$
\begin{aligned}
[E^*] = &\, k_2\left([Py^*_{k2}]_{t=0}+[Py^*_{diff}]_{t=0}\exp(-A_3)\sum_{i=0}^{\infty}\frac{A_3{}^i}{i!}\frac{A_2+iA_4}{A_2+iA_4-k_2}\right)\\
&\times\frac{\exp\left(-\frac{t}{\tau_{E0}}\right)-\exp\left(-\left(k_2+\frac{1}{\tau_M}\right)t\right)}{k_2+\frac{1}{\tau_M}-\frac{t}{\tau_{E0}}}+[Py^*_{diff}]_{t=0}\exp(-A_3)\\
&\times\sum_{i=0}^{\infty}\frac{A_3{}^i}{i!}\frac{A_2+iA_4}{A_2+iA_4-k_2}\frac{\exp\left(-\left(A_2+iA_4+\frac{1}{\tau_M}\right)t\right)-\exp\left(-\frac{t}{\tau_{E0}}\right)}{A_2+iA_4+\frac{1}{\tau_M}-\frac{1}{\tau_{E0}}}\\
&+[E0^*]_{t=0}\times\exp\left(-\frac{t}{\tau_{E0}}\right)+[ED^*]_{t=0}\times\exp\left(-\frac{t}{\tau_{ED}}\right)
\end{aligned}
\qquad \text{(S2.2)}
$$

Where the parameters A_2, A_3, and A_4 are described by equations S2.3

$$A_2 = < n > \frac{k_{blob} k_e [blob]}{k_{blob} + k_e [blob]}$$

$$A_3 = < n > \left(\frac{k_{blob}}{k_{blob} + k_e [blob]} \right)^2 \qquad \text{(S2.3)}$$

$$A_4 = k_{blob} + k_e [blob]$$

C] Fluorescence spectra of the Py-PEG$_n$MA samples in organic solvents

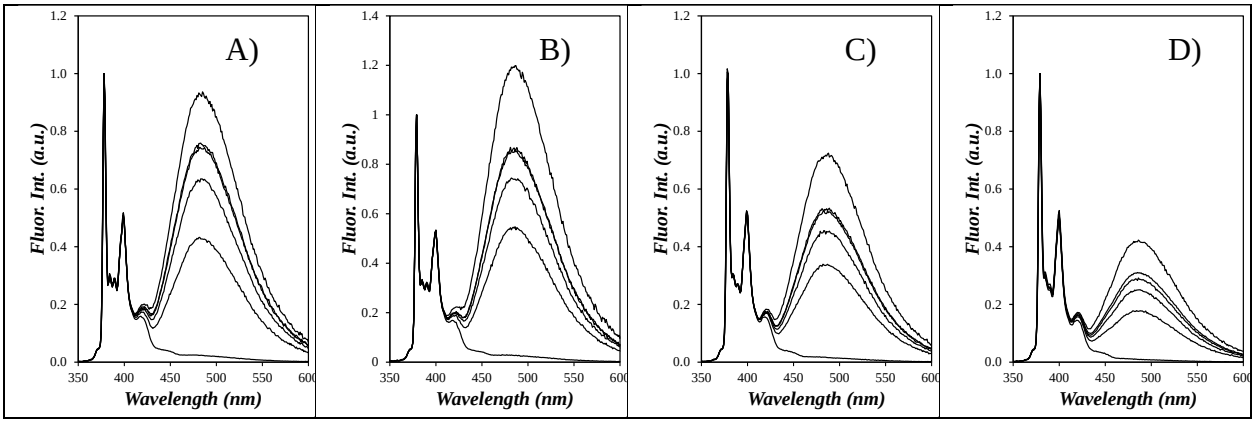

Figure S2.3. Steady-state fluorescence spectra of Py-PEG$_0$MA in (A) tetrahydrofuran, (B) toluene, (C) dimethylformamide, and (D) dimethyl sulfoxide.

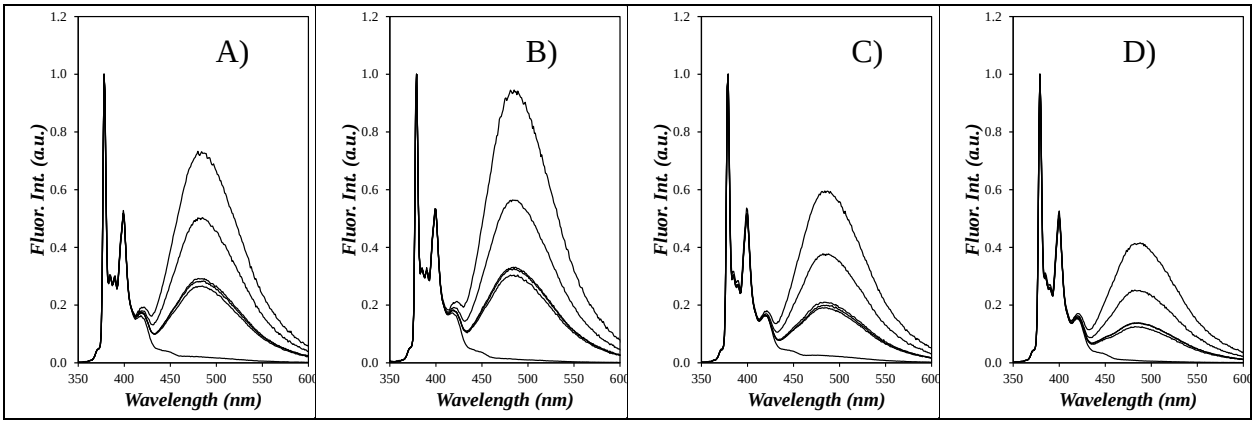

Figure S2.4. Steady-state fluorescence spectra of Py-PEG$_1$MA in (A) THF, (B) toluene, (C) DMF, (D) DMSO.

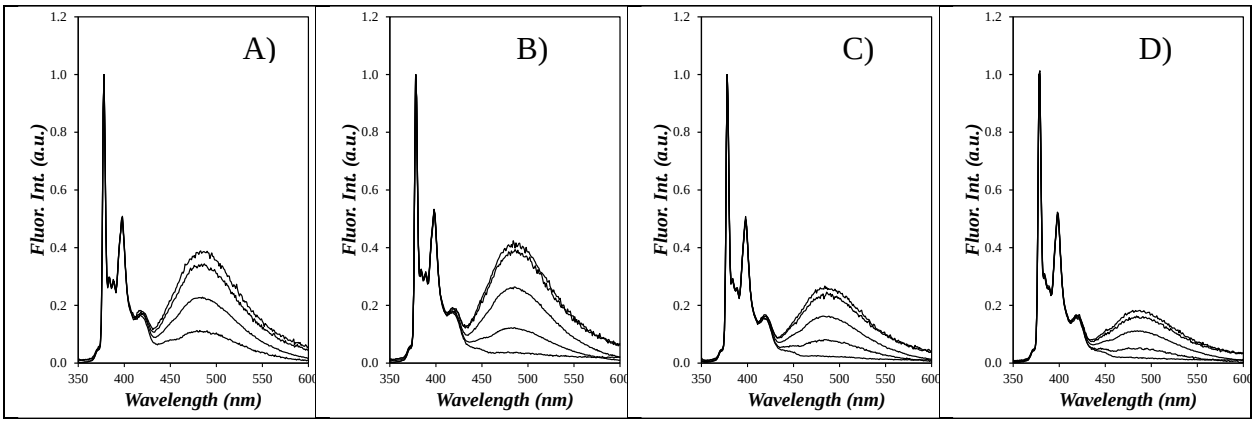

Figure S2.5. Steady-state fluorescence spectra of Py-PEG$_2$MA in (A) THF, (B) toluene, (C) DMF, (D) DMSO.

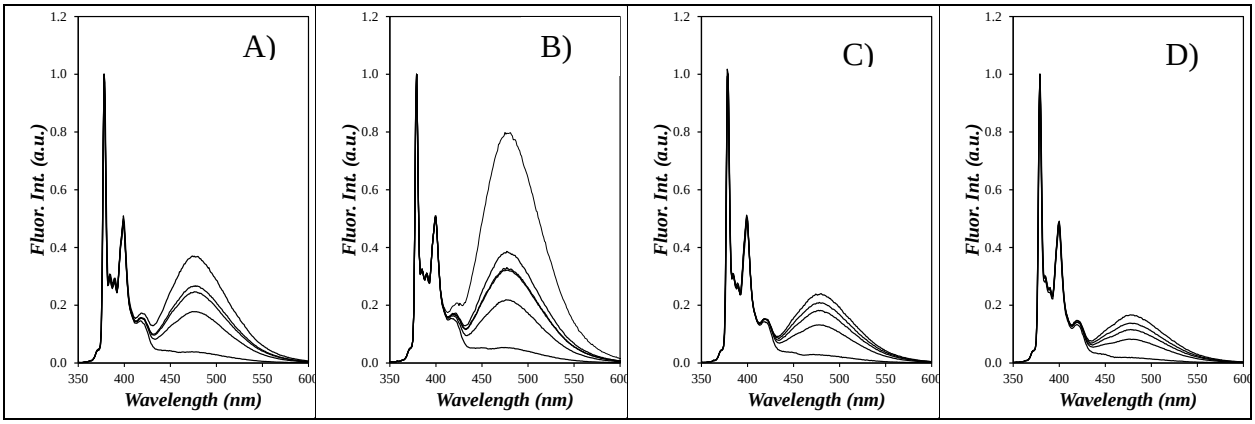

Figure S2.6. Steady-state fluorescence spectra of Py-PEG$_3$MA in (A) THF, (B) toluene, (C) DMF, (D) DMSO.

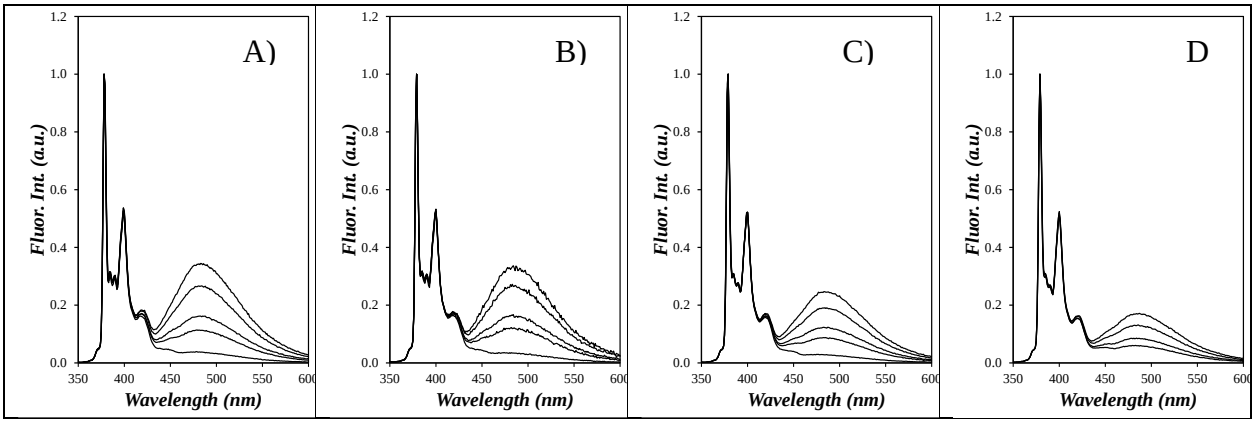

Figure S2.7. Steady-state fluorescence spectra of Py-PEG$_4$MA in (A) THF, (B) toluene, (C) DMF, (D) DMSO.

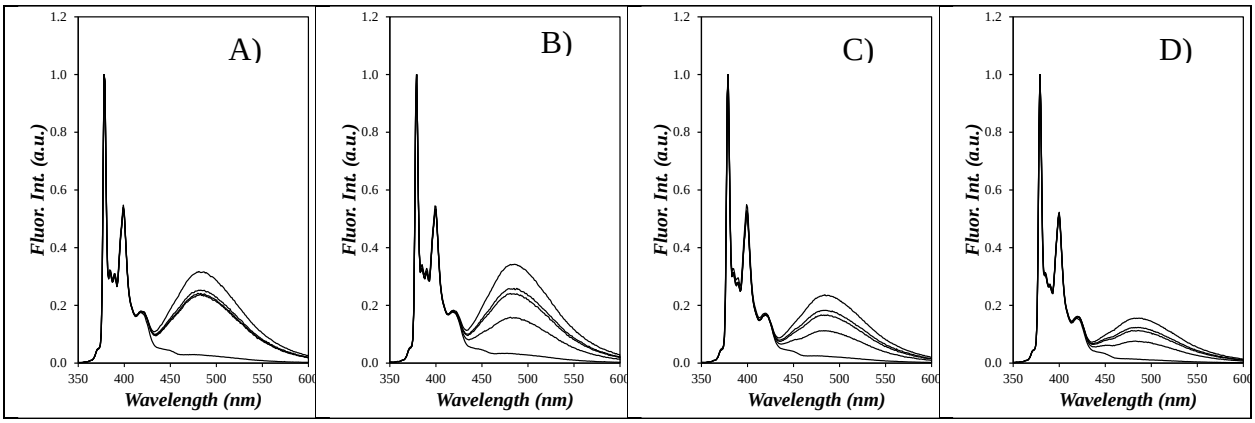

Figure S2.8 Steady-state fluorescence spectra of Py-PEG$_5$MA in (A) THF, (B) toluene, (C) DMF, (D) DMSO.

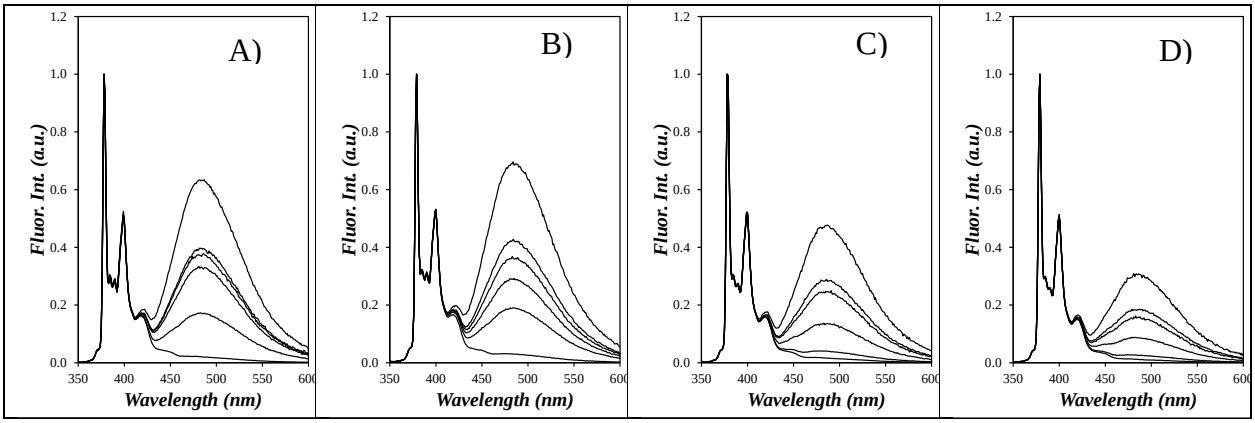

Figure S2.9. Steady-state fluorescence spectra of Py-PEG$_9$MA in (A) THF, (B) toluene, (C) DMF, (D) DMSO.

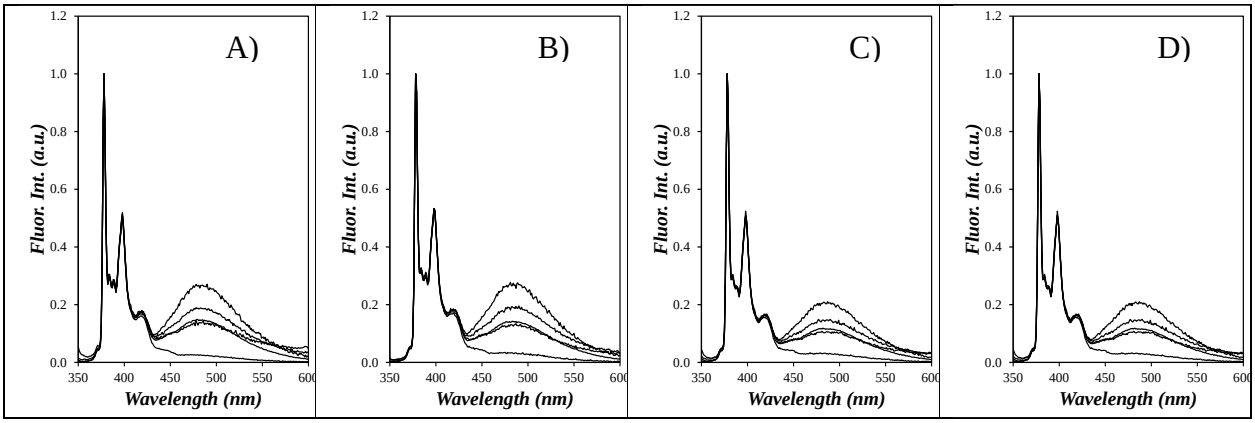

Figure S2.10 Steady-state fluorescence spectra of Py-PEG$_{16}$MA in (A) THF, (B) toluene, (C) DMF, (D) DMSO.

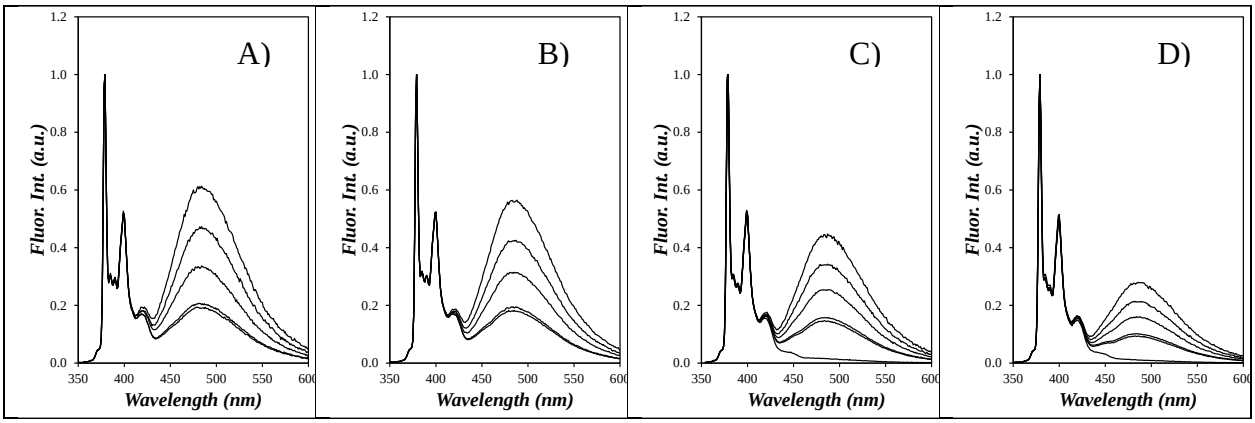

Figure S2.11 Steady-state fluorescence spectra of Py-PEG$_{19}$MA in (A) THF, (B) toluene, (C) DMF, (D) DMSO.

D] Fluorescence decays of the Py(9.2)-PEG$_3$MA samples in different organic solvents

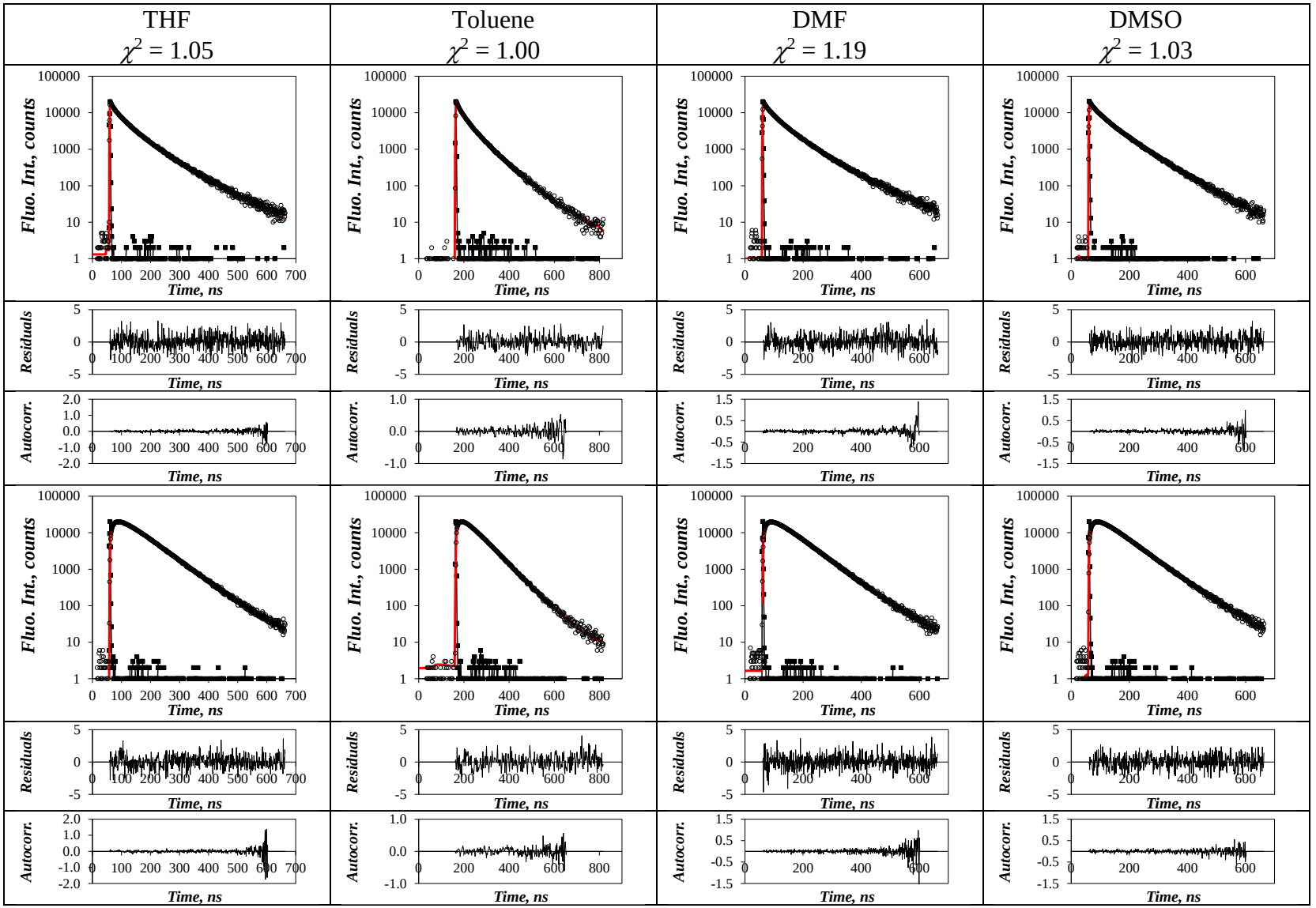

Figure S2.12. Example fits of the monomer and excimer decays of Py(9.2)-PEG$_3$MA using the program *globmis90bbg*.

E] Plots of the FBM parameters N_{blob} and k_{blob}

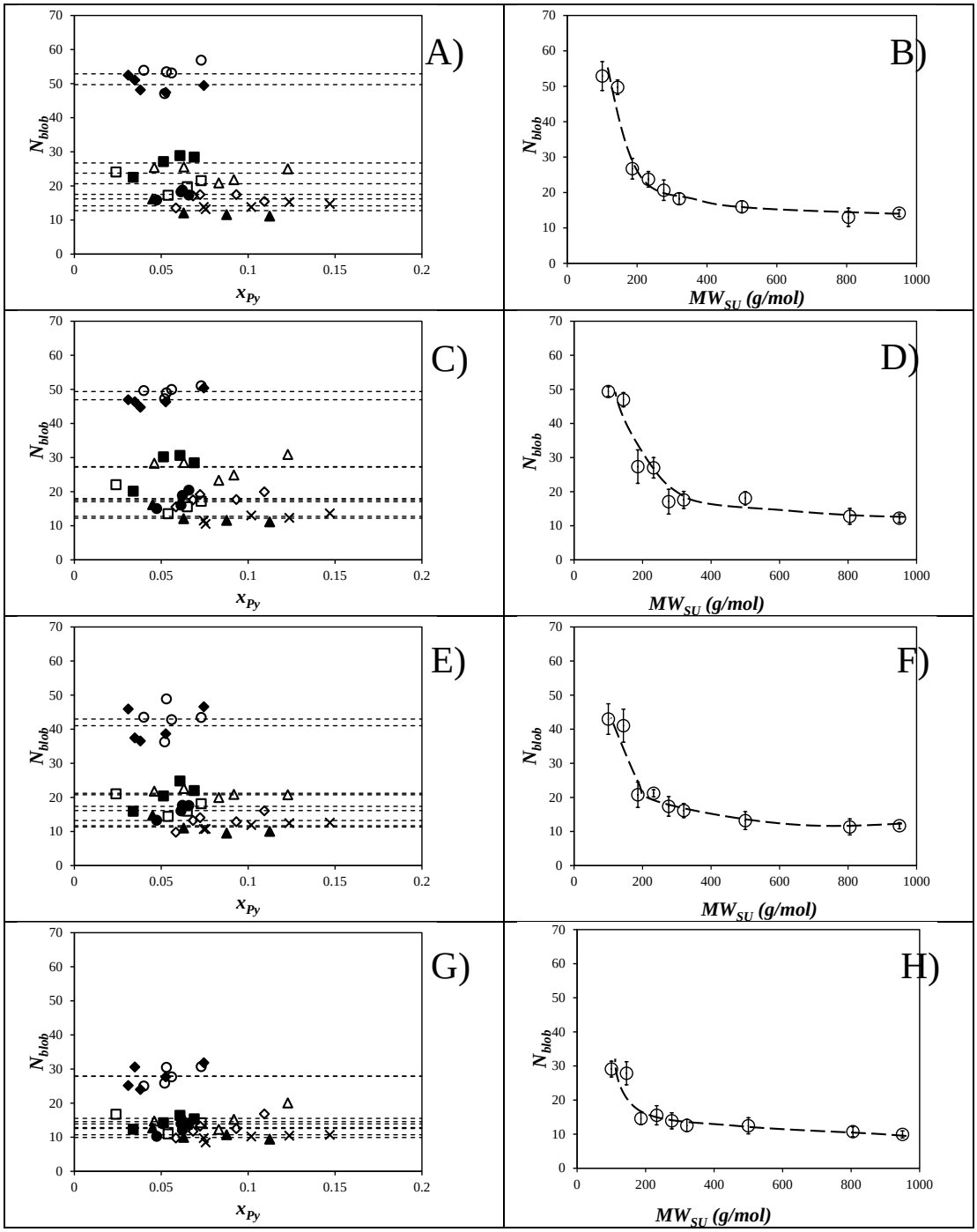

Figure S2.13. Plot of N_{blob} as a function of mole fraction of pyrene in (A, C, E, G) or N_{blob} as a function of MW_{SU} (B, D, F, H) in (A, B) THF, (C, D) toluene, (E, F) DMF, and (G, H) DMSO where (○) Py-PEG$_0$MA, (◆) Py-PEG$_1$MA, (■) Py-PEG$_2$MA, (△) Py-PEG$_3$MA, (□) Py-PEG$_4$MA, (●) Py-PEG$_5$MA, (◇) Py-PEG$_9$MA, (▲) Py-PEG$_{16}$MA and (×) Py-PEG$_{19}$MA.

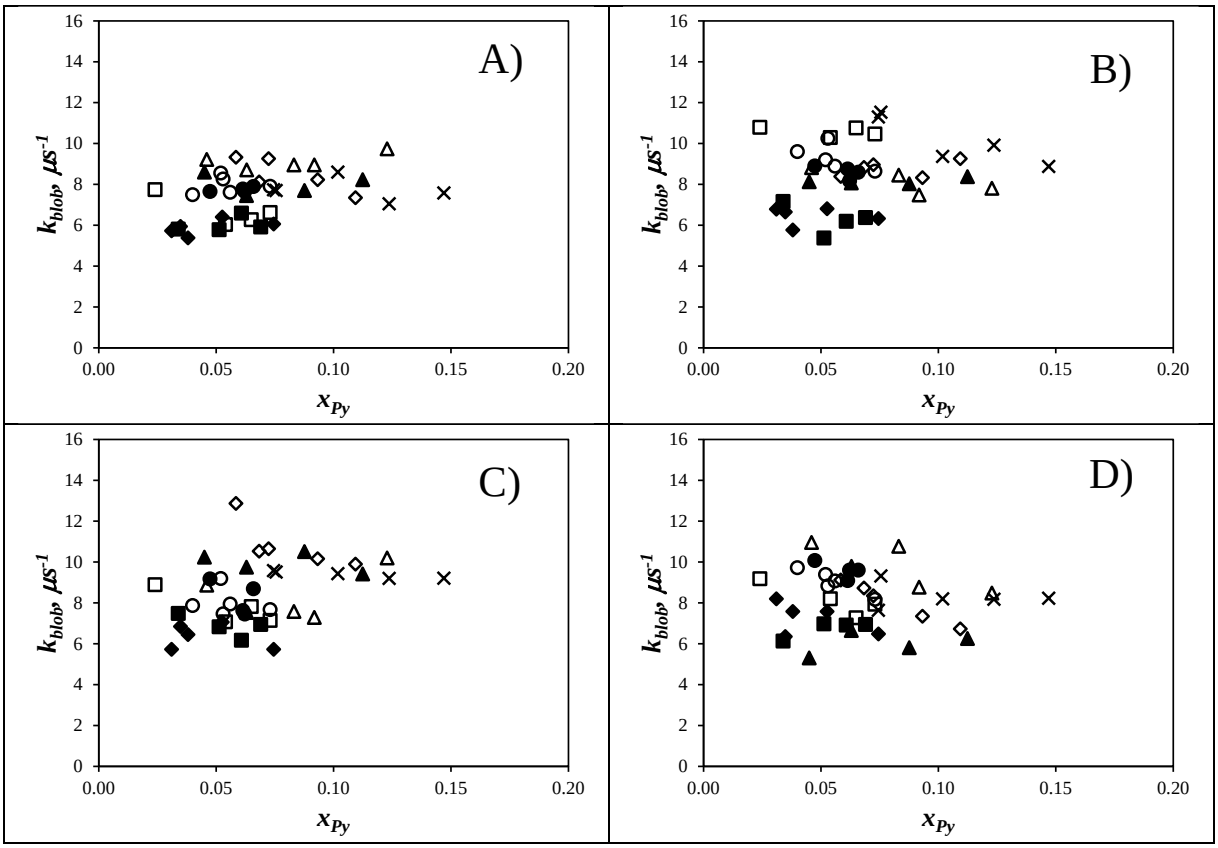

Figure S2.14. Plot of k_{blob} as a function of mole fraction of pyrene in (A) THF, (B) toluene, (C) DMF, and (D) DMSO where (○) Py-PEG$_0$MA, (◆) Py-PEG$_1$MA, (■) Py-PEG$_2$MA, (▲) Py-PEG$_3$MA, (□) Py-PEG$_4$MA, (●) Py-PEG$_5$MA, (◇) Py-PEG$_9$MA, (▲) Py-PEG$_{16}$MA, and (×) Py-PEG$_{19}$MA.

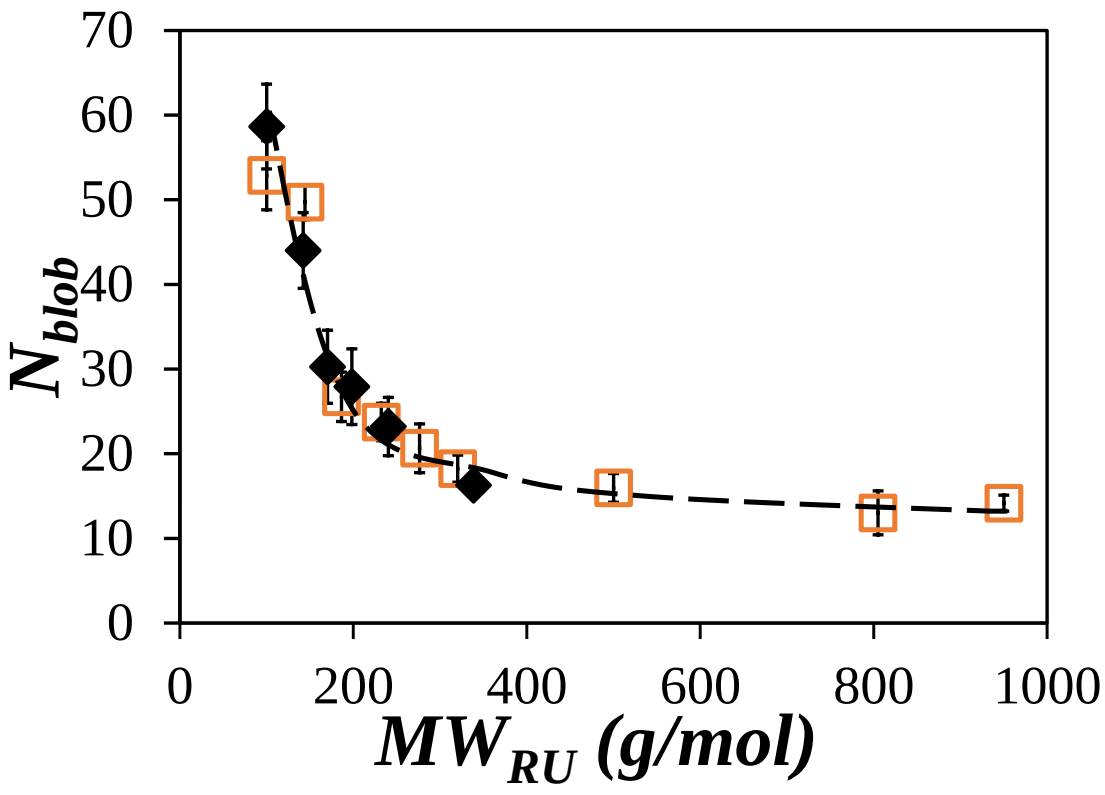

Figure S2.15. Comparison between the <N_{blob}> values obtained in THF for (▣) Py-PEG$_n$MA and (◆) Py-PAMA samples

F] Parameters retrieved from the FBM analysis of the Py-PEG$_n$MA fluorescence decays

Table S2.1. Parameters retrieved from the monomer in THF fit with the program *globmis90gbg* where k_2 is fixed in the analysis.

Sample	Mol %	k_{blob} (10^{-6} s^{-1})	<*n*>	k_e[*blob*] (10^{-6} s^{-1})	f_{Mdiff}	f_{k2}	f_{Mfree}	χ^2
PyPEG$_0$MA	4.0	7.49	2.22	4.41	0.77	0.21	0.027	1.06
k_2 = 1.50 ×10^{-8} s^{-1}	5.2	8.55	2.46	3.66	0.71	0.28	0.007	1.07
τ_M = 186 ns	5.3	8.26	2.87	6.39	0.69	0.30	0.013	1.04
	5.6	7.61	2.99	5.67	0.69	0.30	0.005	1.20
	7.3	7.90	4.16	7.94	0.61	0.39	0.001	1.18
PyPEG$_1$MA	3.1	5.73	1.71	4.02	0.77	0.18	0.05	1.09
k_2 = 1.22 ×10^{-8} s^{-1}	3.5	5.94	1.82	4.51	0.77	0.20	0.02	1.10
τ_M = 200 ns	3.8	5.38	1.90	4.31	0.77	0.20	0.04	0.97
	5.3	6.40	2.57	5.57	0.68	0.29	0.03	1.14
	7.5	6.06	3.81	5.56	0.58	0.39	0.03	1.09
PyPEG$_2$MA	3.4	5.81	0.95	4.77	0.69	0.11	0.20	1.03
k_2 = 1.12 ×10^{-8} s^{-1}	5.1	5.78	1.51	4.53	0.76	0.16	0.08	1.26
τ_M = 197 ns	6.1	6.59	1.80	4.50	0.79	0.19	0.03	1.24
	6.9	5.91	2.00	5.10	0.73	0.25	0.02	1.08
PyPEG$_3$MA	4.6	9.22	1.26	7.19	0.73	0.19	0.07	1.26
k_2 = 1.57 ×10^{-8} s^{-1}	6.3	8.71	1.65	6.36	0.73	0.25	0.02	1.26
τ_M = 181 ns	8.3	8.95	1.76	6.33	0.73	0.26	0.01	1.12
	9.2	8.95	2.03	6.33	0.68	0.30	0.01	1.05
	12.3	9.74	3.13	7.62	0.55	0.43	0.02	1.28
PyPEG$_4$MA	2.4	7.74	0.82	5.59	0.55	0.15	0.30	1.16
k_2 = 1.01 ×10^{-8} s^{-1}	5.4	6.03	1.02	3.77	0.70	0.20	0.09	1.09
τ_M = 188 ns	6.5	6.27	1.35	4.16	0.69	0.25	0.05	1.09
	7.3	6.62	1.64	4.00	0.65	0.30	0.04	1.03
PyPEG$_5$MA	4.7	8.90	0.83	5.49	0.67	0.18	0.15	1.11
k_2 = 1.14 ×10^{-8} s^{-1}	6.1	8.75	1.03	4.24	0.70	0.25	0.04	1.13
τ_M = 192 ns	6.2	8.17	1.24	5.65	0.69	0.25	0.06	1.13
	6.6	8.59	1.39	4.55	0.66	0.30	0.03	1.21
PyPEG$_9$MA	5.8	9.33	0.95	5.81	0.65	0.18	0.17	1.13
k_2 = 1.12 ×10^{-8} s^{-1}	6.8	8.12	1.28	5.75	0.65	0.26	0.09	1.05
τ_M = 187 ns	7.2	9.26	1.32	5.55	0.66	0.30	0.04	1.11
	9.3	8.23	1.66	5.66	0.66	0.32	0.02	1.12
	10.9	7.35	1.73	4.09	0.65	0.33	0.02	1.24
PyPEG$_{16}$MA	4.5	8.60	0.99	4.49	0.56	0.20	0.24	0.95
k_2 = 1.00 ×10^{-8} s^{-1}	6.3	7.45	1.06	3.55	0.53	0.20	0.26	1.10
τ_M = 191 ns	8.8	7.70	1.39	4.34	0.51	0.25	0.24	1.07
	11.2	8.23	1.34	4.48	0.61	0.29	0.09	1.17
PyPEG$_{19}$MA	7.4	7.74	1.26	3.81	0.57	0.24	0.18	1.10
k_2 = 0.95 ×10^{-8} s^{-1}	7.6	7.70	1.21	3.8	0.59	0.23	0.18	1.06
τ_M = 190 ns	10.2	8.60	1.53	4.5	0.58	0.34	0.08	1.16
	12.4	7.05	1.95	2.85	0.55	0.41	0.03	1.12
	14.7	7.58	2.23	2.35	0.48	0.48	0.03	1.00

Table S2.2. Parameters retrieved from the excimer decays in THF fit with the program *globmis90gbg* where k_2 is fixed in the analysis.

Sample	Mol %	f_{Ek2}	τ_{E0} (ns)	f_{E0diff}	f_{EE0}	τ_D (ns)	f_{ED}	χ^2
$PyPEG_0MA$	4	0.20	56	0.75	0.0002	108	0.05	1.06
	5.2	0.28	54	0.69	0.0001	103	0.03	1.07
	5.3	0.29	54	0.67	0.0092	102	0.03	1.04
	5.6	0.29	53	0.67	0.0001	98	0.03	1.20
	7.3	0.36	45	0.58	0.0003	76	0.06	1.18
$PyPEG_1MA$	3.1	0.19	55	0.79	0.0051	116	0.02	1.09
	3.5	0.21	55	0.78	0.0058	114	0.01	1.10
	3.8	0.20	55	0.78	0.0064	132	0.01	0.97
	5.3	0.28	55	0.67	0.0310	104	0.02	1.14
	7.5	0.37	53	0.56	0.0019	88	0.07	1.09
$PyPEG_2MA$	3.4	0.14	60	0.85	0.0029	180	0.01	1.03
	5.1	0.17	54	0.78	0.0007	120	0.05	1.26
	6.1	0.18	54	0.73	0.0004	99	0.10	1.24
	6.9	0.24	55	0.72	0.0001	104	0.04	1.08
$PyPEG_3MA$	4.6	0.20	56	0.77	0.0049	132	0.02	1.26
	6.3	0.24	55	0.73	0.0010	119	0.03	1.26
	8.3	0.25	55	0.71	0.0122	108	0.02	1.12
	9.2	0.30	55	0.67	0.0136	113	0.02	1.05
	12.3	0.41	55	0.53	0.0367	116	0.02	1.28
$PyPEG_4MA$	2.4	0.21	58	0.76	0.0001	172	0.03	1.16
	5.4	0.22	55	0.76	0.0029	148	0.02	1.09
	6.5	0.26	53	0.71	0.0011	118	0.03	1.09
	7.3	0.30	53	0.64	0.0057	108	0.06	1.03
$PyPEG_5MA$	4.7	0.20	54	0.77	0.0011	142	0.03	1.11
	6.1	0.24	53	0.72	0.0031	124	0.04	1.13
	6.2	0.25	53	0.70	0.0034	121	0.05	1.13
	6.6	0.27	54	0.68	0.0079	113	0.03	1.21
$PyPEG_9MA$	5.8	0.20	58	0.74	0.0235	150	0.03	1.13
	6.8	0.27	56	0.69	0.0237	134	0.02	1.05
	7.2	0.29	58	0.66	0.0372	135	0.01	1.11
	9.3	0.31	55	0.63	0.0522	145	0.01	1.12
	10.9	0.32	54	0.63	0.0000	107	0.05	1.24
$PyPEG_{16}MA$	4.5	0.25	55	0.71	0.0066	147	0.03	0.95
	6.3	0.26	53	0.69	0.0151	139	0.03	1.10
	8.8	0.32	54	0.63	0.0213	142	0.03	1.07
	11.2	0.31	55	0.64	0.0322	142	0.02	1.17
$PyPEG_{19}MA$	7.4	0.28	54	0.66	0.0361	135	0.03	1.10
	7.6	0.27	52	0.68	0.0002	125	0.05	1.06
	10.2	0.35	55	0.59	0.0167	115	0.06	1.16
	12.4	0.40	53	0.53	0.0116	99	0.06	1.12
	14.7	0.43	57	0.43	0.1040	106	0.04	1.00

Table S2.3. Parameters retrieved from the monomer decays in DMSO fit with the program *globmis90gbg* where k_2 is fixed in the analysis.

Sample	Mol %	k_{blob} (10^{-6} s^{-1})	<*n*>	k_e[*blob*] (10^{-6} s^{-1})	f_{Mdiff}	f_{k2}	f_{Mfree}	χ^2
$PyPEG_0MA$	4	9.72	1.06	8.29	0.77	0.17	0.05	1.10
$k_2 = 1.31 \times 10^{-8}$ s^{-1}	5.2	9.39	1.39	7.48	0.74	0.22	0.03	1.04
τ_M = 138 ns	5.3	8.83	1.67	7.65	0.72	0.25	0.03	1.09
	5.6	9.07	1.59	7.96	0.74	0.24	0.02	1.19
	7.3	8.17	2.26	6.54	0.68	0.31	0.01	1.15
$PyPEG_1MA$	3.1	8.20	0.86	8.72	0.75	0.16	0.09	1.00
$k_2 = 1.01 \times 10^{-8}$ s^{-1}	3.5	6.35	1.16	6.69	0.75	0.18	0.08	1.04
τ_M = 141 ns	3.8	7.58	1.00	8.15	0.75	0.17	0.08	1.18
	5.3	7.58	1.53	9.69	0.69	0.26	0.05	1.04
	7.5	6.48	2.42	5.96	0.61	0.37	0.02	1.23
$PyPEG_2MA$	3.4	6.13	0.77	7.95	0.47	0.07	0.45	1.07
$k_2 = 0.84 \times 10^{-8}$ s^{-1}	5.1	6.97	0.81	5.56	0.75	0.16	0.10	1.12
τ_M = 140 ns	6.1	6.91	1.08	6.73	0.73	0.19	0.08	1.03
	6.9	6.94	1.13	7.23	0.74	0.20	0.06	1.08
$PyPEG_3MA$	4.6	10.96	0.79	7.14	0.72	0.14	0.14	1.22
$k_2 = 1.20 \times 10^{-8}$ s^{-1}	6.3	9.79	1.04	7.37	0.75	0.18	0.07	1.01
τ_M = 134 ns	8.3	10.77	1.07	8.09	0.76	0.19	0.05	1.08
	9.2	8.77	1.45	6.56	0.73	0.24	0.03	1.03
	12.3	8.48	2.53	7.8	0.59	0.38	0.03	1.13
$PyPEG_4MA$	2.4	9.18	0.67	7.05	0.50	0.10	0.40	0.98
$k_2 = 0.91 \times 10^{-8}$ s^{-1}	5.4	8.20	0.79	6.26	0.61	0.14	0.25	1.03
τ_M = 139 ns	6.5	7.27	1.00	5.22	0.71	0.19	0.10	1.11
	7.3	7.93	1.14	6.26	0.70	0.21	0.09	1.13
$PyPEG_5MA$	4.7	10.07	0.69	6.12	0.59	0.12	0.30	1.09
$k_2 = 1.08 \times 10^{-8}$ s^{-1}	6.1	9.09	0.94	7.77	0.74	0.17	0.09	1.19
τ_M = 140 ns	6.2	9.60	0.89	6.71	0.69	0.16	0.16	1.11
	6.6	9.60	1.03	7.46	0.71	0.18	0.11	1.10
$PyPEG_9MA$	5.8	9.12	0.72	6.13	0.66	0.13	0.21	1.08
$k_2 = 0.89 \times 10^{-8}$ s^{-1}	6.8	8.73	0.90	5.81	0.71	0.18	0.11	1.07
τ_M = 145 ns	7.2	8.35	1.05	5.53	0.72	0.20	0.09	1.12
	9.3	7.35	1.22	4.61	0.72	0.23	0.04	1.22
	10.9	6.73	1.86	3.44	0.67	0.31	0.01	1.04
$PyPEG_{16}MA$	4.5	5.31	1.11	3.19	0.52	0.14	0.34	1.04
$k_2 = 0.67 \times 10^{-8}$ s^{-1}	6.3	6.65	1.06	4.79	0.44	0.15	0.41	1.08
τ_M = 140 ns	8.8	5.81	1.39	5.03	0.48	0.20	0.32	1.04
	11.2	6.26	1.28	4.5	0.60	0.23	0.17	1.01
$PyPEG_{19}MA$	7.4	7.64	1.05	5.21	0.57	0.12	0.31	1.09
$k_2 = 0.95 \times 10^{-8}$ s^{-1}	7.6	9.32	0.88	5.77	0.59	0.13	0.27	1.15
τ_M = 144 ns	10.2	8.20	1.16	3.51	0.69	0.20	0.10	1.07
	12.4	8.18	1.42	5.93	0.67	0.24	0.09	1.11
	14.7	8.23	1.67	3.81	0.63	0.31	0.05	1.12

Table S2.4. Parameters retrieved from the excimer decays in DMSO fit with the program *globmis90gbg* where k_2 is fixed in the analysis.

Sample	Mol %	f_{Ek2}	τ_{E0} (ns)	f_{E0diff}	f_{EE0}	τ_D (ns)	f_{ED}	χ^2
$PyPEG_0MA$	4	0.17	51	0.78	0.036	128	0.01	1.1
	5.2	0.22	49	0.72	0.025	105	0.04	1.04
	5.3	0.24	49	0.69	0.012	95	0.06	1.09
	5.6	0.23	50	0.71	0.047	128	0.02	1.19
	7.3	0.28	49	0.63	0.008	86	0.08	1.15
$PyPEG_1MA$	3.1	0.16	51	0.78	0.052	125	0.01	1.00
	3.5	0.18	48	0.76	0.004	102	0.06	1.04
	3.8	0.17	51	0.77	0.053	129	0.01	1.18
	5.3	0.25	51	0.66	0.081	137	0.01	1.04
	7.5	0.33	48	0.54	0.001	82	0.13	1.23
$PyPEG_2MA$	3.4	0.13	49	0.83	0.001	138	0.04	1.07
	5.1	0.16	52	0.79	0.000	108	0.05	1.12
	6.1	0.20	51	0.74	0.012	108	0.05	1.03
	6.9	0.20	50	0.74	0.009	101	0.05	1.08
$PyPEG_3MA$	4.6	0.15	51	0.79	0.005	109	0.05	1.22
	6.3	0.18	50	0.76	0.002	100	0.06	1.01
	8.3	0.19	51	0.75	0.042	113	0.02	1.08
	9.2	0.24	49	0.71	0.006	97	0.05	1.03
	12.3	0.36	49	0.55	0.027	88	0.07	1.13
$PyPEG_4MA$	2.4	0.16	50	0.80	0.000	130	0.04	0.98
	5.4	0.18	51	0.78	0.018	131	0.03	1.03
	6.5	0.20	48	0.76	0.012	112	0.03	1.11
	7.3	0.22	48	0.73	0.012	104	0.04	1.13
$PyPEG_5MA$	4.7	0.16	53	0.80	0.014	128	0.03	1.09
	6.1	0.18	47	0.78	0.023	93	0.01	1.19
	6.2	0.18	49	0.78	0.010	111	0.03	1.11
	6.6	0.20	50	0.76	0.020	124	0.02	1.1
$PyPEG_9MA$	5.8	0.15	49	0.79	0.001	101	0.06	1.08
	6.8	0.19	50	0.75	0.016	103	0.04	1.07
	7.2	0.20	50	0.74	0.009	100	0.05	1.12
	9.3	0.23	52	0.72	0.022	109	0.03	1.22
	10.9	0.29	50	0.62	0.002	88	0.09	1.04
$PyPEG_{16}MA$	4.5	0.21	48	0.74	0.000	119	0.05	1.04
	6.3	0.24	50	0.69	0.028	121	0.04	1.08
	8.8	0.27	49	0.65	0.053	123	0.03	1.04
	11.2	0.26	50	0.67	0.027	116	0.04	1.01
$PyPEG_{19}MA$	7.4	0.17	49	0.77	0.008	110	0.06	1.09
	7.6	0.17	51	0.77	0.017	115	0.04	1.15
	10.2	0.21	50	0.72	0.000	98	0.07	1.07
	12.4	0.25	51	0.68	0.044	114	0.02	1.11
	14.7	0.30	50	0.60	0.000	83	0.10	1.12

Table S2.5. Parameters retrieved from the monomer decays in DMF fit with the program *globmis90gbg* where k_2 is fixed in the analysis.

Sample	Mol %	k_{blob} (10^{-6} s^{-1})	<*n*>	k_e[*blob*] (10^{-6} s^{-1})	f_{Mdiff}	f_{k2}	f_{Mfree}	χ^2
$PyPEG_0MA$	4	7.87	1.75	6.29	0.74	0.21	0.00	1.04
$k_2 = 1.35 \times 10^{-8}$ s^{-1}	5.2	9.19	1.96	7.73	0.72	0.25	0.04	1.13
τ_M = 149 ns	5.3	7.46	2.64	5.5	0.68	0.31	0.02	1.18
	5.6	7.94	2.42	5.89	0.70	0.29	0.01	1.03
	7.3	7.67	3.20	6.41	0.63	0.36	0.01	1.19
$PyPEG_1MA$	3.1	5.73	1.52	4.83	0.76	0.18	0.07	1.14
$k_2 = 1.12 \times 10^{-8}$ s^{-1}	3.5	6.45	1.46	5.31	0.77	0.18	0.05	1.01
τ_M = 169 ns	3.8	6.85	1.36	5.73	0.77	0.19	0.04	1.05
	5.3	7.06	2.08	6.13	0.69	0.29	0.02	1.04
	7.5	5.73	3.52	3.48	0.60	0.39	0.02	1.15
$PyPEG_2MA$	3.4	7.48	0.72	5.89	0.62	0.12	0.25	1.04
$k_2 = 1.20 \times 10^{-8}$ s^{-1}	5.1	6.83	1.16	5.81	0.74	0.16	0.10	1.14
τ_M = 165 ns	6.1	6.17	1.57	5.32	0.76	0.20	0.04	1.16
	6.9	6.94	1.56	5.67	0.74	0.23	0.03	1.08
$PyPEG_3MA$	4.6	8.87	1.10	6.6	0.72	0.19	0.09	1.07
$k_2 = 1.18 \times 10^{-8}$ s^{-1}	6.3	7.53	1.47	5.08	0.71	0.26	0.03	1.24
τ_M = 153ns	8.3	7.58	1.70	5.22	0.72	0.26	0.02	1.08
	9.2	7.29	1.98	6.24	0.67	0.30	0.03	1.19
	12.3	10.20	2.62	12.73	0.52	0.45	0.03	1.18
$PyPEG_4MA$	2.4	8.89	0.72	6.89	0.56	0.14	0.30	1.07
$k_2 = 1.00 \times 10^{-8}$ s^{-1}	5.4	7.07	0.94	4.87	0.66	0.17	0.17	1.04
τ_M = 162 ns	6.5	7.82	1.13	5.62	0.69	0.23	0.08	1.15
	7.3	7.14	1.40	4.97	0.67	0.27	0.06	1.01
$PyPEG_5MA$	4.7	9.17	0.80	5.55	0.63	0.16	0.22	1.05
$k_2 = 1.08 \times 10^{-8}$ s^{-1}	6.1	7.62	1.11	5.04	0.68	0.20	0.12	1.16
τ_M = 163 ns	6.2	7.45	1.21	5.07	0.68	0.22	0.09	1.06
	6.6	8.69	1.23	5.56	0.69	0.25	0.06	1.09
$PyPEG_9MA$	5.8	12.87	0.78	7.07	0.59	0.15	0.26	1.08
$k_2 = 1.16 \times 10^{-8}$ s^{-1}	6.8	10.53	1.08	6.67	0.63	0.21	0.16	1.09
τ_M = 154 ns	7.2	10.65	1.11	6.08	0.69	0.23	0.08	1.08
	9.3	10.16	1.28	5.73	0.68	0.25	0.06	1.26
	10.9	9.90	1.82	6.12	0.62	0.35	0.03	1.14
$PyPEG_{16}MA$	4.5	10.24	0.94	6.39	0.54	0.16	0.29	0.98
$k_2 = 1.05 \times 10^{-8}$ s^{-1}	6.3	9.75	1.07	5.93	0.48	0.17	0.35	1.13
τ_M = 161 ns	8.8	10.51	1.14	6.2	0.51	0.22	0.27	1.00
	11.2	9.42	1.26	4.53	0.63	0.26	0.10	1.07
$PyPEG_{19}MA$	7.4	9.58	0.95	3.19	0.65	0.19	0.16	1.23
$k_2 = 1.06 \times 10^{-8}$ s^{-1}	7.6	9.51	1.01	5.49	0.60	0.20	0.20	1.07
τ_M = 167 ns	10.2	9.43	1.32	4.41	0.64	0.27	0.09	1.16
	12.4	9.20	1.60	3.92	0.64	0.32	0.04	1.12
	14.7	9.21	1.94	3.48	0.57	0.39	0.04	1.09

Table S2.6. Parameters retrieved from the excimer decays in DMF fit with the program *globmis90gbg* where k_2 is fixed in the analysis.

Sample	Mol %	f_{Ek2}	τ_{E0} (ns)	f_{E0diff}	f_{EE0}	τ_D (ns)	f_{ED}	χ^2
$PyPEG_0MA$	4	0.22	53	0.75	0.000	108	0.03	1.04
	5.2	0.24	50	0.69	0.006	95	0.07	1.13
	5.3	0.30	52	0.66	0.003	93	0.04	1.18
	5.6	0.28	52	0.67	0.003	91	0.05	1.03
	7.3	0.34	50	0.59	0.000	84	0.07	1.19
$PyPEG_1MA$	3.1	0.18	52	0.78	0.016	118	0.02	1.14
	3.5	0.19	53	0.78	0.010	91	0.02	1.01
	3.8	0.19	52	0.78	0.010	103	0.03	1.05
	5.3	0.28	53	0.67	0.029	93	0.02	1.04
	7.5	0.36	52	0.56	0.045	98	0.03	1.15
$PyPEG_2MA$	3.4	0.16	61	0.82	0.002	157	0.02	1.04
	5.1	0.17	53	0.81	0.001	129	0.02	1.14
	6.1	0.20	52	0.77	0.009	116	0.03	1.16
	6.9	0.23	55	0.74	0.007	112	0.02	1.08
$PyPEG_3MA$	4.6	0.20	56	0.76	0.027	136	0.02	1.07
	6.3	0.26	55	0.72	0.001	121	0.01	1.24
	8.3	0.24	52	0.68	0.011	97	0.06	1.08
	9.2	0.30	51	0.66	0.002	98	0.04	1.19
	12.3	0.41	54	0.47	0.097	110	0.02	1.18
$PyPEG_4MA$	2.4	0.19	54	0.78	0.000	142	0.03	1.07
	5.4	0.20	51	0.77	0.000	129	0.03	1.04
	6.5	0.24	52	0.72	0.007	123	0.03	1.15
	7.3	0.27	51	0.68	0.005	104	0.04	1.01
$PyPEG_5MA$	4.7	0.19	54	0.77	0.007	137	0.03	1.05
	6.1	0.22	51	0.74	0.000	117	0.03	1.16
	6.2	0.24	51	0.73	0.002	117	0.03	1.06
	6.6	0.25	52	0.71	0.014	120	0.02	1.09
$PyPEG_9MA$	5.8	0.19	56	0.76	0.000	134	0.05	1.08
	6.8	0.24	54	0.73	0.004	127	0.03	1.09
	7.2	0.24	55	0.72	0.012	120	0.03	1.08
	9.3	0.26	54	0.69	0.002	108	0.05	1.26
	10.9	0.34	53	0.60	0.013	106	0.04	1.14
$PyPEG_{16}MA$	4.5	0.22	52	0.74	0.009	147	0.03	0.98
	6.3	0.25	52	0.71	0.006	134	0.04	1.13
	8.8	0.28	53	0.66	0.039	143	0.02	1.00
	11.2	0.28	54	0.67	0.017	118	0.03	1.07
$PyPEG_{19}MA$	7.4	0.22	55	0.73	0.000	110	0.06	1.23
	7.6	0.24	53	0.72	0.002	124	0.04	1.07
	10.2	0.28	52	0.66	0.024	112	0.04	1.16
	12.4	0.31	52	0.61	0.014	97	0.07	1.12
	14.7	0.36	50	0.52	0.000	86	0.12	1.09

Table S2.7. Parameters retrieved from the monomer decays in toluene fit with the program *globmis90gbg* where k_2 is fixed in the analysis.

Sample	Mol %	k_{blob} (10^{-6} s^{-1})	<*n*>	k_e[*blob*] (10^{-6} s^{-1})	f_{Mdiff}	f_{k2}	f_{Mfree}	χ^2
$PyPEG_0MA$	4	9.60	2.02	7.68	0.77	0.21	0.02	1.02
$k_2 = 1.90 \times 10^{-8}$ s^{-1}	5.2	9.20	2.47	3.52	0.73	0.26	0.01	1.27
τ_M = 140 ns	5.3	10.25	2.66	8.55	0.69	0.29	0.02	1.01
	5.6	8.89	2.83	6.07	0.71	0.28	0.01	1.13
	7.3	8.64	3.75	4.89	0.63	0.36	0.01	1.09
$PyPEG_1MA$	3.1	6.79	1.58	6.38	0.74	0.18	0.08	1.06
$k_2 = 1.12 \times 10^{-8}$ s^{-1}	3.5	6.65	1.72	5.80	0.74	0.20	0.06	1.14
τ_M = 158 ns	3.8	5.77	1.80	4.87	0.74	0.20	0.06	1.15
	5.3	6.81	2.57	9.58	0.66	0.29	0.05	1.14
	7.5	6.33	3.85	8.89	0.56	0.42	0.02	1.09
$PyPEG_2MA$	3.4	7.16	0.92	5.48	0.62	0.12	0.26	1.08
$k_2 = 1.17 \times 10^{-8}$ s^{-1}	5.1	5.37	1.65	4.87	0.75	0.19	0.06	1.13
τ_M = 171 ns	6.1	6.19	1.91	5.09	0.73	0.24	0.03	1.08
	6.9	6.37	2.01	5.63	0.72	0.26	0.02	1.11
$PyPEG_3MA$	4.6	8.82	1.37	6.30	0.73	0.23	0.05	1.08
$k_2 = 1.40 \times 10^{-8}$ s^{-1}	6.3	8.67	1.84	6.20	0.67	0.31	0.02	1.20
τ_M = 159 ns	8.3	8.45	1.97	5.60	0.70	0.29	0.01	1.17
	9.2	7.48	2.30	4.67	0.67	0.32	0.01	1.00
	12.3	7.81	3.83	7.08	0.48	0.51	0.01	1.27
$PyPEG_4MA$	2.4	10.79	0.74	7.91	0.59	0.59	0.28	1.11
$k_2 = 1.42 \times 10^{-8}$ s^{-1}	5.4	10.29	0.88	7.14	0.66	0.66	0.17	0.97
τ_M = 169 ns	6.5	10.76	1.09	7.68	0.71	0.71	0.07	1.09
	7.3	10.46	1.33	6.65	0.68	0.68	0.06	1.15
$PyPEG_5MA$	4.7	8.90	0.83	5.49	0.67	0.18	0.15	1.11
$k_2 = 1.15 \times 10^{-8}$ s^{-1}	6.1	8.75	1.03	4.24	0.70	0.25	0.04	1.13
τ_M = 163 ns	6.2	8.17	1.24	5.65	0.69	0.25	0.06	1.13
	6.6	8.59	1.39	4.55	0.66	0.30	0.03	1.21
$PyPEG_9MA$	5.8	8.39	1.08	5.22	0.65	0.19	0.16	1.13
$k_2 = 1.28 \times 10^{-8}$ s^{-1}	6.8	8.83	1.29	4.96	0.67	0.26	0.07	1.19
τ_M = 171 ns	7.2	8.96	1.44	4.72	0.68	0.28	0.04	1.04
	9.3	8.33	1.69	3.91	0.66	0.32	0.03	1.11
	10.9	9.26	2.22	5.01	0.56	0.42	0.02	1.05
$PyPEG_{16}MA$	4.5	8.13	1.01	4.73	0.54	0.18	0.28	1.18
$k_2 = 1.10 \times 10^{-8}$ s^{-1}	6.3	8.07	1.08	3.50	0.52	0.18	0.29	1.17
τ_M = 165 ns	8.8	8.03	1.32	3.48	0.53	0.24	0.23	1.08
	11.2	8.38	1.38	3.83	0.63	0.28	0.09	1.08
$PyPEG_{19}MA$	7.4	11.30	1.19	6.40	0.50	0.22	0.28	1.04
$k_2 = 1.18 \times 10^{-8}$ s^{-1}	7.6	11.53	1.11	6.51	0.52	0.20	0.28	1.09
τ_M = 158 ns	10.2	9.37	1.51	4.37	0.60	0.28	0.12	1.02
	12.4	9.92	1.64	4.9	0.60	0.34	0.07	1.21
	14.7	8.88	2.12	3.3	0.52	0.42	0.06	1.18

Table S2.8. Parameters retrieved from the excimer decays in Toluene fit with the program *globmis90gbg* where k_2 is fixed in the analysis.

Sample	Mol %	f_{Ek2}	τ_{E0} (ns)	f_{E0diff}	f_{EE0}	τ_D (ns)	f_{ED}	χ^2
$PyPEG_0MA$	4	0.21	49	0.75	0.021	105	0.02	1.02
	5.2	0.25	52	0.69	0.001	85	0.06	1.27
	5.3	0.28	50	0.67	0.007	89	0.05	1.01
	5.6	0.27	52	0.46	0.005	87	0.05	1.13
	7.3	0.34	51	0.60	0.046	96	0.02	1.09
$PyPEG_1MA$	3.1	0.19	54	0.76	0.018	127	0.03	1.06
	3.5	0.20	54	0.75	0.034	141	0.02	1.14
	3.8	0.21	52	0.76	0.003	117	0.03	1.15
	5.3	0.28	49	0.64	0.024	97	0.05	1.14
	7.5	0.38	49	0.51	0.000	77	0.11	1.09
$PyPEG_2MA$	3.4	0.16	57	0.82	0.001	146	0.02	1.08
	5.1	0.19	51	0.77	0.010	121	0.02	1.13
	6.1	0.24	51	0.71	0.001	99	0.05	1.08
	6.9	0.25	52	0.69	0.020	103	0.04	1.11
$PyPEG_3MA$	4.6	0.23	53	0.73	0.035	140	0.01	1.08
	6.3	0.30	53	0.64	0.051	139	0.01	1.2
	8.3	0.27	51	0.65	0.000	91	0.08	1.17
	9.2	0.30	50	0.62	0.021	79	0.06	1
	12.3	0.46	50	0.43	0.068	83	0.04	1.27
$PyPEG_4MA$	2.4	0.18	53	0.80	0.000	178	0.02	1.11
	5.4	0.20	53	0.77	0.014	157	0.02	0.97
	6.5	0.22	50	0.74	0.025	137	0.02	1.09
	7.3	0.27	52	0.68	0.034	124	0.01	1.15
$PyPEG_5MA$	4.7	0.20	51	0.76	0.001	118	0.03	1.11
	6.1	0.25	53	0.70	0.011	96	0.04	1.13
	6.2	0.25	50	0.70	0.032	125	0.02	1.13
	6.6	0.29	53	0.65	0.044	116	0.01	1.21
$PyPEG_9MA$	5.8	0.22	50	0.74	0.006	122	0.03	1.13
	6.8	0.27	51	0.69	0.031	128	0.02	1.19
	7.2	0.28	49	0.67	0.005	95	0.05	1.04
	9.3	0.30	50	0.63	0.003	98	0.06	1.11
	10.9	0.39	50	0.52	0.030	87	0.06	1.05
$PyPEG_{16}MA$	4.5	0.24	49	0.72	0.002	133	0.04	1.18
	6.3	0.24	49	0.70	0.010	122	0.05	1.17
	8.8	0.29	48	0.64	0.010	110	0.06	1.08
	11.2	0.29	49	0.65	0.003	109	0.06	1.08
$PyPEG_{19}MA$	7.4	0.29	53	0.67	0.007	143	0.04	1.04
	7.6	0.26	53	0.69	0.000	140	0.04	1.09
	10.2	0.29	50	0.63	0.005	106	0.07	1.02
	12.4	0.34	50	0.60	0.001	99	0.07	1.21
	14.7	0.41	49	0.50	0.005	92	0.08	1.18

G] Derivation of the Scaling Laws for N_{blob} and $k_{blob} \times N_{blob}$

The bending function f_{b1} parameters *a*, *b*, and the pre-factor *c* were optimized by the minimizing the χ^2 of Equation S2.4, which resulted in the matrix presented in Equation S2.5. In solving the matrix, Py-PEG0MA was not used, nor were the polymers where $MW_{SU} > 500$ g/mol.

$$\chi^2 = \sum \left[\left(\frac{N_{blob}}{N_{blob}^{\infty}} - 1 \right) - \left(c \times {MW_{SU}}^{a} \times \eta^{b} \right) \right] \tag{S2.4}$$

$$\begin{pmatrix} c \\ a \\ b \end{pmatrix} = \begin{pmatrix} \sum 1 & \sum \ln(MW_{SU}) & \sum \ln(\eta) \\ \sum \ln(\eta) & \sum \ln(MW_{SU}) \times \ln(\eta) & \sum (\ln(\eta))^2 \\ \sum \ln(MW_{SU}) & \sum (\ln(MW_{SU}))^2 & \sum \ln(MW_{SU}) \times \ln(\eta) \end{pmatrix}^{-1} \bullet \begin{pmatrix} \sum \ln\left(\frac{N_{blob}}{N_{blob}^{\infty}} + 1 \right) \\ \sum \ln\left(\frac{N_{blob}}{N_{blob}^{\infty}} + 1 \right) \times \ln(\eta) \\ \sum \ln\left(\frac{N_{blob}}{N_{blob}^{\infty}} + 1 \right) \times \ln(MW_{SU}) \end{pmatrix} \tag{S2.5}$$

A similar procedure could be implemented for $k_{blob} \times N_{blob}$, with the greatest difference being that the values of $k_{blob} \times N_{blob}$ for the Py-PEG$_{16}$MA and Py-PEG$_{19}$MA did not scale linearly with η^{-1} but instead took a constant value at solvent viscosities greater than 0.79 mPa·s after which they began to decrease. The χ^2 of the bending function f_{b2} is described by equation S2.6, and the parameters retrieved from the matrix given in Equation S2.7

$$\chi^2 = \sum \left[\left(\frac{(k_{blob} \times N_{blob})}{(k_{blob} \times N_{blob})^{\infty}} - 1 \right) - \left(c \times {MW_{SU}}^{a} \times \eta^{b} \right) \right] \tag{S2.6}$$

$$\begin{pmatrix} c \\ a \\ b \end{pmatrix} = \begin{pmatrix} \sum 1 & \sum \ln(MW_{SU}) & \sum \ln(\eta) \\ \sum \ln(\eta) & \sum \ln(MW_{SU}) \times \ln(\eta) & \sum (\ln(\eta))^2 \\ \sum \ln(MW_{SU}) & \sum (\ln(MW_{SU}))^2 & \sum \ln(MW_{SU}) \times \ln(\eta) \end{pmatrix}^{-1} \bullet \begin{pmatrix} \sum \ln\left(\frac{(k_{blob} \times N_{blob})}{(k_{blob} \times N_{blob})^{\infty}} + 1 \right) \\ \sum \ln\left(\frac{(k_{blob} \times N_{blob})}{(k_{blob} \times N_{blob})^{\infty}} + 1 \right) \times \ln(\eta) \\ \sum \ln\left(\frac{(k_{blob} \times N_{blob})}{(k_{blob} \times N_{blob})^{\infty}} + 1 \right) \times \ln(MW_{SU}) \end{pmatrix} \tag{S2.7}$$

Appendix B Supporting Information for Chapter 3

A] Equations describing the MFA

The monomer and excimer decays were fit globally according to the Model Free Analysis (MFA) with Equations S3.1 and S3.2, respectively. In Equation S3.1, the parameters τ_i are the decay times and their associated pre-exponential factors (a_i) were normalized to unity ($\Sigma a_i = 1$) and their values were kept the same in Equations S3.1 and S3.2 during the MFA of the fluorescence decays. The molar fractions f_{Mdiff} and f_{Mfree} represents the pyrene species that are detected in the monomer decays which form excimer by diffusive encounters between an excited and a ground-state pyrene and are isolated in the macromolecule and cannot form excimer.

$$[Py^*] = [Py^*]_{t=0}\left[f_{Mdiff} \times \sum_{i=1}^{n} a_i \exp\left(\frac{-t}{\tau_i}\right) + f_{Mfree} \exp\left(\frac{-t}{\tau_M}\right)\right] \quad \text{(S3.1)}$$

Equations S3.2 accounts for pyrenyl labels forming a short (*E*0*) and long-lived (*D**) excimer species. The pyrenyl species generating *E*0* and *D** by direct excitation are represented by the molar fractions f_{EE0} and f_{ED}, respectively, and the pyrenyl species forming *E*0* by diffusive encounters are represented by the molar fraction $f_{EdiffE0}$. The index "E" in the molar fractions indicates that these pyrenyl species were only detected in the excimer fluorescence decays. The excimer *E*0* and *D** have a lifetime τ_{E0} and τ_D, respectively.

$$[E^*] = [Py^*]_{t=0}\left[-f_{EdiffE0} \times \sum_{i=1}^{n} a_i \frac{\frac{1}{\tau_i} - \frac{1}{\tau_M}}{\frac{1}{\tau_i} - \frac{1}{\tau_{E0}}} \exp\left(\frac{t}{\tau_i}\right) + \left(f_{EE0} + f_{EdiffE0}\right) \times \sum_{i=1}^{n} a_i \frac{\frac{1}{\tau_i} - \frac{1}{\tau_M}}{\frac{1}{\tau_i} - \frac{1}{\tau_{E0}}} \exp\left(\frac{t}{\tau_{E0}}\right) + f_{ED} \exp\left(\frac{t}{\tau_D}\right)\right] \quad \text{(S3.2)}$$

B] Determination of the molar fractions

Since the monomer and excimer fluorescence decays probe different populations of pyrenyl species, the molar fractions f_{Mdiff}, f_{Mfree}, f_{EdiffE0}, f_{EE0}, and f_{ED} represent a subset of the total population of pyrenyl species. Equations S3.3 – S3.6 were used to express the molar fractions f_{diffE0}, f_{free}, f_{E0}, and f_{D} from the fractions f_{Mdiff}, f_{Mfree}, f_{EdiffE0}, f_{EE0}, and f_{ED}.

$$f_{diffE0} = \frac{[Py_{diffE0}{}^*]_0}{[Py_{diffE0}{}^*]_0 + [Py_{free}{}^*]_0 + [E0^*]_0 + [D^*]_0} = \left(1 + \frac{f_{Mfree}}{f_{Mdiff}} + \frac{f_{E0}}{f_{EdiffE0}} + \frac{f_{ED}}{f_{EdiffE0}}\right)^{-1} \tag{3.3}$$

$$f_{free} = \frac{[Py_{free}{}^*]_0}{[Py_{diffE0}{}^*]_0 + [Py_{free}{}^*]_0 + [E0^*]_0 + [D^*]_0} = f_{diffE0} \times \frac{f_{Mfree}}{f_{Mdiff}} \tag{3.4}$$

$$f_{E0} = \frac{[E0^*]_0}{[Py_{diffE0}{}^*]_0 + [Py_{free}{}^*]_0 + [E0^*]_0 + [D^*]_0} = f_{diffE0} \times \frac{f_{EE0}}{f_{Ediff}} \tag{3.5}$$

$$f_{D} = \frac{[D^*]_0}{[Py_{diffE0}{}^*]_0 + [Py_{free}{}^*]_0 + [E0^*]_0 + [D^*]_0} = f_{diffE0} \times \frac{f_{ED}}{f_{Ediff}} \tag{3.6}$$

C] Fluorescence Decays of Py(6.1)-PEG_5MA samples in different organic solvents.

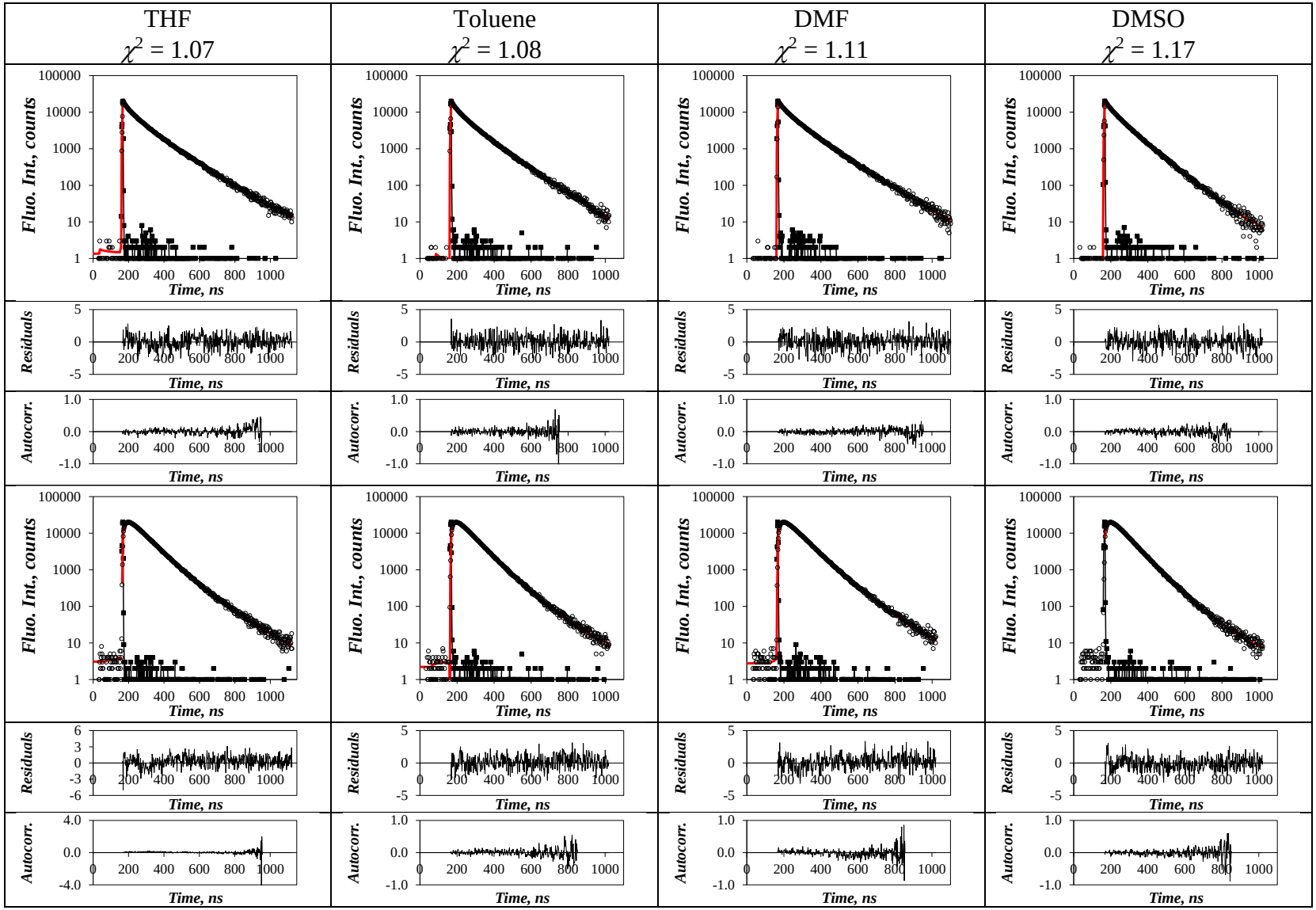

Figure S3.1. Example fits of monomer and excimer decays of Py(6.1)-PEG_5MA using the program *sumegs17bg*.

D] Plots of the MFA parameter $<k^{MF}>^{blob}$

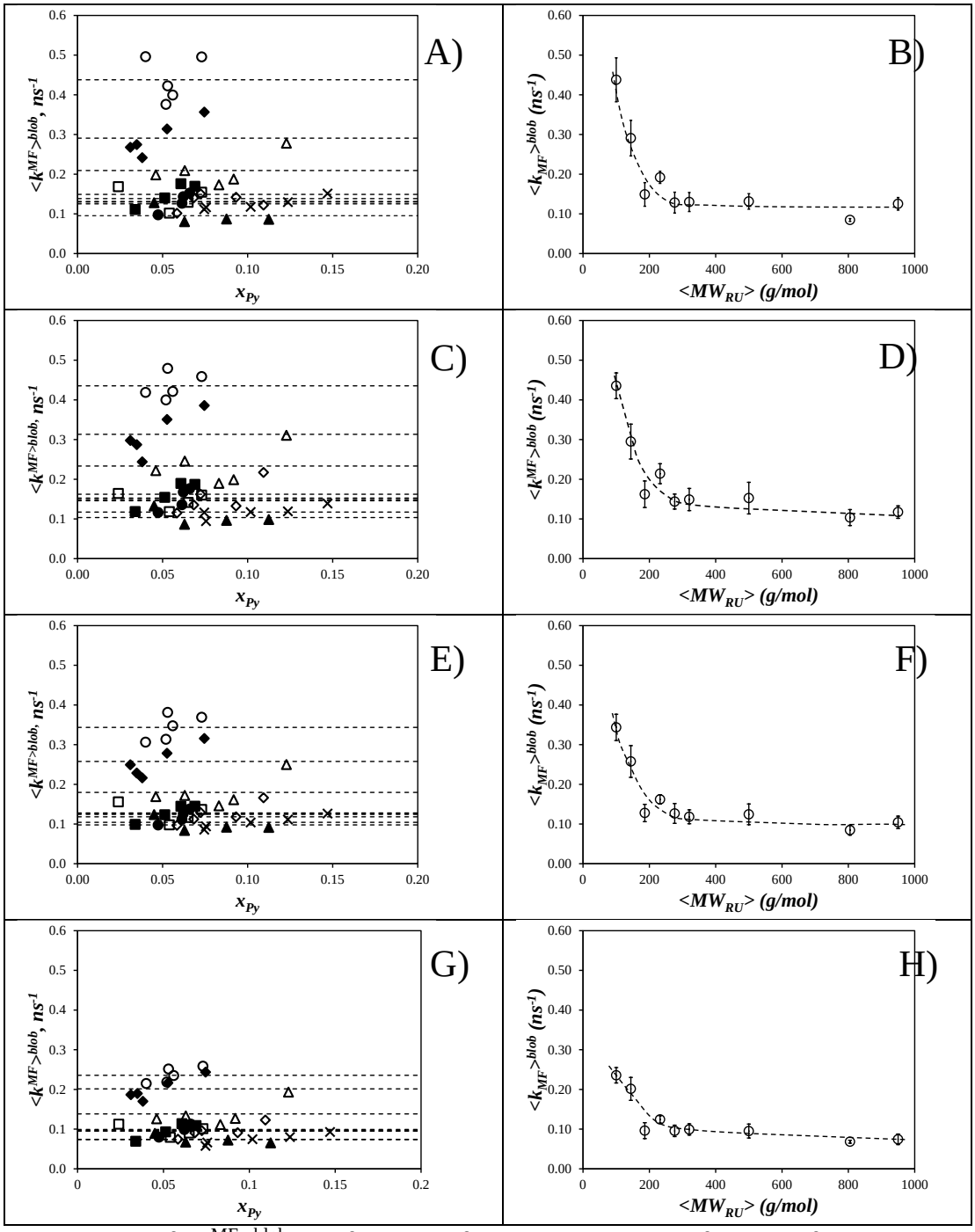

Figure S3.2. Plot of $<k^{MF}>^{blob}$ as a function of (A, C, E, G) molar fraction of pyrene or (B, D, F, H) MW_{SU} in (A, B) THF, (C, D) toluene, (E, F) DMF, and (G, H) DMSO. (O) Py-PEG$_0$MA, (◆) Py-PEG$_1$MA, (■) Py-PEG$_2$MA, (▲) Py-PEG$_3$MA, (□) Py-PEG$_4$MA, (●) Py-PEG$_5$MA, (◇) Py-PEG$_9$MA, (▲) Py-PEG$_{16}$MA, and (×) Py-PEG$_{19}$MA.

E] Parameters retrieved from the FBM analysis of the Py-PEG$_n$MA fluorescence decays

Table S3.1. Parameters retrieved from the monomer in THF fit with the program *sumegs17bg*

Sample	Mol %	τ_1 (ns)	a_1	τ_2 (ns)	a_2	τ_3 (ns)	a_3	f_{Mfree}	χ^2
PyPEG$_0$MA	4.0	7.2	0.17	31.2	0.44	62.7	0.39	0.00	1.11
τ_M = 186 ns	5.2	8.1	0.21	31.2	0.48	75.3	0.31	0.01	1.08
	5.3	9.1	0.23	30.6	0.48	66.5	0.28	0.01	1.06
	5.6	7.2	0.20	28.6	0.49	66.1	0.31	0.00	1.18
	7.3	5.0	0.20	19.4	0.49	43.9	0.31	0.00	1.21
PyPEG$_1$MA	3.1	11.2	0.15	52.2	0.39	116.2	0.42	0.04	1.02
τ_M = 200 ns	3.5	12.2	0.19	53.5	0.42	112.1	0.38	0.01	1.09
	3.8	10.5	0.16	50.5	0.40	110.7	0.41	0.03	1.10
	5.3	6.9	0.17	30.5	0.38	74.3	0.42	0.03	1.13
	7.5	4.4	0.17	20.3	0.42	53.9	0.38	0.03	1.08
PyPEG$_2$MA	3.4	10.2	0.09	50.2	0.19	138.7	0.57	0.15	1.09
τ_M = 197 ns	5.1	9.7	0.12	47.4	0.29	111.5	0.51	0.08	1.11
	6.1	9.9	0.19	46.0	0.38	101.3	0.41	0.02	1.10
	6.9	7.3	0.15	34.7	0.32	88.2	0.51	0.03	1.04
PyPEG$_3$MA	4.6	9.2	0.18	44.4	0.31	102.0	0.46	0.06	1.22
τ_M = 181 ns	6.3	7.0	0.19	34.3	0.35	86.8	0.44	0.02	1.29
	8.3	7.9	0.21	35.3	0.37	83.8	0.41	0.01	1.08
	9.2	9.6	0.29	40.6	0.42	84.7	0.27	0.01	1.08
	12.3	6.1	0.29	20.2	0.41	49.6	0.29	0.02	1.24
PyPEG$_4$MA	2.4	11.2	0.11	48.2	0.15	125.1	0.43	0.31	1.11
τ_M = 188 ns	5.4	11.4	0.15	55.1	0.25	126.5	0.48	0.11	1.11
	6.5	9.7	0.20	46.5	0.29	113.5	0.45	0.05	1.10
	7.3	8.9	0.22	38.3	0.32	99.8	0.41	0.05	1.01
PyPEG$_5$MA	4.7	12.6	0.15	60.6	0.24	136.5	0.48	0.13	1.19
τ_M = 192 ns	6.1	10.8	0.20	49.4	0.29	119.2	0.45	0.05	1.07
	6.2	8.0	0.17	36.3	0.28	106.5	0.48	0.08	1.10
	6.6	9.6	0.23	44.3	0.33	110.7	0.40	0.04	1.11
PyPEG$_9$MA	5.8	10.2	0.15	38.9	0.23	123.4	0.50	0.12	1.26
τ_M = 187 ns	6.8	7.5	0.18	32.8	0.29	105.3	0.45	0.08	1.03
	7.2	12.1	0.31	53.1	0.36	117.2	0.31	0.02	1.12
	9.3	10.7	0.27	44.4	0.38	98.8	0.33	0.02	1.10
	10.9	9.8	0.29	41.6	0.35	99.3	0.35	0.02	1.13
PyPEG$_{16}$MA	4.5	11.2	0.17	47.2	0.23	127.5	0.38	0.23	0.99
τ_M = 191 ns	6.3	11.4	0.15	54.6	0.25	135.7	0.35	0.25	1.17
	8.8	12.7	0.23	50.9	0.26	123.1	0.29	0.22	1.11
	11.2	10.6	0.23	43.5	0.33	113.8	0.36	0.09	1.21
PyPEG$_{19}$MA	7.4	9.7	0.21	40.2	0.28	119.2	0.36	0.15	1.26
τ_M = 190 ns	7.6	10.4	0.22	41.1	0.28	116.0	0.35	0.15	1.17
	10.2	11.4	0.31	43.8	0.34	113.2	0.30	0.06	1.17
	12.4	8.9	0.28	32.7	0.38	94.4	0.31	0.04	1.09
	14.7	7.4	0.32	28.7	0.39	82.8	0.24	0.04	1.18

Table S3.2. Parameters retrieved from the excimer decays in THF fit with the program *sumegs17bg*.

Sample	Mol %	f_{diff}^{E0}	τ_{E0} (ns)	τ_D (ns)	f_{EE0}	f_{ED}	χ^2
$PyPEG_0MA$	4	0.98	42.7	88.0	0.001	0.024	1.11
	5.2	0.96	54.6	94.2	0.003	0.033	1.08
	5.3	0.94	54.1	89.7	0.016	0.041	1.06
	5.6	0.96	53.4	91.1	0.000	0.036	1.18
	7.3	0.97	45.4	88.8	0.000	0.031	1.21
$PyPEG_1MA$	3.1	0.96	57.5	98.9	0.030	0.007	1.02
	3.5	0.97	56.7	98.4	0.022	0.008	1.09
	3.8	0.97	57.3	101.4	0.020	0.008	1.10
	5.3	0.96	54.3	96.2	0.002	0.040	1.13
	7.5	0.96	54.0	99.4	0.007	0.033	1.08
$PyPEG_2MA$	3.4	0.98	66.1	91.1	0.165	0.004	1.09
	5.1	0.97	54.8	110.2	0.000	0.029	1.11
	6.1	0.96	57.0	107.0	0.013	0.024	1.10
	6.9	0.97	54.7	109.7	0.000	0.033	1.04
$PyPEG_3MA$	4.6	0.96	56.7	118.5	0.018	0.025	1.22
	6.3	0.97	56.0	111.2	0.009	0.022	1.29
	8.3	0.95	54.4	101.5	0.009	0.036	1.08
	9.2	0.94	54.3	99.0	0.015	0.041	1.08
	12.3	0.95	53.9	89.8	0.000	0.053	1.24
$PyPEG_4MA$	2.4	0.96	56.6	174.4	0.014	0.027	1.11
	5.4	0.96	50.4	139.7	0.000	0.040	1.11
	6.5	0.97	53.6	123.0	0.004	0.029	1.10
	7.3	0.94	54.6	116.0	0.025	0.038	1.01
$PyPEG_5MA$	4.7	0.95	52.5	114.0	0.000	0.048	1.19
	6.1	0.95	53.5	106.2	0.000	0.049	1.07
	6.2	0.95	53.6	113.1	0.000	0.051	1.10
	6.6	0.95	53.9	109.4	0.000	0.046	1.11
$PyPEG_9MA$	5.8	0.94	65.2	102.5	0.059	0.001	1.26
	6.8	0.96	58.8	101.3	0.036	0.005	1.03
	7.2	0.94	57.1	104.1	0.009	0.053	1.12
	9.3	0.93	51.6	102.6	0.004	0.069	1.10
	10.9	0.95	55.3	102.2	0.002	0.050	1.13
$PyPEG_{16}MA$	4.5	0.94	50.0	115.2	0.006	0.062	0.99
	6.3	0.93	52.1	110.5	0.000	0.073	1.17
	8.8	0.94	53.0	109.7	0.000	0.060	1.11
	11.2	0.95	54.9	127.8	0.000	0.049	1.21
$PyPEG_{19}MA$	7.4	0.95	58.6	115.8	0.003	0.049	1.26
	7.6	0.93	57.5	118.7	0.000	0.070	1.17
	10.2	0.92	55.8	101.8	0.028	0.050	1.17
	12.4	0.93	56.0	102.0	0.034	0.036	1.09
	14.7	0.93	53.5	100.3	0.004	0.061	1.18

Table S3.3. Parameters retrieved from the monomer decays in DMSO fit with the program *sumegs17bg*.

Sample	Mol %	τ_1 (ns)	a_1	τ_2 (ns)	a_2	τ_3 (ns)	a_3	f_{Mfree}	χ^2
$PyPEG_0MA$	4	7.2	0.11	31.7	0.25	84.1	0.59	0.05	1.11
τ_M = 138 ns	5.2	13.1	0.28	50.8	0.39	91.5	0.33	0.00	1.23
	5.3	12.7	0.29	47.0	0.41	85.5	0.29	0.01	1.22
	5.6	10.6	0.25	43.4	0.42	84.2	0.33	0.00	1.22
	7.3	8.2	0.23	31.6	0.42	66.8	0.34	0.01	1.16
$PyPEG_1MA$	3.1	12.7	0.14	49.0	0.21	100.6	0.59	0.05	1.00
τ_M = 141 ns	3.5	10.9	0.14	46.6	0.24	96.1	0.56	0.06	1.08
	3.8	10.3	0.11	39.7	0.21	93.2	0.61	0.07	1.21
	5.3	12.1	0.26	51.7	0.41	90.6	0.31	0.02	1.13
	7.5	10.0	0.31	38.9	0.40	73.2	0.27	0.02	1.27
$PyPEG_2MA$	3.4	20.2	0.12	75.4	0.12	117.4	0.37	0.40	1.21
τ_M = 140 ns	5.1	12.3	0.12	48.3	0.19	104.2	0.58	0.11	1.03
	6.1	10.1	0.12	36.8	0.22	91.7	0.57	0.09	1.15
	6.9	9.2	0.10	31.8	0.22	86.6	0.60	0.08	1.06
$PyPEG_3MA$	4.6	12.2	0.12	42.4	0.22	97.0	0.55	0.11	1.19
τ_M = 134 ns	6.3	8.5	0.12	32.5	0.25	84.3	0.56	0.07	0.98
	8.3	11.9	0.18	41.3	0.30	86.0	0.49	0.03	1.07
	9.2	10.1	0.21	40.3	0.37	84.2	0.40	0.02	1.08
	12.3	7.7	0.25	24.6	0.37	55.1	0.35	0.03	1.15
$PyPEG_4MA$	2.4	15.6	0.09	57.3	0.16	118.1	0.51	0.22	1.11
τ_M = 139 ns	5.4	11.9	0.10	45.3	0.19	105.1	0.50	0.07	1.07
	6.5	14.2	0.15	54.3	0.30	105.7	0.48	0.04	1.14
	7.3	14.7	0.19	53.5	0.35	102.1	0.42	0.01	1.17
$PyPEG_5MA$	4.7	13.1	0.10	47.8	0.18	109.2	0.47	0.25	1.01
τ_M = 140 ns	6.1	16.9	0.16	45.2	0.18	93.3	0.58	0.08	1.17
	6.2	11.8	0.13	42.1	0.22	96.7	0.51	0.14	1.08
	6.6	13.2	0.16	46.0	0.29	95.8	0.47	0.08	1.09
$PyPEG_9MA$	5.8	12.3	0.08	40.7	0.18	104.5	0.53	0.21	1.06
τ_M = 145 ns	6.8	12.6	0.13	42.0	0.23	101.3	0.53	0.10	0.99
	7.2	14.5	0.17	50.7	0.31	104.5	0.46	0.06	1.10
	9.3	9.8	0.14	36.9	0.30	93.6	0.51	0.05	1.19
	10.9	9.5	0.19	32.9	0.38	80.5	0.41	0.02	1.03
$PyPEG_{16}MA$	4.5	15.2	0.13	47.6	0.17	105.7	0.34	0.37	1.10
τ_M = 140 ns	6.3	9.9	0.10	33.9	0.20	88.2	0.38	0.32	1.03
	8.8	10.6	0.12	36.7	0.24	88.3	0.45	0.19	1.05
	11.2	15.1	0.11	50.6	0.19	108.3	0.38	0.31	1.02
$PyPEG_{19}MA$	7.4	13.5	0.17	44.8	0.25	116.0	0.39	0.18	1.17
τ_M = 144 ns	7.6	8.3	0.12	32.4	0.25	104.0	0.44	0.20	1.10
	10.2	13.6	0.30	45.9	0.30	107.5	0.34	0.07	1.29
	12.4	10.3	0.24	35.4	0.39	94.0	0.33	0.04	1.15
	14.7	9.1	0.27	30.0	0.40	81.4	0.28	0.05	1.17

Table S3.4. Parameters retrieved from the excimer decays in DMSO fit with the program *sumegs17bg*.

Sample	Mol %	f_{diff}^{E0}	τ_{E0} (ns)	τ_D (ns)	f_{EE0}	f_{ED}	χ^2
$PyPEG_0MA$	4	0.95	49.8	104.3	0.009	0.038	1.11
	5.2	0.93	50.7	91.8	0.021	0.053	1.23
	5.3	0.91	50.4	89.8	0.032	0.056	1.22
	5.6	0.93	50.4	93.0	0.019	0.052	1.22
	7.3	0.91	48.5	86.1	0.001	0.088	1.16
$PyPEG_1MA$	3.1	0.93	52.0	98.5	0.042	0.023	1.00
	3.5	0.93	48.3	100.3	0.001	0.065	1.08
	3.8	0.93	46.8	98.4	0.000	0.069	1.21
	5.3	0.91	49.7	88.1	0.022	0.070	1.13
	7.5	0.89	49.7	88.4	0.039	0.076	1.27
$PyPEG_2MA$	3.4	0.94	61.3	125.8	0.000	0.058	1.21
	5.1	0.96	53.0	107.2	0.000	0.041	1.03
	6.1	0.94	51.8	105.3	0.000	0.058	1.15
	6.9	0.94	51.0	106.7	0.016	0.041	1.06
$PyPEG_3MA$	4.6	0.94	50.4	104.5	0.000	0.062	1.19
	6.3	0.94	49.7	100.6	0.005	0.056	0.98
	8.3	0.93	48.6	95.7	0.000	0.071	1.07
	9.2	0.94	49.5	97.4	0.009	0.050	1.08
	12.3	0.91	47.7	87.5	0.000	0.089	1.17
$PyPEG_4MA$	2.4	0.96	49.8	112.1	0.000	0.044	1.11
	5.4	0.95	49.3	108.1	0.000	0.048	1.07
	6.5	0.95	46.1	102.1	0.001	0.050	1.14
	7.3	0.94	46.5	99.8	0.001	0.059	1.17
$PyPEG_5MA$	4.7	0.95	49.9	112.6	0.000	0.051	1.01
	6.1	0.94	46.5	109.5	0.053	0.007	1.17
	6.2	0.95	47.8	109.9	0.010	0.039	1.08
	6.6	0.95	47.0	108.7	0.000	0.051	1.09
$PyPEG_9MA$	5.8	0.94	48.8	102.2	0.014	0.042	1.06
	6.8	0.94	50.4	102.2	0.028	0.027	0.99
	7.2	0.94	49.9	102.9	0.017	0.046	1.10
	9.3	0.95	51.4	103.4	0.015	0.033	1.19
	10.9	0.91	52.0	100.7	0.056	0.033	1.03
$PyPEG_{16}MA$	4.5	0.95	52.0	125.5	0.022	0.027	1.10
	6.3	0.93	53.4	123.2	0.043	0.029	1.03
	8.8	0.93	49.5	121.8	0.040	0.029	1.05
	11.2	0.94	48.8	117.9	0.011	0.044	1.02
$PyPEG_{19}MA$	7.4	0.95	58.6	115.8	0.003	0.049	1.17
	7.6	0.93	57.5	118.7	0.000	0.070	1.10
	10.2	0.92	55.8	101.8	0.028	0.050	1.29
	12.4	0.93	56.0	102.0	0.034	0.036	1.15
	14.7	0.93	53.5	100.3	0.004	0.061	1.17

Table S3.5. Parameters retrieved from the monomer decays in DMF fit with the program *sumegs17bg*.

Sample	Mol %	τ_1 (ns)	a_1	τ_2 (ns)	a_2	τ_3 (ns)	a_3	f_{Mfree}	χ^2
$PyPEG_0MA$	4	7.5	0.13	31.9	0.34	76.8	0.48	0.05	1.06
τ_M = 149 ns	5.2	7.5	0.15	28.4	0.38	66.9	0.43	0.04	1.13
	5.3	7.0	0.20	28.4	0.43	63.8	0.35	0.02	1.19
	5.6	6.0	0.17	26.6	0.42	63.7	0.40	0.01	1.07
	7.3	7.1	0.25	23.8	0.40	51.8	0.35	0.01	1.14
$PyPEG_1MA$	3.1	10.1	0.14	45.5	0.32	100.4	0.49	0.05	1.06
τ_M = 169 ns	3.5	9.8	0.14	46.4	0.31	103.3	0.49	0.06	1.04
	3.8	10.1	0.24	40.9	0.40	82.3	0.35	0.02	1.23
	5.3	11.4	0.15	50.6	0.34	104.8	0.47	0.03	1.01
	7.5	6.7	0.24	28.3	0.44	63.2	0.30	0.02	1.16
$PyPEG_2MA$	3.4	9.9	0.10	54.5	0.16	125.7	0.53	0.21	1.17
τ_M = 165 ns	5.1	10.7	0.12	48.6	0.26	106.9	0.53	0.09	1.14
	6.1	10.1	0.15	46.6	0.34	97.7	0.47	0.04	1.13
	6.9	10.0	0.19	48.2	0.39	99.7	0.40	0.02	1.15
$PyPEG_3MA$	4.6	9.9	0.15	40.4	0.27	97.2	0.51	0.07	1.07
τ_M = 153ns	6.3	8.8	0.20	38.8	0.33	92.1	0.44	0.02	1.25
	8.3	10.6	0.21	39.8	0.36	86.7	0.41	0.02	1.11
	9.2	9.1	0.24	38.2	0.38	80.8	0.35	0.03	1.21
	12.3	6.8	0.24	18.7	0.35	46.0	0.37	0.03	1.16
$PyPEG_4MA$	2.4	13.7	0.11	51.4	0.16	119.4	0.47	0.26	1.09
τ_M = 162 ns	5.4	10.8	0.13	47.8	0.22	112.3	0.48	0.17	1.09
	6.5	13.5	0.20	50.6	0.28	106.3	0.45	0.07	1.19
	7.3	9.9	0.20	39.2	0.29	95.7	0.45	0.06	1.03
$PyPEG_5MA$	4.7	14.4	0.17	52.5	0.19	125.7	0.51	0.13	1.11
τ_M = 163 ns	6.1	10.1	0.16	45.1	0.26	107.9	0.47	0.11	1.11
	6.2	15.5	0.24	49.9	0.21	102.6	0.46	0.09	1.25
	6.6	15.7	0.24	49.4	0.28	99.9	0.42	0.06	1.18
$PyPEG_9MA$	5.8	8.5	0.10	29.8	0.22	107.8	0.47	0.21	1.22
τ_M = 154 ns	6.8	14.1	0.24	52.7	0.24	104.3	0.39	0.13	1.22
	7.2	11.3	0.22	40.3	0.29	101.4	0.43	0.05	1.15
	9.3	10.6	0.21	37.0	0.31	90.9	0.42	0.06	1.22
	10.9	7.7	0.22	26.6	0.37	71.9	0.37	0.04	1.13
$PyPEG_{16}MA$	4.5	12.8	0.14	46.6	0.22	109.1	0.37	0.28	0.99
τ_M = 161 ns	6.3	14.9	0.16	58.4	0.27	122.3	0.26	0.30	1.13
	8.8	9.8	0.16	37.8	0.25	98.4	0.33	0.26	1.01
	11.2	9.4	0.19	35.5	0.31	96.1	0.39	0.11	1.07
$PyPEG_{19}MA$	7.4	13.5	0.17	44.8	0.25	116.0	0.39	0.18	1.17
τ_M = 167 ns	7.6	8.3	0.12	32.4	0.25	104.0	0.44	0.20	1.10
	10.2	13.6	0.30	45.9	0.30	107.5	0.34	0.07	1.29
	12.4	10.3	0.24	35.4	0.39	94.0	0.33	0.04	1.15
	14.7	9.1	0.27	30.0	0.40	81.4	0.28	0.05	1.17

Table S3.6. Parameters retrieved from the excimer decays in DMF fit with the program *sumegs17bg*.

Sample	Mol %	f_{diff}^{E0}	τ_{E0} (ns)	τ_D (ns)	f_{EE0}	f_{ED}	χ^2
$PyPEG_0MA$	4	0.97	53.5	101.8	0.000	0.032	1.06
	5.2	0.93	50.3	94.9	0.000	0.070	1.13
	5.3	0.96	52.0	94.7	0.000	0.041	1.19
	5.6	0.97	52.0	97.2	0.001	0.033	1.07
	7.3	0.95	51.7	102.9	0.029	0.022	1.14
$PyPEG_1MA$	3.1	0.96	53.4	101.0	0.009	0.031	1.06
	3.5	0.96	51.9	97.0	0.012	0.031	1.04
	3.8	0.96	52.6	101.6	0.018	0.024	1.23
	5.3	0.94	51.4	95.5	0.006	0.049	1.01
	7.5	0.94	50.6	93.5	0.004	0.052	1.16
$PyPEG_2MA$	3.4	0.97	59.2	127.0	0.000	0.029	1.17
	5.1	0.97	53.1	115.8	0.000	0.032	1.14
	6.1	0.96	51.4	113.0	0.000	0.041	1.13
	6.9	0.97	53.7	113.2	0.000	0.034	1.15
$PyPEG_3MA$	4.6	0.95	54.8	105.9	0.000	0.050	1.07
	6.3	0.98	55.5	102.9	0.000	0.019	1.25
	8.3	0.92	54.1	102.5	0.055	0.026	1.11
	9.2	0.95	51.6	99.1	0.012	0.036	1.21
	12.3	0.98	52.7	99.6	0.067	0.041	1.16
$PyPEG_4MA$	2.4	0.95	0.5	124.8	0.000	0.051	1.09
	5.4	0.96	49.6	134.8	0.001	0.037	1.09
	6.5	0.94	51.5	137.8	0.032	0.027	1.19
	7.3	0.95	52.8	139.4	0.039	0.010	1.03
$PyPEG_5MA$	4.7	0.95	58.8	109.8	0.026	0.029	1.11
	6.1	0.97	50.8	109.7	0.000	0.034	1.11
	6.2	0.92	51.8	106.2	0.015	0.061	1.25
	6.6	0.92	48.2	107.2	0.000	0.075	1.18
$PyPEG_9MA$	5.8	0.96	62.7	117.7	0.014	0.026	1.22
	6.8	0.95	55.5	104.8	0.024	0.028	1.22
	7.2	0.95	57.2	97.3	0.015	0.040	1.15
	9.3	0.94	53.8	106.2	0.011	0.050	1.22
	10.9	0.95	53.2	107.3	0.015	0.037	1.13
$PyPEG_{16}MA$	4.5	0.95	50.2	125.6	0.000	0.049	0.99
	6.3	0.94	50.9	121.1	0.007	0.050	1.13
	8.8	0.94	50.5	117.2	0.010	0.051	1.01
	11.2	0.95	54.2	122.4	0.024	0.027	1.07
$PyPEG_{19}MA$	7.4	0.94	55.9	101.1	0.004	0.057	1.17
	7.6	0.97	55.2	123.4	0.013	0.017	1.10
	10.2	0.93	54.8	91.5	0.020	0.051	1.29
	12.4	0.91	53.5	96.2	0.036	0.049	1.15
	14.7	0.90	52.1	94.0	0.047	0.054	1.17

Table S3.7. Parameters retrieved from the monomer decays in toluene fit with the program *sumegs17bg*.

Sample	Mol %	τ_1 (ns)	a_1	τ_2 (ns)	a_2	τ_3 (ns)	a_3	f_{Mfree}	χ^2
$PyPEG_0MA$	4	8.7	0.19	34.7	0.47	70.5	0.33	0.01	1.02
τ_M = 140 ns	5.2	9.0	0.22	28.0	0.44	62.8	0.33	0.02	1.10
	5.3	9.4	0.31	32.1	0.47	59.6	0.19	0.02	1.08
	5.6	12.1	0.34	32.9	0.38	57.0	0.27	0.01	1.22
	7.3	7.9	0.33	26.6	0.52	54.4	0.15	0.01	1.10
$PyPEG_1MA$	3.1	8.8	0.13	38.2	0.29	87.9	0.51	0.07	1.22
τ_M = 158 ns	3.5	9.0	0.13	40.8	0.35	87.3	0.46	0.06	1.12
	3.8	10.8	0.15	47.4	0.37	93.6	0.42	0.05	1.14
	5.3	4.7	0.14	21.4	0.30	58.0	0.51	0.05	1.10
	7.5	6.8	0.22	19.7	0.33	45.4	0.42	0.03	1.12
$PyPEG_2MA$	3.4	12.1	0.11	56.3	0.21	125.2	0.47	0.21	1.07
τ_M = 171 ns	5.1	9.5	0.13	47.0	0.31	101.7	0.50	0.06	1.10
	6.1	8.6	0.17	39.1	0.35	88.1	0.45	0.03	1.06
	6.9	7.3	0.17	34.6	0.34	82.3	0.46	0.02	1.11
$PyPEG_3MA$	4.6	9.4	0.18	41.3	0.34	93.4	0.44	0.04	1.07
τ_M = 159 ns	6.3	9.0	0.27	39.7	0.41	85.7	0.31	0.01	1.20
	8.3	9.5	0.25	39.3	0.42	81.0	0.32	0.01	1.17
	9.2	7.3	0.24	31.4	0.40	73.3	0.35	0.01	1.02
	12.3	8.0	0.45	28.0	0.43	57.4	0.11	0.01	1.27
$PyPEG_4MA$	2.4	12.1	0.10	56.1	0.23	127.3	0.45	0.21	1.01
τ_M = 169 ns	5.4	6.7	0.12	35.2	0.21	106.5	0.51	0.16	1.04
	6.5	9.8	0.18	39.5	0.27	96.7	0.49	0.07	1.11
	7.3	10.1	0.23	39.4	0.30	91.3	0.41	0.06	1.09
$PyPEG_5MA$	4.7	9.9	0.14	43.3	0.21	113.8	0.52	0.14	1.19
τ_M = 163 ns	6.1	9.0	0.17	39.1	0.26	100.6	0.48	0.08	1.08
	6.2	9.9	0.21	43.4	0.30	100.5	0.35	0.05	1.12
	6.6	8.6	0.22	37.5	0.34	94.5	0.40	0.04	1.13
$PyPEG_9MA$	5.8	9.1	0.16	43.7	0.25	111.9	0.45	0.14	1.16
τ_M = 171 ns	6.8	11.5	0.23	51.4	0.37	113.6	0.35	0.05	1.11
	7.2	9.8	0.23	40.2	0.34	96.0	0.39	0.04	1.05
	9.3	13.5	0.33	54.2	0.46	118.6	0.21	0.00	1.18
	10.9	6.7	0.30	26.1	0.39	70.4	0.29	0.02	1.03
$PyPEG_{16}MA$	4.5	11.1	0.16	48.5	0.22	110.2	0.34	0.28	1.16
τ_M = 165 ns	6.3	11.7	0.16	54.1	0.26	123.6	0.30	0.28	1.13
	8.8	9.7	0.20	42.1	0.26	105.6	0.30	0.23	1.09
	11.2	7.6	0.20	34.4	0.32	96.7	0.38	0.10	1.07
$PyPEG_{19}MA$	7.4	10.0	0.18	37.0	0.24	94.6	0.31	0.28	1.06
τ_M = 158 ns	7.6	14.4	0.19	50.1	0.26	106.4	0.28	0.27	1.10
	10.2	10.5	0.25	40.7	0.33	95.6	0.29	0.12	1.01
	12.4	10.3	0.26	35.9	0.37	87.6	0.30	0.07	1.18
	14.7	9.5	0.34	32.0	0.37	80.3	0.23	0.06	1.16

Table S3.8. Parameters retrieved from the excimer decays in Toluene fit with the program *sumegs17bg*.

Sample	Mol %	f_{diff}^{E0}	τ_{E0} (ns)	τ_D (ns)	f_{EE0}	f_{ED}	χ^2
$PyPEG_0MA$	4	0.95	47.9	84.4	0.000	0.055	1.02
	5.2	0.91	52.3	93.5	0.051	0.037	1.10
	5.3	0.92	51.2	88.8	0.044	0.034	1.08
	5.6	0.90	52.5	89.0	0.070	0.032	1.22
	7.3	0.90	51.1	83.1	0.065	0.030	1.10
$PyPEG_1MA$	3.1	0.95	53.8	111.3	0.003	0.046	1.22
	3.5	0.95	51.5	111.3	0.004	0.051	1.12
	3.8	0.96	51.1	109.4	0.009	0.036	1.14
	5.3	0.95	49.4	99.4	0.004	0.044	1.10
	7.5	0.89	47.8	81.2	0.000	0.106	1.12
$PyPEG_2MA$	3.4	0.96	57.7	121.5	0.000	0.035	1.07
	5.1	0.96	50.3	102.9	0.000	0.039	1.10
	6.1	0.95	50.7	100.3	0.001	0.052	1.06
	6.9	0.95	51.1	101.1	0.000	0.047	1.11
$PyPEG_3MA$	4.6	0.94	49.6	99.0	0.004	0.060	1.07
	6.3	0.92	51.8	99.1	0.037	0.041	1.20
	8.3	0.91	49.7	94.6	0.002	0.086	1.17
	9.2	0.92	51.0	97.2	0.063	0.018	1.02
	12.3	0.86	51.1	90.5	0.124	0.018	1.27
$PyPEG_4MA$	2.4	0.91	46.4	118.8	0.000	0.088	1.04
	5.4	0.97	51.7	125.5	0.000	0.028	1.04
	6.5	0.94	48.9	116.9	0.024	0.039	1.11
	7.3	0.92	50.9	119.5	0.058	0.018	1.09
$PyPEG_5MA$	4.7	0.95	50.2	104.7	0.000	0.046	1.19
	6.1	0.95	48.1	100.5	0.000	0.054	1.08
	6.2	0.95	47.7	108.5	0.009	0.045	1.12
	6.6	0.94	49.3	98.9	0.000	0.060	1.13
$PyPEG_9MA$	5.8	0.95	50.1	104.8	0.000	0.049	1.16
	6.8	0.93	46.8	100.5	0.002	0.069	1.11
	7.2	0.93	47.3	97.6	0.002	0.064	1.05
	9.3	0.89	47.7	98.4	0.026	0.086	1.18
	10.9	0.92	50.2	88.1	0.019	0.061	1.03
$PyPEG_{16}MA$	4.5	0.95	48.9	134.1	0.011	0.041	1.16
	6.3	0.93	48.0	119.6	0.015	0.050	1.13
	8.8	0.92	49.1	111.8	0.025	0.053	1.09
	11.2	0.95	49.5	113.1	0.002	0.049	1.07
$PyPEG_{19}MA$	7.4	0.94	51.9	125.5	0.001	0.057	1.06
	7.6	0.92	49.2	119.3	0.000	0.079	1.10
	10.2	0.91	50.4	105.9	0.018	0.067	1.01
	12.4	0.90	47.7	97.3	0.001	0.095	1.18
	14.7	0.88	51.0	98.3	0.070	0.054	1.16

F] Global pyrene fractions determined from Equations S3.3–S3.6

Table S3.9. Globally pyrene fractions in THF.

Sample	Mol %	f_{diff}	f_{free}	f_{E0}	f_{D}
$PyPEG_0MA$	4	0.97	0.002	0.001	0.02
	5.2	0.96	0.005	0.003	0.03
	5.3	0.93	0.011	0.016	0.04
	5.6	0.96	0.004	0.000	0.04
	7.3	0.97	0.001	0.000	0.03
$PyPEG_1MA$	3.1	0.93	0.035	0.029	0.01
	3.5	0.96	0.014	0.022	0.01
	3.8	0.94	0.028	0.019	0.01
	5.3	0.93	0.031	0.002	0.04
	7.5	0.93	0.033	0.007	0.03
$PyPEG_2MA$	3.4	0.74	0.134	0.125	0.00
	5.1	0.90	0.076	0.000	0.03
	6.1	0.94	0.023	0.012	0.02
	6.9	0.94	0.027	0.000	0.03
$PyPEG_3MA$	4.6	0.90	0.057	0.017	0.02
	6.3	0.95	0.023	0.009	0.02
	8.3	0.94	0.014	0.009	0.04
	9.2	0.94	0.008	0.015	0.04
	12.3	0.93	0.019	0.000	0.05
$PyPEG_4MA$	2.4	0.67	0.298	0.010	0.02
	5.4	0.86	0.109	0.000	0.04
	6.5	0.92	0.052	0.003	0.03
	7.3	0.89	0.046	0.024	0.04
$PyPEG_5MA$	4.7	0.83	0.127	0.000	0.04
	6.1	0.90	0.049	0.000	0.05
	6.2	0.88	0.072	0.000	0.05
	6.6	0.92	0.037	0.000	0.04
$PyPEG_9MA$	5.8	0.83	0.117	0.052	0.00
	6.8	0.89	0.076	0.033	0.00
	7.2	0.92	0.020	0.009	0.05
	9.3	0.91	0.016	0.004	0.07
	10.9	0.93	0.019	0.002	0.05
$PyPEG_{16}MA$	4.5	0.75	0.217	0.000	0.04
	6.3	0.71	0.238	0.004	0.05
	8.8	0.73	0.208	0.000	0.06
	11.2	0.86	0.082	0.000	0.05
$PyPEG_{19}MA$	7.4	0.81	0.146	0.002	0.04
	7.6	0.80	0.140	0.000	0.06
	10.2	0.87	0.058	0.027	0.05
	12.4	0.90	0.033	0.033	0.03
	14.7	0.90	0.041	0.004	0.06

Table S3.10. Globally pyrene fractions in DMSO.

Sample	Mol %	f_{diff}	f_{free}	f_{E0}	f_{D}
$PyPEG_0MA$	4	0.91	0.049	0.009	0.04
	5.2	0.92	0.004	0.021	0.05
	5.3	0.90	0.008	0.032	0.06
	5.6	0.93	0.002	0.019	0.05
	7.3	0.90	0.007	0.001	0.09
$PyPEG_1MA$	3.1	0.89	0.051	0.040	0.02
	3.5	0.88	0.058	0.001	0.06
	3.8	0.87	0.069	0.000	0.06
	5.3	0.89	0.018	0.022	0.07
	7.5	0.87	0.015	0.038	0.07
$PyPEG_2MA$	3.4	0.58	0.383	0.000	0.04
	5.1	0.86	0.103	0.000	0.04
	6.1	0.86	0.084	0.000	0.05
	6.9	0.87	0.077	0.015	0.04
$PyPEG_3MA$	4.6	0.84	0.102	0.000	0.06
	6.3	0.87	0.069	0.005	0.05
	8.3	0.90	0.031	0.000	0.07
	9.2	0.92	0.017	0.009	0.05
	12.3	0.89	0.025	0.000	0.09
$PyPEG_4MA$	2.4	0.74	0.228	0.000	0.03
	5.4	0.75	0.208	0.000	0.04
	6.5	0.89	0.065	0.001	0.05
	7.3	0.90	0.042	0.001	0.06
$PyPEG_5MA$	4.7	0.72	0.243	0.000	0.04
	6.1	0.87	0.072	0.049	0.01
	6.2	0.82	0.139	0.008	0.03
	6.6	0.88	0.074	0.000	0.05
$PyPEG_9MA$	5.8	0.75	0.201	0.011	0.03
	6.8	0.86	0.094	0.025	0.02
	7.2	0.89	0.052	0.016	0.04
	9.3	0.91	0.047	0.015	0.03
	10.9	0.89	0.023	0.055	0.03
$PyPEG_{16}MA$	4.5	0.66	0.303	0.015	0.02
	6.3	0.60	0.355	0.028	0.02
	8.8	0.64	0.309	0.028	0.02
	11.2	0.77	0.186	0.009	0.04
$PyPEG_{19}MA$	7.4	0.74	0.212	0.011	0.04
	7.6	0.69	0.269	0.021	0.02
	10.2	0.82	0.117	0.010	0.05
	12.4	0.87	0.066	0.012	0.05
	14.7	0.87	0.063	0.017	0.05

Table S3.11. Globally pyrene fractions in DMF.

Sample	Mol %	f_{diff}	f_{free}	f_{E0}	f_D
$PyPEG_0MA$	4	0.93	0.044	0.000	0.03
	5.2	0.90	0.034	0.000	0.07
	5.3	0.94	0.018	0.000	0.04
	5.6	0.96	0.010	0.001	0.03
	7.3	0.94	0.011	0.029	0.02
$PyPEG_1MA$	3.1	0.91	0.055	0.009	0.03
	3.5	0.93	0.031	0.012	0.03
	3.8	0.92	0.044	0.017	0.02
	5.3	0.93	0.018	0.006	0.05
	7.5	0.93	0.016	0.004	0.05
$PyPEG_2MA$	3.4	0.77	0.205	0.000	0.02
	5.1	0.89	0.084	0.000	0.03
	6.1	0.92	0.036	0.000	0.04
	6.9	0.95	0.018	0.000	0.03
$PyPEG_3MA$	4.6	0.88	0.071	0.000	0.05
	6.3	0.96	0.024	0.000	0.02
	8.3	0.90	0.017	0.054	0.03
	9.2	0.93	0.026	0.011	0.03
	12.3	0.88	0.026	0.060	0.04
$PyPEG_4MA$	2.4	0.71	0.254	0.000	0.04
	5.4	0.80	0.168	0.001	0.03
	6.5	0.87	0.070	0.030	0.02
	7.3	0.90	0.057	0.037	0.01
$PyPEG_5MA$	4.7	0.83	0.124	0.023	0.03
	6.1	0.86	0.107	0.000	0.03
	6.2	0.84	0.088	0.014	0.06
	6.6	0.87	0.056	0.000	0.07
$PyPEG_9MA$	5.8	0.76	0.203	0.011	0.02
	6.8	0.83	0.122	0.021	0.02
	7.2	0.90	0.047	0.014	0.04
	9.3	0.89	0.056	0.010	0.05
	10.9	0.92	0.033	0.015	0.04
$PyPEG_{16}MA$	4.5	0.70	0.267	0.000	0.04
	6.3	0.66	0.292	0.000	0.05
	8.8	0.70	0.250	0.007	0.04
	11.2	0.85	0.105	0.022	0.02
$PyPEG_{19}MA$	7.4	0.78	0.173	0.003	0.05
	7.6	0.78	0.191	0.011	0.01
	10.2	0.87	0.063	0.018	0.05
	12.4	0.88	0.037	0.035	0.05
	14.7	0.86	0.045	0.045	0.05

Table S3.12. Globally pyrene fractions in toluene.

Sample	Mol %	f_{diff}	f_{free}	f_{E0}	f_D
$PyPEG_0MA$	4	0.94	0.010	0.000	0.05
	5.2	0.90	0.014	0.050	0.04
	5.3	0.90	0.021	0.043	0.03
	5.6	0.89	0.011	0.069	0.03
	7.3	0.90	0.006	0.064	0.03
$PyPEG_1MA$	3.1	0.88	0.070	0.003	0.04
	3.5	0.89	0.057	0.004	0.05
	3.8	0.91	0.051	0.009	0.03
	5.3	0.91	0.049	0.004	0.04
	7.5	0.87	0.022	0.000	0.10
$PyPEG_2MA$	3.4	0.76	0.208	0.000	0.03
	5.1	0.91	0.054	0.000	0.04
	6.1	0.92	0.026	0.001	0.05
	6.9	0.93	0.023	0.000	0.05
$PyPEG_3MA$	4.6	0.90	0.036	0.004	0.06
	6.3	0.91	0.013	0.037	0.04
	8.3	0.90	0.012	0.002	0.08
	9.2	0.91	0.008	0.063	0.02
	12.3	0.85	0.007	0.123	0.02
$PyPEG_4MA$	2.4	0.74	0.196	0.003	0.07
	5.4	0.82	0.156	0.000	0.02
	6.5	0.88	0.062	0.022	0.04
	7.3	0.88	0.053	0.055	0.02
$PyPEG_5MA$	4.7	0.83	0.131	0.000	0.04
	6.1	0.87	0.080	0.000	0.05
	6.2	0.90	0.048	0.008	0.04
	6.6	0.90	0.038	0.000	0.06
$PyPEG_9MA$	5.8	0.82	0.138	0.000	0.04
	6.8	0.89	0.044	0.002	0.07
	7.2	0.90	0.038	0.002	0.06
	9.3	0.88	0.004	0.026	0.09
	10.9	0.90	0.018	0.019	0.06
$PyPEG_{16}MA$	4.5	0.69	0.269	0.008	0.03
	6.3	0.69	0.264	0.011	0.04
	8.8	0.72	0.220	0.019	0.04
	11.2	0.86	0.094	0.002	0.04
$PyPEG_{19}MA$	7.4	0.69	0.264	0.001	0.04
	7.6	0.69	0.253	0.000	0.06
	10.2	0.81	0.111	0.016	0.06
	12.4	0.85	0.063	0.001	0.09
	14.7	0.83	0.054	0.066	0.05

G] Derivation of the Scaling Laws for $<k^{MF}>^{blob}$

The optimal parameters *a*, *b*, and the pre-factor *c*, of the bending function f_{b3}were obtained by minimizing the χ^2 of Equation S3.7 which resulted in the matrix presented in Equation S3.8. In solving the matrix, Py-PEG$_2$MA was not used, nor were the polymers where MW_{SU} > 500 g/mol.

$$\chi^2 = \sum \left[\left(\frac{< k^{MF} >^{blob}}{< k^{MF} >^{blob,\infty}} - 1 \right) - \left(c \times {MW_{SU}}^{a} \times \eta^{b} \right) \right]^2 \tag{S3.7}$$

$$\begin{pmatrix} c \\ a \\ b \end{pmatrix} = \begin{pmatrix} \sum 1 & \sum \ln(MW_{SU}) & \sum \ln(\eta) \\ \sum \ln(\eta) & \sum \ln(MW_{SU}) \times \ln(\eta) & \sum \left(\ln(\eta)\right)^2 \\ \sum \ln(MW_{SU}) & \sum \left(\ln(MW_{SU})\right)^2 & \sum \ln(MW_{SU}) \times \ln(\eta) \end{pmatrix}^{-1} \bullet \begin{pmatrix} \sum \ln\left(\frac{< k^{MF} >^{blob}}{< k^{MF} >^{blob,\infty}} + 1 \right) \\ \sum \ln\left(\frac{< k^{MF} >^{blob}}{< k^{MF} >^{blob,\infty}} + 1 \right) \times \ln(\eta) \\ \sum \ln\left(\frac{< k^{MF} >^{blob}}{< k^{MF} >^{blob,\infty}} + 1 \right) \times \ln(MW_{SU}) \end{pmatrix} \tag{S3.8}$$